Laboratory Evaluation of Layer Structural Coefficients for HMA Pavements

Volume 1 – Hot Mix Asphalt

Submitted to the Tennessee Department of Transportation

Research Development and Technology Program

Project #: RES – 1271

Baoshan Huang

Eric Drumm

Department of Civil and Environmental Engineering

The University of Tennessee, Knoxville

March 2008

Acknowledgements

We would like to begin by thanking Tennessee Department of Transportation (TDOT) for funding this research project. During this research, we have collaborated closely with many engineers and technicians at the TDOT Materials and Test Division. They have provided valuable support towards the fulfillment of the research objectives. Without their support, it would be impossible for us to finish this research project. We would also like to thank the administrative staffs from the TDOT research office who have working very closely with our research team and kept the whole project on the proposed schedule. Thanks are also due to many graduate and undergraduate students who have worked in this project.

Table of Contents

CHAPTER 1 INTRODUCTION

1.1 Background

Asphalt covers more than ninety percent of all covered pavements in the United States, and the majority of them have been designed by the design guide published by the American Association of State Highway Officials (AASHTO). The AASHTO design guide, first published in 1972 (with revised editions in 1981, 1986 and 1993), has been almost exclusively used by all state Departments of Transportation (DOT) as the design procedure for pavement thickness design. The latest AASHTO Mechanistic Empirical (M-E) design guide (published in 2004) employs a more mechanistic approach in determining the structural capacities of each pavement layer. However, it will take many years before the new M-E design guide will be fully implemented and many aspects of the current guide (AASHTO Guide 1993) remain in the new (M-E) design guide. Under the current design guide, the structural capacity of each pavement layer is represented by a layer structural coefficient (a_i) that is intimately related to the fundamental mechanical properties of the material. Under the new AASHTO M-E Design Guide, the structural capacities of pavement will be calculated directly from the fundamental mechanical properties of the paving materials.

The current Tennessee Department of Transportation (TDOT) design procedure assigns layer structural coefficients to standard HMA mixtures, granular base and treated

granular layers. These values have been proven to be adequate over the past few decades. However, there have been numerous technological developments in the hot-mix asphalt paving industry since the 1990's, including both new materials and new design procedures. The primary example is the routine use of polymer modified asphalt cement in HMA mixtures. Other examples include the introduction of stone mastic asphalt (SMA), Superpave mixture design, open-graded friction courses (OGFC), and the use of recycled asphalt pavements as stone bases and interlayers. These changes have significantly improved the performance of the pavements, yet these changes may not be reflected in design because the layer coefficients have not been evaluated for these improved materials.

Numerous state DOTs have adjusted the layer structural coefficients of HMA mixtures and granular base layers to reflect the increase of structural capacities as a result of the implementation of new technologies. For example, the Louisiana Department of Transportation and Development (LADOTD), after a systematic investigation of material properties and the design approach, increased the layer coefficient of HMA mixtures with polymer modified asphalt from the original value of 0.42 to 0.44 (5% increase), and the coefficient for SMA mixtures from 0.42 to 0.48 (14% increase). Thus, when a high performance HMA mix design is selected, the designer can take advantage of a slightly larger layer coefficient, and effectively evaluate the economics of using these alternative mixtures.

1.2 Objective

The objective of this research was to systematically evaluate the potential increase in structural capacity of the asphalt mixture and granular base layers used in Tennessee, and, if adjustments to the layer structural coefficients of these materials are warranted, determine new layer coefficients. Specifically, the following materials should be evaluated for new structural layer coefficients: five HMA mixtures utilizing both conventional and polymer modified asphalt ("D", SMA, "BM-2", "A", and "A-S" mixes), and five granular base materials (unbound gravel base, unbound limestone base, cement treated stone base, fly ash treated stone bases, recycled asphalt pavement (RAP) and recycled concrete aggregate).

1.3 Scope of Study

The scope of the research work, summarized in Tables 1-1 and 1-2, is:

1. To evaluate the viscoelastic properties of the five HMA mixtures through dynamic modulus testing (ASTM D3497);
2. To evaluate the permanent deformation (rutting) characteristics of the five HMA mixtures through Asphalt Pavement Analyzer (APA – ASSHTO TP 63-03) ,E* and creep compliance test (AASHTO TP9);
3. To evaluate the fatigue cracking characteristics of the five HMA mixture through indirect tensile strength (ASTM D4123), beam fatigue test (AASHTO

TP8), and semi-circular notched fracture test;

4. To evaluate the resilient properties of the six granular base materials through repeated load triaxial resilient modulus test (AASHTO T307-99) on 6 inch (150mm) diameter specimens;
5. To evaluate the strength characteristics of the six granular base materials through triaxial strength tests (AASHTO T307-99) on 6 inch (150mm) diameter specimens;
6. To evaluate the shear strength characteristics of granular base materials through large scale direct shear testing (AASHTO T236-03) and confirm that the sample size is sufficient for the aggregate particle size;
7. For the five HMA mixtures, two types of asphalt binders (conventional and polymer modified) and two coarse aggregates (limestone and gravels) will be considered;
8. For the five granular base materials, three moisture content levels (low, medium and high) will be considered.

Table 1-1 HMA Test Factorials (Numbers in cells represent the number of samples tested)

Mixtures			Mix Performance Test					
Mixture Types	Asphalt Cement	Coarse Aggregate	Dynamic Modulus	APA[1]	Creep	IDT[2]	Beam Fatigue	SCB[3] Fracture
"D"	PG64-22	Limestone	3	6	3	3	3	9
		Gravel	3	6	3	3	3	9
	PG76-22	Limestone	3	6	3	3	3	9
		Gravel	3	6	3	3	3	9
SMA	PG64-22	Limestone	3	6	3	3	3	9
		Gravel	3	6	3	3	3	9
	PG76-22	Limestone	3	6	3	3	3	9
		Gravel	3	6	3	3	3	9
"BM-2"	PG64-22	Limestone	3	6	3	3	3	9
		Gravel	3	6	3	3	3	9
	PG76-22	Limestone	3	6	3	3	3	9
		Gravel	3	6	3	3	3	9
"A"	PG64-22	Limestone	3	6	3	3	3	9
		Gravel	3	6	3	3	3	9
	PG76-22	Limestone	3	6	3	3	3	9
		Gravel	3	6	3	3	3	9
"A-S"	PG64-22	Limestone	3	6	3	3	3	9
		Gravel	3	6	3	3	3	9
	PG76-22	Limestone	3	6	3	3	3	9
		Gravel	3	6	3	3	3	9

Note: Each test will be conducted on triplicate samples and total number of test will be 540.

1. APA – Asphalt Pavement Analyzer
2. IDT – Indirect Tensile Strength Test
3. SCB – Semi-Circular Bending Test

Table 1-2 Granular Base Test Factorials

Granular Base Type	Characterization Tests		Performance Tests				
	In-Place Density	Moisture Density	Moisture Levels	Resilient Modulus	Triaxial Strength[1]	CBR[2]	Direct Shear
Unbound Limestone Base	6	6[3,4]	Optimum	3	3	3	3
			Optimum +	3	3	3	3
			Optimum ++	3	3	3	3
Cement Treated Limestone Base	6	6[5]	Note				
			N/A	3	3	3	
			Optimum ++				
Unbound Gravel Base	6	6[3,4]	Optimum	3	3	3	3
			Optimum +	3	3	3	3
			Optimum ++	3	3	3	3
Cement Treated Gravel Base	6	6[5]					
			N/A	3	3	3	
Recycled Asphalt Pavement (RAP)	6	6[3,4]	Optimum	3	3	3	3
			Optimum +	3	3	3	3
			Optimum ++	3	3	3	3
Recycled Concrete Aggregate (RCA)	6	6[3,4]	Optimum	3	3	3	3
			Optimum +	3	3	3	3
			Optimum ++	3	3	3	3

Note: Each test will be conducted on triplicate samples and total number of test will be 180.

1. Triaxial Strength determined at conclusion of Resilient Modulus Test
2. CBR – California Bearing Ratio (AASHTO T 193-99 (2003))
3. Standard Proctor Test (AASHTO T 99-01)
4. Modified Proctor Test (AASHTO T 180-01)
5. Moisture Density Relations of Soil-Cement Mixtures AASHTO T 134-95 (2000), ASTMD 558-82

CHAPTER 2 LITERATURE REVIEW

2.1 Background

During the late 1950s to the early 1960s, the American Association of State Highway Officials (AASHO) conducted a comprehensive road test to determine the methodology for pavement structural design. The results from the AASHO Road Test provided the basis for the structural number design approach and the structural layer coefficient concept that were developed first in 1961 in the "AASHO Interim Guide for the Design of Rigid and Flexible Pavements". The organization, AASHO, later became the American Association of State Highway and Transportation Officials (AASHTO). The AASHTO Design Guide was later revised in 1972, 1981, 1986, and 1993 and is still widely used in the United States.

The structural design for flexible pavements is to solve the following equation for structural number (SN) (Huang 2004):

$$\log W18 = Z_R S_0 + 9.36\log(\mathrm{SN}+1) - 0.20 + \frac{\log\left[\frac{\Delta \mathrm{PSI}}{4.2-1.5}\right]}{0.40 + \frac{1094}{(\mathrm{SN}+1)^{5.19}}} + 2.32\log M_R - 8.07 \qquad (2\text{-}1)$$

where,

W_{18} = predicted number of 18-kip equivalent single-axle loads (ESALs),

Z_R = standard normal deviate,

S_0 = combined standard error of the traffic prediction and performance prediction,

SN = structural number of pavement,

ΔPSI = difference between the initial design serviceability index, p0, and the design terminal serviceability index, pt, and

M_R = subgrade resilient modulus in psi.

The structural number is an abstract number that represents the capacity of an pavement structure to last for the expected service life under the conditions of given traffic loads (ESALs), subgrade soil support, terminal serviceability index, and regional factors. The structural number is also a linear combination of the supporting capacities of different layer materials in the pavement structure. Structural number is initially computed as (Huang 2004):

$$\text{SN} = a_1 D_1 + a_2 D_2 + a_3 D_3 \tag{2-2}$$

where,

a_1, a_2, and a_3 = structural layer coefficients for the surface, base, and subbase, respectively, and

D_1, D_2, and D_3 = thicknesses for the surface, base, and subbase, respectively.

Equation (2-2) was later modified to the following form to take into account local precipitation and drainage conditions:

$$\text{SN} = a_1 D_1 + a_2 m_2 D_2 + a_3 m_3 D_3 \tag{2-3}$$

where,

m_2 and m_3 = drainage coefficients for the base and subbase, respectively.

From Equation (2-3), it is obvious that the structural number concept combines the effects of the structural layer coefficients, layer thicknesses, and drainage coefficients on the structural capacity of pavements. The structural layer coefficient a_i is a measure of the relative ability of a unit thickness of a given material to function as a structural component of the pavement and thus used to convert the actual thicknesses of asphalt layers into the structural number required in the structural design of pavement.

The original structural layer coefficients are actually regression constants obtained by correlating pavement layer thicknesses with the pavement performance based on the results from the AASHO Road Test. According to the most recent AASHTO design guide (1993), the layer coefficients a_i vary considerably depending upon a number of factors. These factors include:

- Layer thickness
- Material type
- Material properties
- Layer location (surface, base, subbase)
- Traffic level
- Failure criterion

Except for the initial layer coefficients, the determination of layer coefficient

values are usually based on the empirical relationships between layer coefficients and the layer material properties. Resilient modulus has long been used as a fundamental material property to estimate layer coefficients from.

2.2 Determination of Layer Coefficients from Resilient Modulus

Except for the initial structural layer coefficients, resilient modulus of pavement layer materials has long been identified as the primary property to determine the layer coefficient values. In the AASHTO design guide, charts have been provided to determine the structural layer coefficient value based on the relationships between layer coefficient and resilient modulus. Figure 2-1 shows the relationships of layer coefficient, Marshall stability, cohesiometer values, and resilient modulus for HMA. Figure 2-2 shows the correlation charts for untreated granular base, bituminous-treated base, and cement-treated base. Figure 2-3 shows the correlation chart for estimating layer coefficient of granular subbases from California Bearing Ratio (CBR), R values, and Texas triaxial classification.

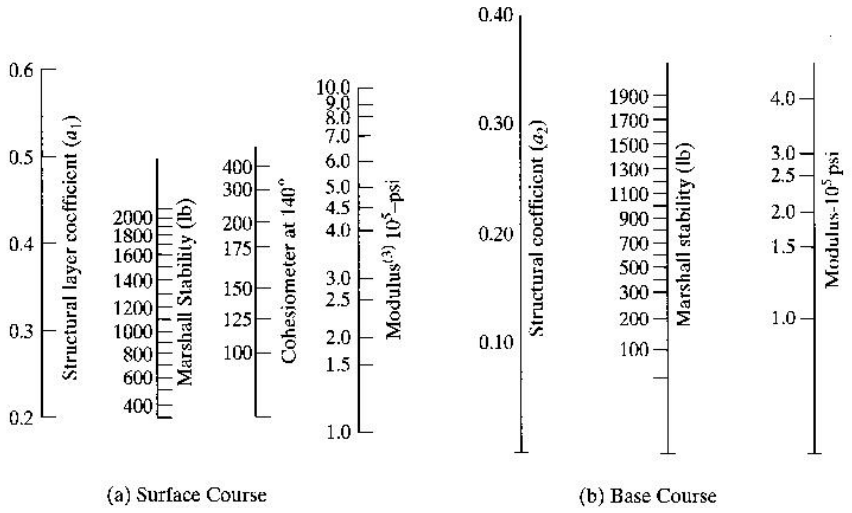

Figure 2-1 Correlation Charts for Determining Layer Coefficient of HMA (After Huang 2004)

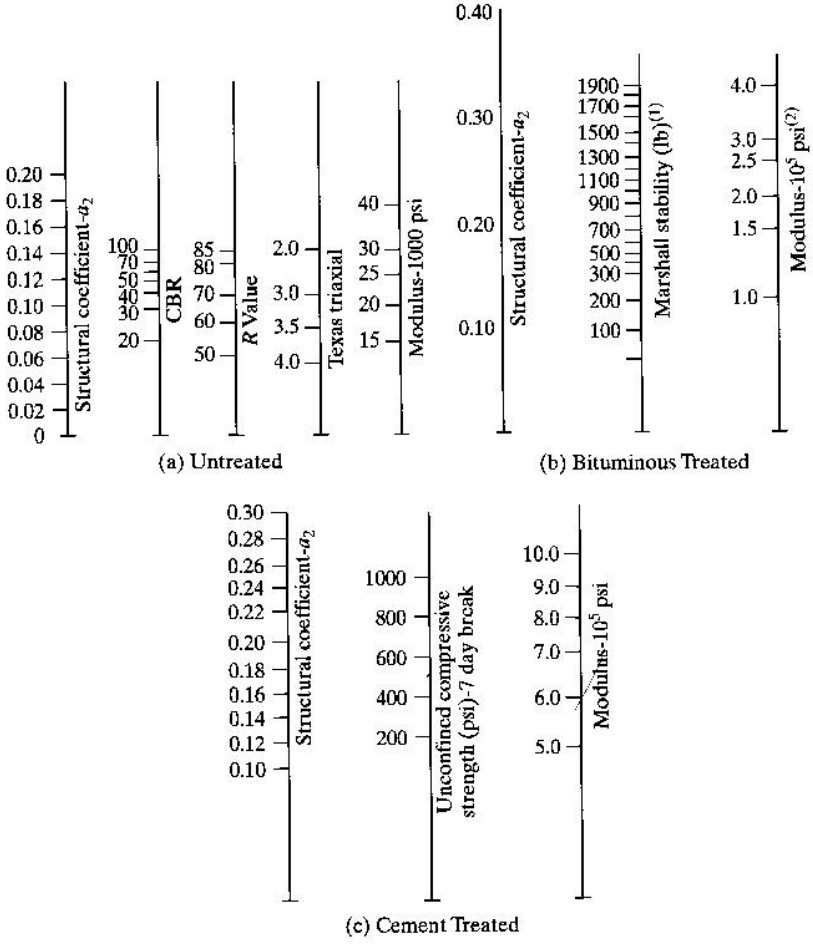

Figure 2-2 Correlation Charts for Determining Layer Coefficient of Bases (After Huang 2004)

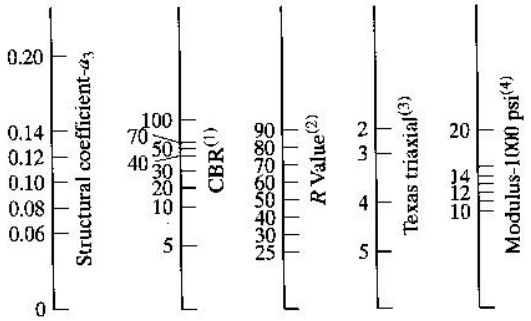

Figure 2-3 Correlation Charts for Determining Layer Coefficient of Subbases (After Huang 2004)

It is noted that in the previous charts, not only resilient modulus but also other material properties are used for for determining layer coefficient values. For dense-graded asphalt concrete surface course, layer coefficient can be estimated from only resilient modulus measured at 70 °F (21 °C) as shown in Figure 2-4.

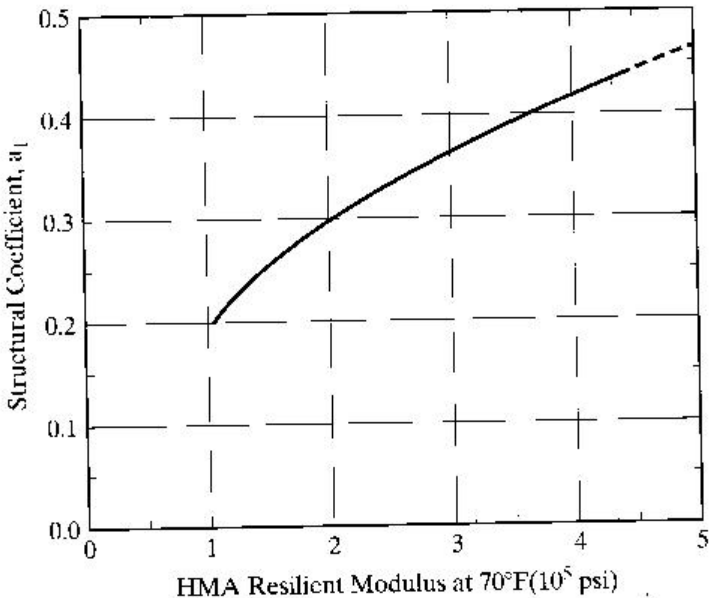

Figure 2-4 Chart for Estimating Layer Coefficient of Dense-Graded Asphalt Concrete (After Huang 2004)

In addition to the previous correlation charts, equations can also be used to determine layer coefficients (Huang 2004):

Granular Base:

$$a_2 = 0.249\log(E_2) - 0.977 \tag{2-4}$$

where E_2 = resiliment modulus of granular base material (in psi).

Granular Subbase:

$$a_3 = 0.227\log(E_3) - 0.839 \tag{2-5}$$

where E_2 = resiliment modulus of granular subbase material (in psi).

Other researchers also gave some empirical relationships for the determination of layer coefficients from resilient modulus of pavement materials. Following are some of the commonly used equations (Ullidtz 1987):

Asphalt concrete:

$$a_1 = 0.40 * \log\left(\frac{E}{3000\text{MPa}}\right) + 0.44 \qquad 0.20 < a_1 < 0.44 \tag{2-6}$$

Bituminous-treated base:

$$a_2 = 0.30 * \log\left(\frac{E}{3000\text{MPa}}\right) + 0.33 \qquad 0.10 < a_2 < 0.30 \tag{2-7}$$

Granular subbase:

$$a_3 = 0.23 * \log\left(\frac{E}{160\text{MPa}}\right) + 0.15 \qquad 0.06 < a_2 < 0.20 \tag{2-8}$$

Since structural layer coefficients are affected by many factors, such as material type and properties, type of layer, traffic level, and failure criterion, many researchers

believe that using the resilient modulus alone is not sufficient for the determination of layer coefficient values. Actual pavement damage, such as permanent deformation (rutting) and fatigue cracking, must be taken into account in order to formulate a layer coefficient that can reflect actual pavement behavior. In the 1986 AASHTO design guide, three failure criteria were used to determine layer coefficients based on the mechanistic response to traffic loads:

- Surface deflection,
- Tensile strain in the asphalt layer, and
- Vertical compressive strain on the roadbed soil.

Using the layered elastic theory, a wide range of surface layer thickness (D_1) and base layer thickness (D_2) were employed to calculate deflection, tensile strain, and vertical compressive strain. The results were then used to evaluate the increase in base layer thickness for a decrease in the surface layer thickness while keeping the deflection or strain level constant.

2.3 Determination of Layer Coefficients with Falling Weight Deflectometer

The Falling Weight Deflectometer (FWD) test is one of the most commonly used methods to measure the in situ behavior of pavements. FWD devices apply an impact load on a 12 inches (300 mm) diameter circular plate to pavement surface and measure the resulting surface deflections through the sensors located at the loading center and at

various radii from the center. The deflection data usually need to be normalized to a standard load (generally 9000 pounds for highway) and a standard temperature (generally 68 °F). The set of deflections constitutes a bowl-shaped depression known as the deflection basin. The FWD test is relatively quick, inexpensive, and can closely simulate the deflection caused by a moving wheel load. Therefore it has been widely used to evaluate the pavement integrity and the structural capacity of pavements.

Numerous studies have been conducted to utilize FWD for pavement evaluation and material characterization (Hossain et al. 1997; Pologruto 2001; Janoo 1994; Bahia et al. 2000; Noureldin et al. 2005). In the AASHTO design guide, two procedures are recommended to determine layer coefficients from FWD deflections. The first procedure requires the backcalculation of pavement layer modulus and relating the backcalculated modulus to layer coefficients. The second procedure uses the outer deflection sensor to determine subgrade stiffness and then applies the peak deflection, D_0, to determine the structural number of pavements.

Hossain et al. (1997) utilized the FWD deflection data to determine the structural layer coefficients of crumb rubber-modified (CRM) asphalt concrete mixtures. They used three independent methods in the backcalculation process by modeling the pavements as multilayered elastic systems: (a) manual, using the ELSYM5 multilayer elastic analysis program; (b) an automated backcalculation program, MODULUS; and (c) a second automated method, BKCHEVM, developed by the U.S. Army Corps of Engineers and

later slightly modified at the Arizona State University. They also used two methods for computing structural layer coefficients of CRM asphalt mixes: the AASHTO design guide and the equal mechanistic approach, using the vertical compressive strain on top of the subgrade as the mechanistic response. In the AASHTO design guide approach, the equation provided in the AASHTO design guide was used to calculate the effective structural number as follows:

$$SN_{eff} = 0.0045 * D * E_p^{1/3} \quad (2\text{-}9)$$

where

SN_{eff} = structural layer coefficients for the surface, base, and subbase,

D = total thickness of all pavement layers above subgrade (in inches), and

E_p = effective modulus of the pavement layers above subgrade (in psi)

Since the layer thicknesses are known, layer coefficients can be calculated using Equation (2-2) from the structural number value found in Equation (2-9). Hossain et al. (1997) concluded that with the equal the layer coefficients for CRM asphalt mix overlays are lower than those for conventional asphalt concrete mixes. However, they also found that the layer coefficients for newly constructed CRM asphalt pavements are close to the design layer coefficient values used for conventional asphalt concrete layers.

Pologruto (2001) used similar procedure to obtain layer coefficients from the FWD data. In addition to Equations (2-2) and (2-9), Pologruto (2001) used a modified form of Boussinesq's basic deflection form for a semi-infinite half-space to backcalculate

the value of E_p as follows:

$$d_0 = 1.5pa\left(\frac{1}{M_R\sqrt{1+\left(\frac{D}{a}\sqrt[3]{\frac{E_p}{M_R}}\right)^2}}+\frac{\left(1-\frac{1}{\sqrt{1+\left(\frac{D}{a}\right)^2}}\right)}{E_p}\right) \quad (2\text{-}10)$$

where

d_0 = centerline deflection measured by the FWD (in inches),

p = loading plate pressure applied by the FWD (in psi),

a = loading plate radius (in inches),

D = depth of the pavement structure (in inches),

E_p = elastic modulus of the pavement structure (in inches), and

M_R = subgrade resilient modulus (in psi).

It is noted that the subgrade resilient modulus MR must be established by and independent backcalculation before Equation (2-10) can be used for the backcalculation of E_p. Pologruto (2001) found that the layer coefficients determined for unbound subbases were reasonable, whereas layer coefficients estimated for asphalt concrete materials were generally 25 to 35 percent higher than the AASHTO implied maximum of 0.44. However, a statistical analysis indicated considerable support for the predictive qualities of FWD-derived layer coefficients to approximate the in situ layer coefficients

estimated by an elastic layer simulation.

Janoo (1994) used an FWD to measure the deflections on the subgrade and on the top surface of various pavement materials. Layer moduli were backcalculated for these materials and then layer coefficients were computed using several methods, including the correlation between modulus-layer coefficient given in the AASHTO design guide, a procedure recommended by the World Bank, and two methods correlated to the penetration test results.

2.4 Determination of Layer Coefficients with Probabilistic Fatigue Model

George (1984) developed a probability-based fatigue model to derive the structural layer coefficients for several Mississippi pavement materials – surface mixture and base mixture of asphalt concrete, soil-cement, and soil-lime. In this model, traffic load, environment, and subgrade support were regarded as random variables and the inherent uncertainty in these parameters can be taken into account in the fatigue design algorithm.

Although there are three specific distress modes commonly used for the evaluation of pavement performance (fatigue cracking, permanent deformation or rutting, and low-temperature cracking), fatigue cracking is considered the most prevalent type of pavement distress in the United States and justified in the fatigue-life model for the determination of layer coefficients. According to the fatigue model, the material

properties related to layer coefficients are (George 1984):

- Elastic constants, such as resilient modulus and Poisson's ratio
- Fatigue susceptibility expressed in the ε-N diagram.

The structural layer coefficients are determined with the probabilistic fatigue model in two steps. In the first step, an analytical model was developed for predicting the life flexible pavements. In the second step, the "layer equivalence" between different pavement materials and layer coefficients for pavement layers were obtained from the developed model. In order to develop the fatigue life prediction model, a combination of mechanistic and empirical procedures was utilized. It was hypothesized that fatigue cracking is a function of the primary structural response of the pavement (tensile strain at the bottom of base layer) induced by traffic load. This primary structural response can be calculated with a multilayer elastic analysis program. The fatigue life was predicted using the empirical relationship proposed by Hwang and Witczak (1979). The Palmgren-Miner hypothesis of linear damage accumulation was also used for predicting the cumulative fatigue damage caused by mixed traffic loads. Using the developed fatigue model along with the stipulation that fatigue cracking in the wheel paths be less than 45%, George (1984) established the "thickness equivalency" between different pavement layers and hence derived the layer coefficient values. The derived layer coefficients with the model compared satisfactorily with the values proposed in the AASHTO design guide.

Although the inputs are random variables, the resutlsing model equation is

deterministic and amenable to direct solution to the analysis and design of flexible pavements.

CHAPTER 3 RESEARCH METHODOLOGY

3.1 Introduction

This chapter provides information on the type of materials and procedures for the preparation of the HMA samples in the laboratory. Also presented is a summary of the testing procedures and instrumentation used to evaluate the viscoelastic properties, permanent deformation (rutting) characteristics, fatigue cracking characteristics, and resilient properties of asphalt mixtures.

3.2 Materials

The asphalt mixtures used in this study are field collected mixes from 16 locations within the state of Tennessee (Table 3-1). Mixtures were sampled by the University of Tennessee students from dump trucks as they exited asphalt plants. The mixes were placed in 5 gallon steel buckets for ease of handling and transferred back to UT facilities for storage (Figure 3.1). Once acquired, mixtures were only allowed to be reheated once for specimen compaction to avoid stiffening of the mixture. All mixtures meet Tennessee Department of Transportation (TDOT) specifications for 411-D surface mixtures or 307 BM-2, A, or A-S criteria for base mixtures.

Table 3-1 Collected HMA Mixtures

No.	Mixtures
1	411D Limestone PG 64-22
2	411D Limestone PG 70-22
3	411D Limestone PG 76-22
4	411D Gravel PG 64-22
5	411D Gravel PG 70-22
6	411D Gravel PG 76-22
7	411D Granite PG 64-22
8	BM-2 Limestone PG 64-22
9	BM-2 Limestone PG 70-22
10	BM-2 Limestone 76-22
11	BM-2 Gravel PG 82-22
12	A Limestone PG 70-22 (Knoxville)
13	A Limestone PG 70-22 (Davidson)
14	A Limestone PG 76-22
15	AS Limestone PG 70-22 (Knoxville)
16	AS Limestone PG 70-22 (Nashville)

3.2.1 Types of HMA Mixtures

3.2.1.1 411-D Surface Mixtures

Surface mixtures are addressed in Section 411-Asphaltic Concrete Surface (Hot Mix) of the 2006 TDOT Materials Specifications. Three coarse aggregate (D-rock) types were used for evaluation of surface mixes; limestone, gravel, and granite at a maximum aggregate size of ½" for all mixtures. The fine aggregate used in the surface mixes consisted of natural sand and #10 screenings. Only the gravel mixtures contained RAP.

Figure 3.1 Field Collection of HMA Samples

Three types of asphalt binder were used in the study, unmodified asphalt meeting Superpave specifications for PG64-22, and modified asphalts meeting the specifications for both PG70-22 and PG76-22. Asphalt contents of all limestone mixtures were verified to be approximately 5.3%. The gravel mixtures showed much variability in the asphalt content. Mixtures containing PG64-22 binder were tested to show an asphalt content of 5.7%, however the modified binder contents were higher with the PG70-22 and PG76-22 mixtures possessing contents of 6.0% and 6.3% respectively.

3.2.1.2 307 BM-2 Base Mixtures

Base mixtures are addressed in Section 307-Bituminous Plant Mix Base (Hot Mix) of the 2006 TDOT Materials Specifications. Two coarse aggregate types were used for evaluation of BM-2 mixes; limestone and gravel at a maximum aggregate size of ¾" for all mixtures. The fine aggregate used in the surface mixes consisted of #7 stone and #10 screenings. All mixtures contained 20-25% RAP.

Four types of asphalt binder were used in the study, unmodified asphalt meeting Superpave specifications for PG64-22, and modified asphalts meeting the specifications for PG70-22, PG76-22, and PG82-22. Asphalt contents of all limestone mixtures were verified to fall within 4.2% to 4.5%. The gravel mixture had 5.5% asphalt content.

3.2.1.3 307 A and 307 A-S Base Mixtures

307 A and 307 A-S mixtures are also addressed in Section 307 of the TDOT Material Specifications. They differ from a BM-2 mix in that they typically have a larger maximum aggregate size and lower asphalt content. The two mix types differ from one another in that (1) A-S mixes do not allow for the inclusion of RAP and typically exhibit higher asphalt contents; (2) A-S mixes have more air voids and are usually used as drainage layer. Only limestone was evaluated as a coarse aggregate in the study of A and A-S mix types, with a maximum aggregate size of 1 ½" for all mixtures.

Only modified asphalts meeting the specifications for PG70-22 and PG76-22

were used in this study. Asphalt contents of all A type mixes were verified to fall within 3.8% to 4.2%. The A-S type mixtures had 3.0% to 3.6 % asphalt content.

3.2.2 Specimen Preparation

To ensure the quality of each specimen prepared for testing, great care was given to maintain a consistent compaction process. The stored asphalt mixtures were reheated in a force draft oven at 160ºC (320ºF) for 2 hours before compaction.

Two different methods of compaction were used in this study. Beam specimens were compacted with the aid of a vibratory compactor, while 6-inch cylindrical specimens were compacted with a Superpave gyratory compactor (SGC). For the dynamic modulus and flow number tests, once the cylindrical specimens were compacted and allowed to cool they were cored into specimens 100 mm (4 in) in diameter and cut to a final height of 150 mm (6 in.) with a wet blade saw (Figure 3.2). For the other tests, a wet blade saw was also used to cut specimens into their respective sizes. Sawing operations were performed carefully to ensure the ends maintained absolute parallelism.

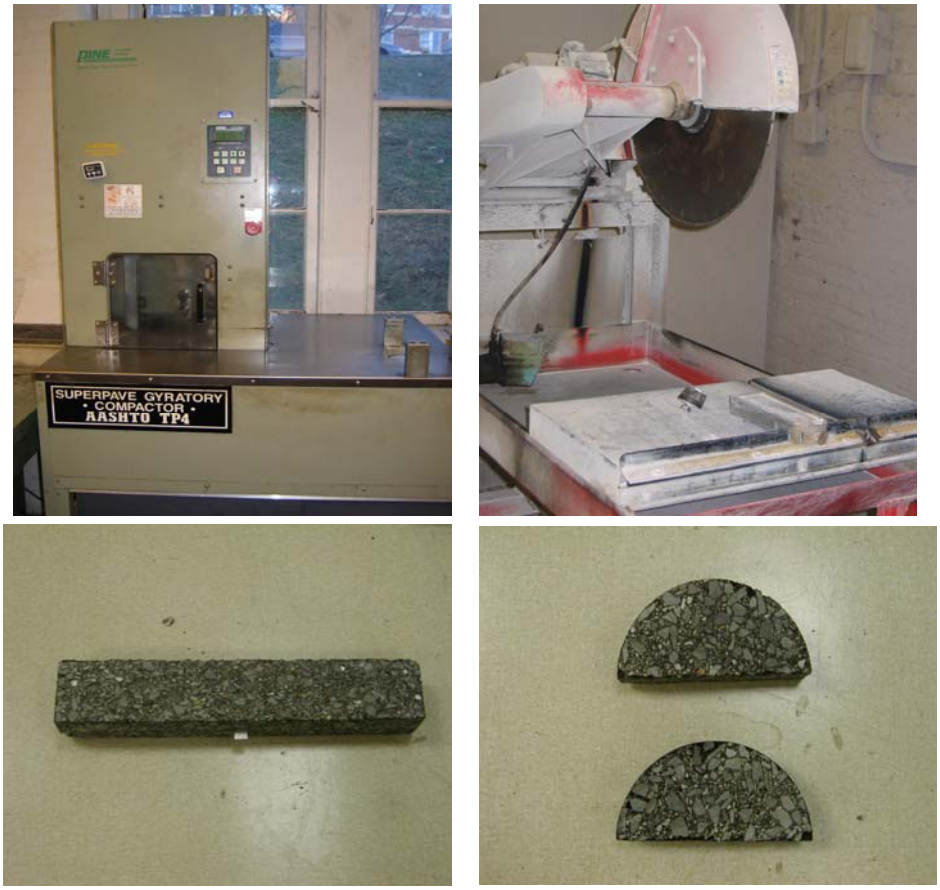

Figure 3.2 Sample Preparation

All of the pills (round gyratory specimens) were compacted to a 4±0.5 percent air voids except that the pills for APA tests were compacted to 7±1 percent air voids. All beam specimens were compacted to 6±1 percent air voids. Prior to testing, all samples were checked for air voids in accordance with AASHTO T-269, *Percent Air Voids in Compacted Dense and Open Bituminous Paving Mixtures*, to validate proper air void requirements. If any specimen was outside the specified air void range, the specimen was discarded and replaced with new one. Specimens that did meet the air void criteria were

stored at 25 °C before testing (Figure 3.3). Table 3-2 presents the HMA mixtures collected and the specimens prepared.

Figure 3.3 Prepared Cylindrical Specimens

Table 3-2 HMA Mixtures Collected and Specimens Prepared

No.	Mixtures	Mix Performance Tests					
		Dynamic Modulus	APA	Creep	IDT	Beam Fatigue	SCB Fracture
1	411D Limestone PG 64-22	3	6	3	3	3	12
2	411D Limestone PG 70-22	3	6	3	3	3	12
3	411D Limestone PG 76-22	3	6	3	3	3	12
4	411D Gravel PG 64-22	3	6	3	3	3	12
5	411D Gravel PG 70-22	3	6	3	3	3	12
6	411D Gravel PG 76-22	3	6	3	3	3	12
7	411D Granite PG 64-22	3	6	3	3	3	12
8	BM-2 Limestone PG 64-22	3	6	3	3	3	12
9	BM-2 Limestone PG 70-22	3	6	3	3	3	12
10	BM-2 Limestone 76-22	3	6	3	3	3	12
11	BM-2 Gravel PG 82-22	3	6	3	3	3	12
12	A Limestone PG 70-22 (Knoxville)	3	6	3	3	3	12
13	A Limestone PG 70-22 (Davidson)	3	6	3	3	3	12
14	A Limestone PG 76-22	3	6	3	3	3	12
15	AS Limestone PG 70-22 (Knoxville)	3	6	3	3	3	12
16	AS Limestone PG 70-22 (Nashville)	3	6	3	3	3	12

3.3 Test Methods

3.3.1 Dynamic Modulus Test ($|E^*|$)

Although first developed in the 1960's through the work of Coffman and Pagen, the dynamic modulus test has gained great acceptance in recent years due to its emphasized inclusion as a choice test in the 2002 AASHTO M-E Design Guide. The current test protocol is a variation of the standard procedure ASTM D3496 with suggestions set forth by Witczak et al. at Arizona State University. The stress-strain relationship for viscoelastic materials, such as asphalt mixes, under continuous sinusoidal

loading can be defined by a complex number, E* (Pellinen and Witczak, 2002). The dynamic modulus test was used to characterize this mechanical relationship in all 16 asphalt mixtures presented in the test matrix of Chapter 1. The dynamic modulus test is a strain controlled test performed as a 100 mm (4 inch) diameter, 150 mm (6 inch) tall cored cylindrical specimen is subjected to a continuous haversine axial compressive load. The test is performed over a range of loading frequencies (25, 20, 10, 5, 2, 1, 0.5, and 0.1 Hz) and temperatures (10, 25, and 54.4ºC) and may or may not be subject to triaxial confining pressure. For research purposes at the University of Tennessee-Knoxville, tests were conducted in triplicate at each temperature with confining stresses of 0 kPa (0 psi), 103.5 kPa (15 psi), and 207.0 kPa (30 psi).

Asphalt mixtures exhibit visco-elastic material behavior. Purely elastic materials exhibit their strain response to applied stress in phase, that is to say they perfectly correspond with no time lag. A purely viscous material exhibits a 90º lag in strain to applied stress; this lag is known as phase angle (δ) and characterizes the extent to which a material is elastic or viscous. Materials exhibiting properties of both elasticity and viscosity have a phase angle falling between the two extremes and are known as visco-elastic materials. Because of this visco-elastic behavior, asphalt mixtures will demonstrate both a storage and loss (dissipation) of energy. Figure 3.4 graphically represents this general behavior.

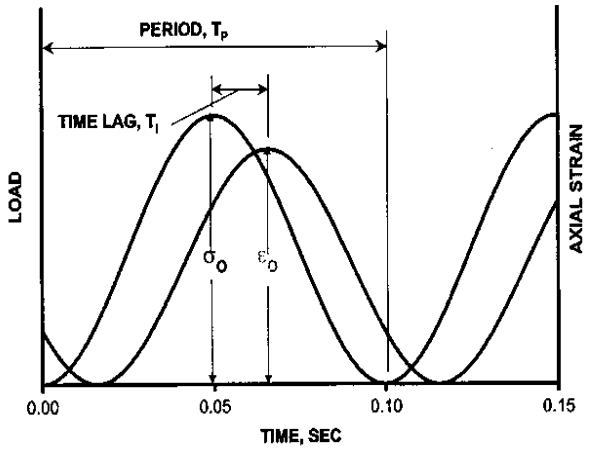

Figure 3.4 Typical Dynamic Modulus Loading and Response

The resulting evaluative material property, $|E^*|$, is defined as the ratio of the amplitude of the sinusoidal stress of pulsation ω applied to the material $\sigma = \sigma_0 \sin(\omega t)$ and the amplitude of the sinusoidal stain $\varepsilon = \varepsilon_0 \sin(\omega t - \delta)$ that results in a steady state:

$$E^* = \frac{\sigma}{\varepsilon} = \frac{\sigma_o e^{i\omega t}}{\varepsilon_o e^{i(\omega t - \delta)}} \tag{3-1}$$

The modulus of this complex number E* is the dynamic modulus $|E^*|$, where σ_o is the stress amplitude and ε_o is the recoverable strain amplitude:

$$|E^*| = \frac{\sigma_o}{\varepsilon_o} \tag{3-2}$$

The Simple Performance Tester (SPT), manufactured by IPC Global of Australia, was used to perform the test. The SPT is a digital servo hydraulic control testing machine equipped with a continuous electronic control and data acquisition system (CDAS). The cored cylindrical samples are placed within the machine and affixed with three radially

mounted linear variable displacement transducers (LVDT). The LVDTs measure displacements across a 70 mm gauge length. Rubber latex membranes are used for triaxial testing. Figure 3.5 shows the test set up within the SPT.

Figure 3.5 Typical Dynamic Modulus Test Setup

Test results were evaluated in comparison with two other tests, the flow number test and the Asphalt Pavement Analyzer (APA), to determine their ability to characterize the permanent deformation characteristics of Tennessee asphalt mixtures. The key rutting parameter is defined as $E^*/\sin\delta$ at 54.4ºC and 5 Hz as established by Witczak et al (2002). However, the same rutting parameter has been used at 10 Hz because the 0.1 second loading time in the laboratory more closely represents the actual traffic loading time in the field (Zhou and Scullion 2003). Both methods were examined in this research. Figure

3.6 represents graphically results from the dynamic modulus test.

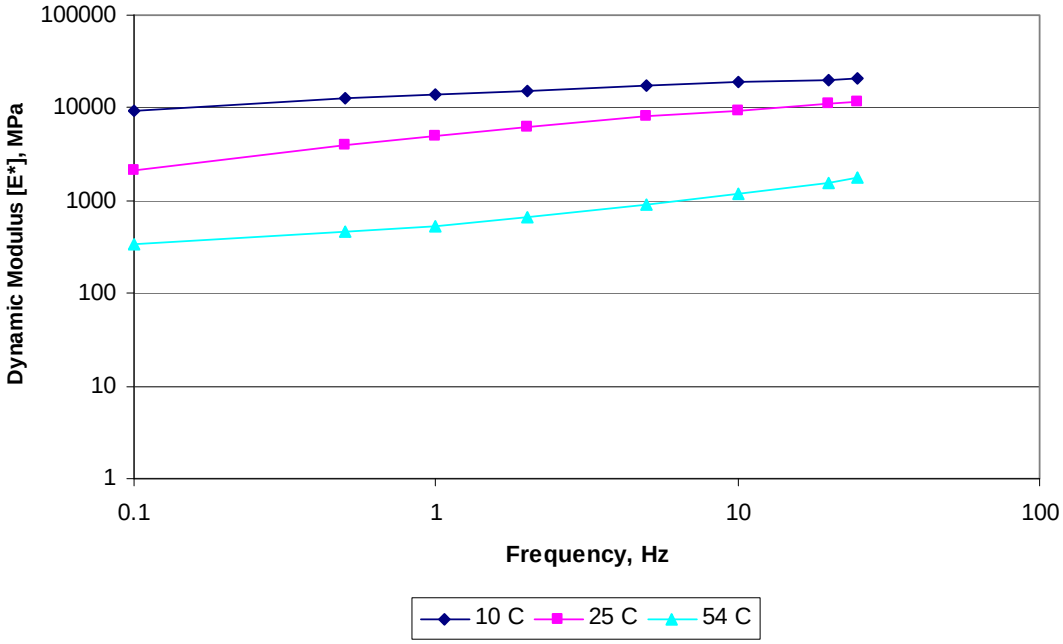

Figure 3.6 Typical Dynamic Modulus Test Results

3.3.2 Flow Number Test (F_N)

The flow number test (F_N) is a repeated-load permanent deformation test used to evaluate the creep characteristics of HMA as related to permanent deformation. The test followed recommended procedures as outlined in NCHRP 9-19 with adopted test parameters as conducted by the Louisiana Transportation Research Center (LTRC) (Mohammad et al. 2005). Tests were performed by applying a uniaxial compressive load to a 100 mm (4 inch) diameter, 150 mm (6 inch) tall cored cylindrical specimen. The compressive load is applied in haversine form with a loading time of 0.1 seconds and a

rest duration of 0.9 seconds for a maximum of 10,000 cycles or until a deformation of 50,000 microstrain is reached. The specimen is tested at 54ºC which closely matches the average maximum effective pavement temperature for the state of Tennessee as determined by LTTPBind Version 2.1 software. Flow number testing was performed in triplicate at both 0 kPa (0 psi) and 103.5 kPa (15 psi) confining pressure states. Because the dynamic modulus test is considered non-destructive, the samples were reused in the unconfined flow number evaluation. New specimens were made for the confined pressure test.

Permanent strain of samples used in flow number evaluation demonstrates itself in three distinct stages. The primary zone is a period of rapid strain accumulation at the beginning of the test. The primary zone is followed by the secondary zone which is identifiable by a constant accumulated strain rate. As the secondary zone continues and the pavement structure breaks down there is eventually a jump to the tertiary zone, marked by an increase in strain rate. The point at which the permanent strain rate is at its minimum and tertiary flow begins is noted as the flow number for that mixture. Figures 3.7 and 3.8 graphically demonstrate this progression of permanent strain.

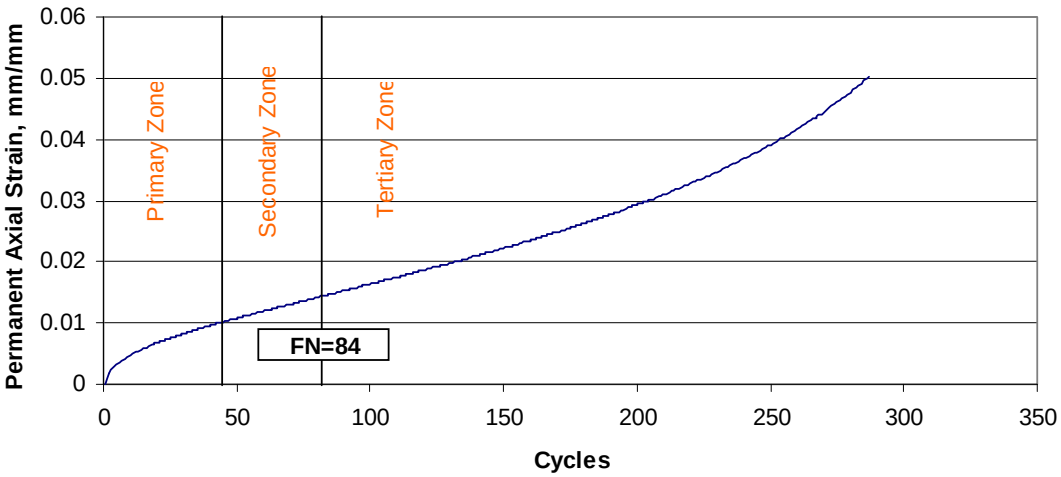

Figure 3.7 Typical Accumulation of Permanent Strain in Flow Number Test

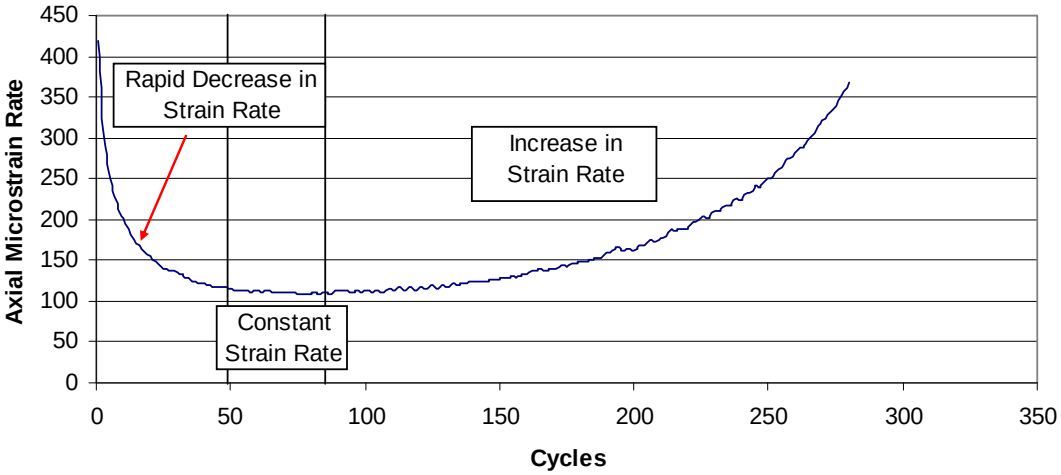

Figure 3.8 Typical Accumulation of Permanent Strain Rate in Flow Number Test

The same SPT used in the dynamic modulus testing is used for flow number testing with exclusion of the previously mentioned LVDTs. Permanent deformations are measured internally by the displacement of the load frame. The CDAS processes

accumulated strain to a strain rate by the following formula:

$$\frac{d\delta i}{dt} \cong \left(\delta_{i+\Delta n} - \delta_{i-\Delta n}\right) / 2\Delta n \qquad (3\text{-}3)$$

where: dδi/dt = strain rate at logged datum "i" (cycle or second);

$\delta_{i+\Delta n}$ = strain at i+Δn samples;

$\delta_{i-\Delta n}$ = strain at i-Δn samples; and

Δn = sampling interval.

The derivatives are smoothed to ensure proper calculation of the minimum strain rate by determining a running average at each point. This eliminates the effects of jumps in the data which may cause anomalies. Two points before and after and also the point in question are summed and then divided by 5.

$$\frac{d\delta i}{dt} \cong \left(\delta_{i-2\Delta n} / dt + \delta_{i-\Delta n} / dt + \delta_i / dt + \delta_{i+\Delta n} / dt + \delta_{i+2\Delta n}\right) / 5 \qquad (3\text{-}4)$$

Data is then analyzed on a comparative basis. Mixtures with higher flow numbers are more stable mixes which should exhibit less permanent deformation in field conditions than mixes with lower flow numbers which are deemed as poorer quality mixes. The collected data is also compared to the previously mentioned rutting parameter from the dynamic modulus test and APA rut depth.

3.3.3 Asphalt Pavement Analyzer (APA)

The APA (Figure 3.9) is an empirical wheel loaded device producing pavement distress by continuously loading 6 identical 150 mm (6in) diameter, 75 mm (3 in) tall

specimens with an inflatable hose and roller. The test is conducted at the temperature of 64 ºC (147.2 ºF) and at the hose pressure of 0.7 MPa for a maximum of 8,000 cycles. The resulting average rut depths are continually recorded. The APA will be used in this study to judge the effectiveness of the dynamic modulus and flow number test to predict the rutting potential of HMA.

Figure 3.9 Asphalt Pavement Analyzer

3.3.4 Superpave IDT Tests

The Superpave IDT tests include the resilient modulus, creep and indirect tensile strength tests and they were conducted according to the procedures developed by Roque and Buttlar (1992) and Buttlar and Roque (1994). Figure 3.10 shows the test setup of the

Superpave IDT tests. The testing system and associated analysis procedures are described in detail by Roque and Buttlar (1992) and Buttlar and Roque (1994).

(a) Without strain gages (b) With strain gages

Figure 3.10 Superpave IDT Test Setup

3.3.4.1 Resilient Modulus Test

The resilient modulus test was performed on the cylindrical samples by applying a repeated peak-load resulting in horizontal deformations within the range of 200-300 microstrains. Each load cycle consists of 0.1-second load application followed by a 0.9-second rest period. The load and deformation were continuously recorded and resilient modulus can be calculated as follows:

$$M_R = \frac{P \times GL}{\Delta H \times t \times D \times C_{cmpl}} \qquad (3\text{-}5)$$

where, M_R = resilient modulus;

P = maximum load;

GL = gage length;

ΔH = horizontal deformation;

t = thickness of specimen;

D = diameter of specimen;

C_{cmpl} = nondimensional creep compliance factor, $C_{cmpl} = 0.6354(X/Y)^{-1} - 0.332$;

(X/Y) = ratio of horizontal to vertical deformation.

3.3.4.2 Creep Test

The creep compliance test was performed on the same specimen used for the resilient modulus test. After allowing the specimen to re-stabilize (5 to 10 minutes) the creep compliance test was performed. During this test the specimen was loaded with a constant load for 1000 seconds. The constant load was chosen such that it produced a horizontal deformation within the range of 200 – 750 microstrains after 1000 seconds of loading. The creep compliance was calculated as follows:

$$D(t) = \frac{\Delta H \times t \times D \times C_{cmpl}}{P \times GL} \tag{3-6}$$

where $D(t)$ = creep compliance at time t;

P, GL, ΔH, t, D, C_{cmpl}, (X/Y) are the same as described above.

The creep compliance $D(t)$ can be represented using the following power function

(Figure 3.11):

$$D(t) = D_0 + D_1 t^m \qquad (3\text{-}7)$$

where D_0, D_1 and m = parameters obtained from the creep test.

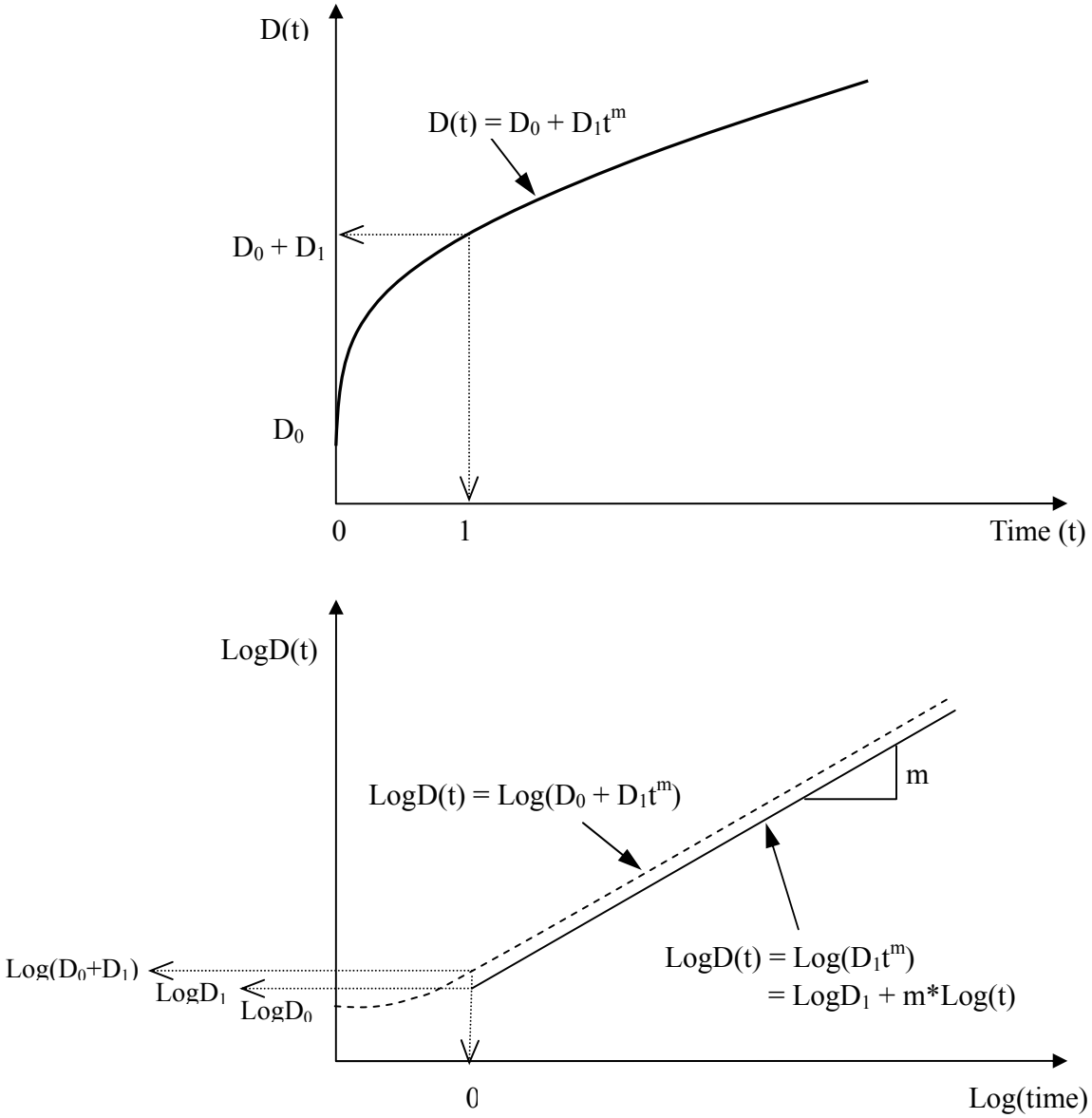

Note: D(t) = Creep compliance at time, t ; D_0, D_1, m = Power model constants

Figure 3.11 Power Model of the Creep Compliance

With these two parameters, D_1 and m, a new term, $DCSE_{min}$, which is the minimum dissipated creep strain energy, was proposed by Roque et al. to characterize the cracking performance of HMA mixtures. $DCSE_{min}$ is expressed as follows:

$$DCSE_{min} = \frac{m^{2.98} \times D_1}{A} \tag{3-8}$$

The parameter A is a function of tensile strength and tensile stress in the asphalt pavement as follows:

$$A = 0.0299\sigma_t^{-3.10}(6.36 - S_t) + 2.46 \times 10^{-8} \tag{3-9}$$

where σ_t = applied tensile stress of asphalt layer;

S_t = indirect tensile strength.

3.3.4.3 Indirect Tensile Strength Test

The IDT strength test was used to determine tensile strength and strain of the mixture specimens compacted to $4 \pm 1\%$ air voids. Cylindrical specimens with 152.4 mm diameter and 50.8 mm thickness were monotonically loaded to failure along the vertical diametric axis at the constant rate of 76.2 mm/min. The indirect tensile strength can be calculated as follows:

$$S_t = \frac{2 \times P \times C_{sx}}{\pi \times t \times D} \tag{3-10}$$

where S_t = indirect tensile strength;

P = failure load;

C_{sx} = horizontal stress correction factor;

$$C_{sx} = 0.948 - 0.01114 \times (t/D) - 0.2693 \times \nu + 1.436 \times (t/D) \times \nu$$

ν = Poisson's ratio, $\nu = -0.1 + 1.480 \times (X/Y)^2 - 0.778 \times (t/D)^2 \times (X/Y)^2$

t, D, (X/Y) are the same as described above.

With the stress strain response from the IDT strength test, the dissipated creep strain energy threshold ($DCSE_f$) was determined by Roque et al. as follows (Figure 3.12):

$$DCSE_f = FE - EE \tag{3-11}$$

where, FE = fracture energy; it is defined as the area under the stress strain curve to the failure strain ε_f, and EE = elastic energy.

$$FE = \int_0^{\varepsilon_f} S(\varepsilon) d\varepsilon \tag{3-12}$$

$$EE = \frac{1}{2} S_t (\varepsilon_f - \varepsilon_0) \tag{3-13}$$

where ε_0 can be found in Figure 3.12.

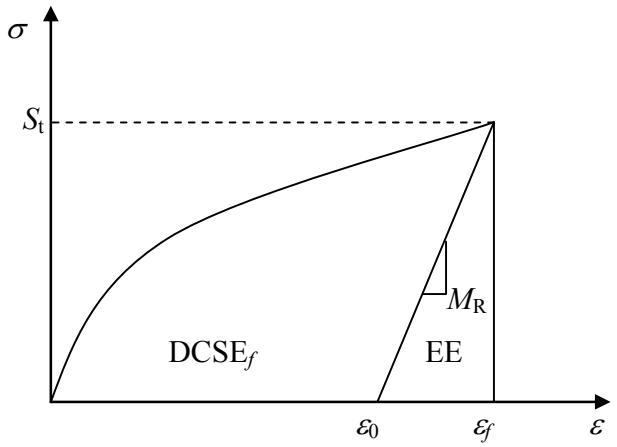

Figure 3.12 Determination of creep strain energy threshold ($DCSE_f$)

With $DCSE_f$ and $DCSE_{min}$, Energy Ratio (ER) was defined as follows (Roque et al., 2004):

$$ER = \frac{DCSE_f}{DCSE_{\min}} \tag{3-14}$$

3.3.5 Beam Fatigue Test

This test was developed under the Strategic Highway Research Program (SHRP) A-003A to evaluate the fatigue response of asphalt paving mixtures and to summarize what is known about the factors that influence pavement life using third point loading. The Flexural Beam Fatigue Test was later modified in SHRP-A-404 to improve the simplicity and reliability of the fatigue test. The Flexural Beam Fatigue test is a strain controlled test to determine the fatigue life of 15 in. long by 2 in. thick by 2.5 in. wide beam specimens sawed from laboratory compacted samples subjected to repeated flexural bending until failure (AASHTO T321-03).

Beam specimens were compacted using the vibratory compactor to 7±1 percent air voids and tested at 25°C according to AASHTO T321-03. Specimens were placed in a beam fatigue fixture (Figure 3.13) that would allow 4-point bending with free rotation and horizontal translation at all load and reaction points using a MTS closed loop computer controlled data acquisition system.

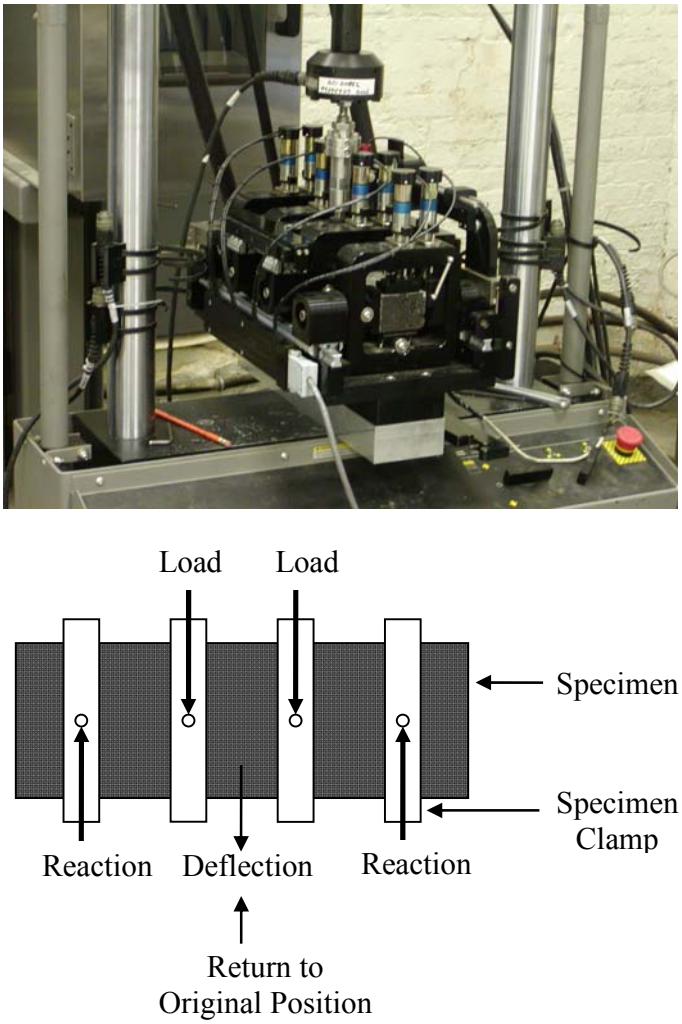

Figure 3.13 Beam fatigue fixture

A strain level of approximately 600 microstrain and a loading frequency of 10 Hz were used such that the specimen will undergo a minimum of 10,000 load cycles. During each load cycle beam deflections were measured at the center of the beam to calculate maximum tensile stress, maximum tensile strain, phase angle, stiffness,

dissipated energy, and cumulative dissipated energy. Figure 3.14 represents a typical stiffness versus load cycle plot using automated fatigue software.

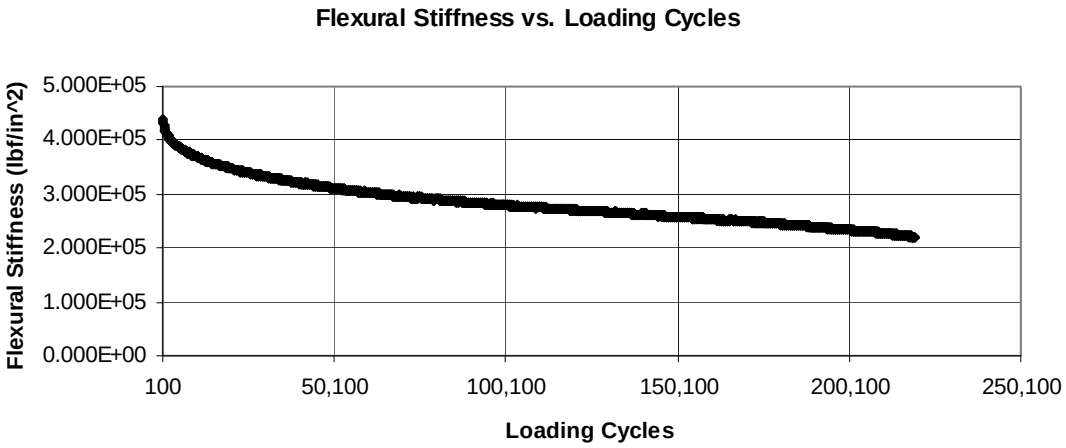

Figure 3.14 Flexural stiffness vs. loading cycles

For the beam fatigue test, fatigue life is traditionally defined as the number of cycles corresponding to a 50 percent reduction in initial stiffness and initial stiffness was measured at the 50th load cycle (AASHTO T321-03). Recently, Carpenter et al. proposed to use RDEC to determine the fatigue life (Ghuzlan and Carpenter 2000; Carpenter et al. 2003; Shen and Carpenter 2005). Figure 3.15 presents a typical RDEC plot. As seen from Figure 3.15, the curve can be divided into three different zones. RDEC value decreases with the load cycle in zone 1. RDEC value is approximately constant in zone 2, representing a period where there is a constant percent of input energy turned into damage. In zone 3, RDEC value increases with the load cycle, indicating that more and

more input energy are turned into damage and ultimately the mixture loses the load carrying capability.

A Plateau Value (PV), or the nearly constant value of RDEC, can be determined and it represents a period where there is a constant percent of input energy being turned into damage. This PV can be used to characterize the fatigue life of HMA mixtures. For a strain-controlled test, the lower the PV, the longer the fatigue life for a specific HMA mixture (Shen and Carpenter, 2005).

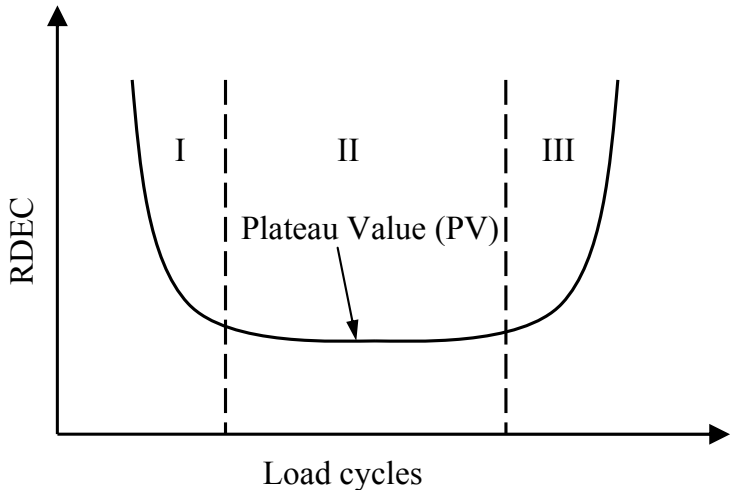

Figure 3.15 Typical RDEC plot with three behavior zone

3.3.6 Semi-Circular Bending (SCB) Test

The semi-circular bending (SCB) test can be used to obtain information on the tensile characteristics and fracture resistance of asphalt mixtures. This simple test is mostly used

in Europe and South Africa and can be performed on any loading frame that is capable of applying monotonic or dynamic loading (Molenaar et al. 2002 and Van de Ven et al. 1997). Figure 3.16 shows a typical setup of an SCB test. A three-point SCB test fixture was fabricated for easy attachment to both the load frame and load cell. The distance between the supports (2a) at the bottom is 4-inches (100mm). The test specimens were produced by means of the Superpave gyratory compactor. Once compacted, the 6-inch (150-mm) diameter cylindrical specimens were cut in half and than sliced into 1-inch (25-mm) thick specimens for testing. Testing was done on triplicate short-term and long-term aged specimens at a temperature of 77°F (25°C). The long-term aged specimens were placed in a forced draft oven and subjected to 85°C for five days.

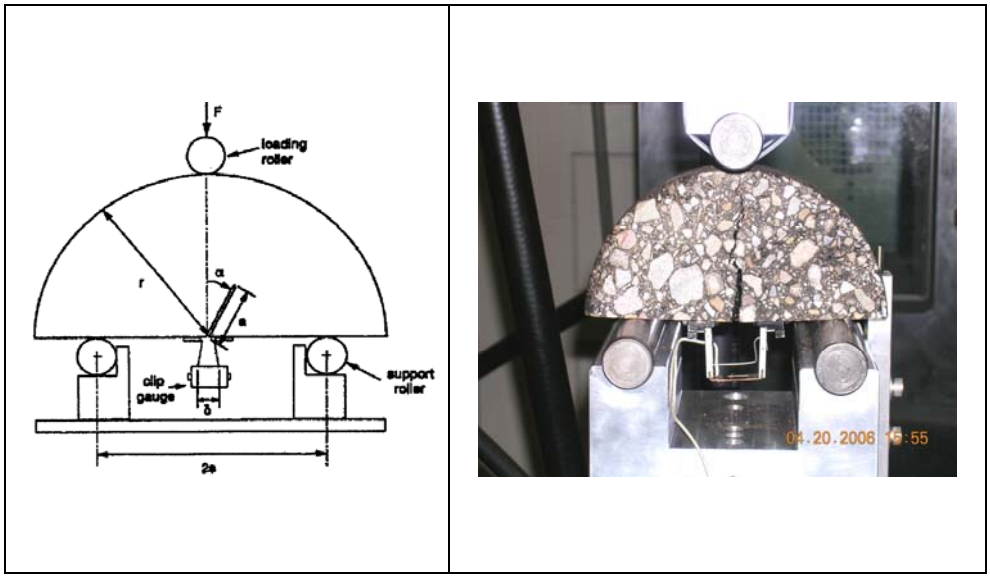

δ – Gage Length of the Strain Gage

Figure 3.16 Typical SCB Setup

3.3.6.1 SCB Tensile Strength Test

In this study the SCB test was used to determine tensile characteristics for HMA mixtures. Similar to the IDT test, the SCB test was set up for monotonic loading where the specimen was loaded at a constant rate of 2 in./min. (50 mm./min.) until failure occurred. Load (F) and deformation (δ) at the bottom of the specimen were continuously recorded during the testing. The deformation of the tested specimens was collected using strain gages mounted at the bottom of the specimens, Figure 3.16. The big advantage of the SCB test over the IDT test is that in the SCB a nice crack develops, without wedging near the loading strip, that helps characterize the tensile characteristics of the mixture (Van de Ven et al., 1997).

Analytical solutions for the SCB test can be accomplished through the proper application of loading and supporting conditions to the constitutive equations of the asphalt mixture. However, even the linear elastic solution between the load and bottom deflection requires complicated mathematical derivation (Van de Ven et al., 1997).
Huang et al. (2004) used the following equation to evaluate the properties of the asphalt RAP mixtures:

$$\sigma_x = 3.564 * \frac{P_{ult}}{D * t} \qquad (3\text{-}15)$$

where, σ_x = maximum tensile stress at the bottom of the specimen;

P_{ult} = load per unit width of the specimen at failure;

D = diameter of specimen; and

t = thickness of specimen.

It should be noted that equation (11) above is only valid if the distance between the two bottom supports equals 0.67 times of the diameter of specimen. The TI parameter used to analyze IDT specimens fatigue properties was also used for the analysis of the toughening characteristics of SCB mixture specimens.

3.3.6.2 SCB Notched Fracture Test

Similar to the SCB test, the semi-circular notched fracture test was conducted at a constant displacement. This test has been used in the past by the researchers to evaluate the fracture resistance of the asphalt mixtures through J-integral (Mull et al. 2002). The first concept of J-integral was introduced by Rice in 1968. Rice defined a J-integral as a path-independent line integral obtained by integrating strain energy density, traction, and displacement along an arbitrary contour around the tip of the crack in counter clockwise direction (Rice 1968). Mull et al. 2002 has used the J-integral concept in the Fracture Resistance Characterization of Chemically Modified Crumb Rubber Asphalt Pavement study to characterize fracture resistance of the asphalt mixtures with different notch depths. He noted that at least two different notched depths should be used to calculate the J-integral, which represents the fracture energies of different notch depths.

Mull et al. (2002) used the following equation to calculate the J-integral:

$$J_c = \left(\frac{U_1}{b_1} - \frac{U_2}{b_2} \right) * \frac{1}{a_2 - a_1} \tag{3-16}$$

where, U = strain energy to failure (area underneath the load-deformation curve up to the peak load;

b = specimen thickness;

a = notch depth.

The subscripts 1 and 2 refer to different notch depths 1 and 2 respectively. Mull et al. (2002) noted that the J-integral value does not reflect the durability or fatigue lifetime of the asphalt mixture.

To increase the accuracy of a J-integral it was decided that three notched depths should be used for this study, 0.5 in. (12.5mm), 1.0 in. (25.4-mm), and 1.5 in. (38-mm). All of the semi-circular notched specimens were loaded monotonically on an MTS machine at a cross-head speed of 0.02 in/min (0.5-mm/min), as shown in Figure 3.17.

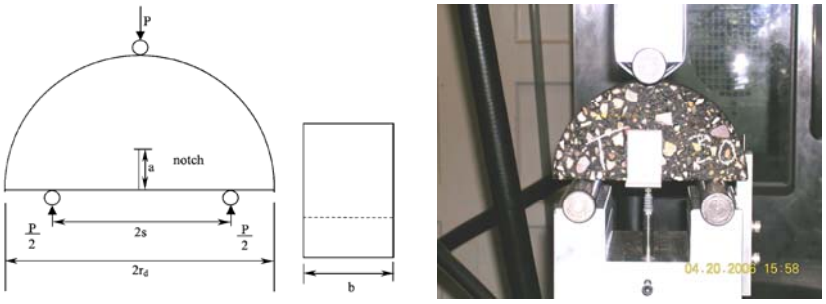

Figure 3.17 SCB Notched Fracture Test Setup

The load (P) was applied on the top of the specimen that was symmetrically supported by two rollers at the bottom with a span (2s) of 4 in. (100-mm), Figure 3.17. The bottom of the fixture was drilled through to create a hole used for mounting the LVDT to the bottom of the specimen so that the deflection on the bottom flat surface can be measured. Each specimen had a diameter ($2r_d$) of 6 in. (150-mm), and the thickness (b) was approximately 1in. (25.4-mm). The loading rate for the semi-circular notched specimens was chosen according to Mull et al. 2002. All of the semi-circular notched specimens were tested at ambient temperature of 25^{o}C.

Figure 3.18 presents a plot of fracture energy per unit thickness versus notched depth. The slope of the lines presented in Figure 3.19, is the fracture resistance J-integral. The fracture resistance consistently increases with the J-integral for any given mixture during the semi-circular notched test.

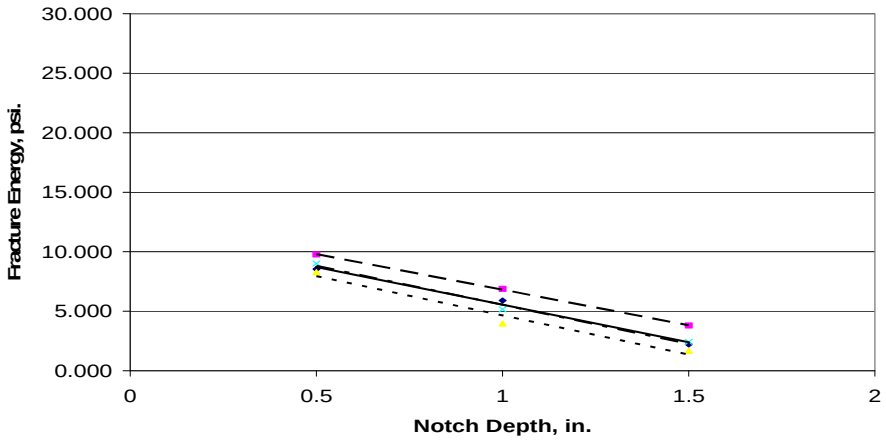

Figure 3.18 J-Integral for Different Notched Depths

CHAPTER 4 SUMMARY AND ANALYSIS OF LABORATIORY RESULTS

4.1 Introduction

This chapter provides a discussion of the laboratory HMA mixture testing results. Mixture properties obtained from the laboratory performance tests included dynamic modulus ($|E^*|$), flow number, APA rut depth, IDT resilient modulus (M_R), IDT creep compliance, IDT strength, toughness index (TI), dissipated creep strain energy threshold ($DCSE_f$), and parameters from the semi-circular bending test and beam fatigue test of HMA mixtures. At the end of this chapter, the layer structural coefficients (a_i) were determined for different HMA mixtures based on their properties.

4.2 Dynamic Modulus Test Results

4.2.1 411-D Asphalt Mixtures

Table 4.1 presents the average dynamic modulus ($|E^*|$) test results along with the corresponding phase angle (δ) for each "D-Criteria" TDOT mixture used in the study. Also presented in the tables are the standard deviation and coefficient of variability for each test set of 3 samples. Figure 4.1 graphically presents the effect of changing the asphalt cement PG grade on dynamic modulus and phase angle for each mixture. It should be noted that the samples tested are field collected mixes from an array of locations within the state of Tennessee; there is no effort to control aggregate source or

gradation in the comparison of results.

As the temperature increases and the loading frequency decreases, the dynamic modulus value decreases for each mixture type. By inspection of Table 4.1 results are seen to be highly repeatable with reasonable coefficients of variation except for select instances involving the 54.4ºC testing temperature.

Table 4.1 Summary of Dynamic Modulus Tests for 411-D Mixtures

(a) Dynamic Modulus (| E* |) Results at 0 kPa Confining Pressure

Mixture	Asphalt Cement	Coarse Agg	|E*| - Dynamic Modulus (Mpa)																									
			Temp	10C								25C								54.4C							
			Freq (Hz)	25	20	10	5	2	1	0.5	0.1	25	20	10	5	2	1	0.5	0.1	25	20	10	5	2	1	0.5	0.1
D	PG 64-22	Gravel	Avg.	16144	15747	14491	13216	11575	10386	9224	6730	7559	7259	6142	5186	4047	3286	2616	1403	1063	835	587	405	246	178	138	82
			STD	1783	1783	1725	1711	1678	1622	1523	1286	315	275	257	201	171	167	169	121	151	159	125	102	77	69	57	44
			%CV	11.0	11.3	11.9	12.9	14.5	15.6	16.5	19.1	4.2	3.8	4.2	3.9	4.2	5.1	6.5	8.6	14.2	19.0	21.3	25.1	31.1	38.7	41.7	54.2
		Limestone	Avg.	15862	15298	13697	12100	10092	8699	7349	4657	7793	7363	6054	4841	3518	2640	1930	866	604	450	321	226	142	95	79	50
			STD	491	524	468	375	311	268	224	131	316	286	252	259	201	169	125	65	48	37	26	19	16	18	16	12
			%CV	3.1	3.4	3.4	3.1	3.1	3.1	3.1	2.8	4.1	3.9	4.2	5.3	5.7	6.4	6.5	7.6	8.0	8.2	8.1	8.4	11.6	19.3	20.1	23.7
		Granite	Avg.	12803	12442	11327	10256	8848	7838	6848	4714	5823	5512	4604	3781	2836	2218	1709	839	651	480	328	227	132	85	65	35
			STD	15	34	93	126	133	132	133	121	418	403	346	296	238	195	156	79	61	63	41	33	20	16	13	6
			%CV	0.1	0.3	0.8	1.2	1.5	1.7	1.9	2.6	7.2	7.3	7.5	7.8	8.4	8.8	9.1	9.4	9.3	13.2	12.4	14.5	15.2	19.4	19.4	17.7
	PG 70-22	Gravel	Avg.	15116	14740	13602	12440	10935	9816	8710	6329	8197	7832	6760	5778	4601	3795	3073	1698	1000	776	539	370	222	149	113	60
			STD	901	865	863	836	794	755	697	573	333	316	301	268	207	182	150	109	114	97	68	48	28	20	13	6
			%CV	6.0	5.9	6.3	6.7	7.3	7.7	8.0	9.1	4.1	4.0	4.4	4.6	4.5	4.8	4.9	6.4	11.3	12.5	12.6	12.9	12.8	13.5	11.8	9.5
		Limestone	Avg.	16070	15672	14437	13195	11580	10333	9062	6306	6907	6526	5434	4454	3316	2579	1974	987	781	637	435	306	191	135	106	58
			STD	244	231	227	224	215	198	206	175	152	157	132	119	95	78	67	44	57	55	39	33	25	19	15	14
			%CV	1.5	1.5	1.6	1.7	1.9	1.9	2.3	2.8	2.2	2.4	2.4	2.7	2.9	3.0	3.4	4.5	7.3	8.6	9.1	10.7	13.1	14.2	14.2	23.9
	PG 76-22	Gravel	Avg.	12089	11821	10905	9993	8776	7867	6967	4994	6085	5798	4951	4167	3250	2641	2106	1139	711	545	399	284	177	120	97	53
			STD	375	399	384	366	352	342	303	208	559	523	464	406	329	274	228	130	69	65	46	30	16	12	8	6
			%CV	3.1	3.4	3.5	3.7	4.0	4.4	4.3	4.2	9.2	9.0	9.4	9.7	10.1	10.4	10.8	11.4	9.8	12.0	11.7	10.5	9.2	9.8	8.2	10.7
		Limestone	Avg.	18693	18148	16674	15171	13275	11859	10442	7380	8931	8494	7204	6012	4611	3695	2908	1584	923	765	542	391	256	183	152	98
			STD	1093	1051	960	914	780	696	583	441	262	252	259	257	245	220	195	148	30	18	10	4	1	3	1	2
			%CV	5.8	5.8	5.8	6.0	5.9	5.9	5.6	6.0	2.9	3.0	3.6	4.3	5.3	6.0	6.7	9.4	3.2	2.4	1.8	1.0	0.4	1.6	0.9	1.9

(b) Phase Angle (δ) Test Results at 0 kPa Confining Pressure

Mixture	Asphalt Cement	Coarse Agg	δ - Phase Angle																									
			Temp	10C								25C								54.4C								
			Freq (Hz)	25	20	10	5	2	1	0.5	0.1	25	20	10	5	2	1	0.5	0.1	25	20	10	5	2	1	0.5	0.1
D	PG 64-22	Gravel	Avg.	11.0	11.6	12.6	13.7	15.3	16.6	18.0	21.8	21.8	22.4	24.3	25.9	28.1	29.8	31.2	34.5	38.9	44.1	43.8	43.1	42.7	40.7	39.7	36.0
			STD	1.2	1.5	1.5	1.6	1.8	1.8	1.8	1.9	0.7	0.7	0.3	0.2	0.1	0.1	0.1	0.1	1.6	2.6	2.7	3.0	4.3	4.4	5.8	7.8
			%CV	10.9	13.1	11.6	11.9	11.6	11.0	10.2	8.8	3.1	3.1	1.3	0.9	0.4	0.5	0.4	0.3	4.1	5.8	6.2	7.1	10.0	10.9	14.6	21.7
		Limestone	Avg.	13.9	14.5	16.2	17.9	20.6	22.6	24.7	29.8	25.6	26.1	28.4	30.8	33.1	34.8	36.1	37.8	34.9	40.9	39.0	37.7	36.2	35.9	32.4	27.2
			STD	0.1	0.1	0.0	0.0	0.1	0.1	0.2	0.2	0.2	0.3	0.2	0.4	0.2	0.2	0.4	0.7	0.3	0.4	0.4	0.7	1.1	2.1	2.1	1.9
			%CV	0.9	0.7	0.1	0.1	0.4	0.5	0.7	0.5	1.0	1.0	0.8	1.4	0.5	0.5	1.0	1.8	0.7	1.0	1.0	1.7	3.0	6.0	6.6	7.1
		Granite	Avg.	11.6	11.7	13.1	14.4	16.3	17.9	19.7	24.3	23.6	24.3	26.3	28.2	30.6	32.3	33.6	36.4	37.8	44.5	44.0	43.2	42.9	42.3	39.3	34.5
			STD	0.2	0.3	0.2	0.2	0.1	0.2	0.1	0.0	0.7	0.8	0.9	1.0	1.1	1.1	1.0	0.7	0.6	0.8	0.8	1.1	1.4	1.4	1.6	2.7
			%CV	1.4	2.7	1.2	1.1	0.9	1.0	0.7	0.2	2.9	3.2	3.5	3.6	3.7	3.4	3.0	1.9	1.7	1.7	1.7	2.6	3.2	3.3	4.1	7.9
	PG 70-22	Gravel	Avg.	10.3	10.6	11.7	12.8	14.5	15.9	17.3	21.2	19.9	20.3	22.2	24.0	26.3	27.9	29.6	33.4	39.1	44.9	45.1	44.0	42.7	42.6	39.4	35.4
			STD	0.6	0.6	0.7	0.7	0.8	0.8	0.8	0.7	0.9	0.8	0.9	0.9	1.0	0.9	0.9	0.8	1.0	1.9	2.8	1.9	1.1	1.8	0.9	1.1
			%CV	5.5	5.3	5.6	5.6	5.3	5.1	4.7	3.3	4.5	4.0	4.2	3.9	3.7	3.1	3.0	2.5	2.6	4.3	6.2	4.4	2.5	4.2	2.3	3.1
		Limestone	Avg.	10.1	10.5	11.6	12.9	14.7	16.4	18.1	23.0	24.4	24.9	27.0	28.9	31.2	32.8	33.8	35.7	38.0	41.7	41.1	40.0	38.9	37.5	35.3	31.4
			STD	0.3	0.3	0.3	0.4	0.4	0.4	0.5	0.5	0.1	0.1	0.0	0.1	0.1	0.2	0.3	0.4	0.6	0.8	0.7	0.9	1.2	1.2	1.0	1.5
			%CV	2.9	2.7	3.0	2.9	2.8	2.7	2.6	2.0	0.6	0.4	0.1	0.2	0.5	0.7	0.8	1.0	1.6	1.8	1.8	2.2	3.1	3.2	2.7	4.8
	PG 76-22	Gravel	Avg.	10.6	10.9	12.0	13.1	14.7	16.2	17.8	21.8	21.3	21.9	23.7	25.5	27.7	29.3	30.7	33.4	36.7	42.5	41.3	40.5	39.5	38.8	36.2	32.3
			STD	0.2	0.2	0.2	0.3	0.3	0.2	0.3	0.3	0.4	0.5	0.5	0.6	0.6	0.7	0.7	0.6	0.7	0.8	1.0	1.0	0.9	0.9	1.1	5.4
			%CV	1.5	1.9	1.8	2.6	1.8	1.5	1.4	1.3	2.1	2.1	2.2	2.3	2.3	2.3	2.3	1.7	2.0	1.9	2.4	2.4	2.3	2.3	3.2	16.9
		Limestone	Avg.	10.5	11.0	12.3	13.7	15.6	17.2	18.9	23.5	22.2	22.6	24.4	26.1	28.3	29.6	30.7	32.0	36.3	39.3	38.3	36.9	35.1	34.4	32.0	28.1
			STD	0.2	0.2	0.3	0.2	0.3	0.4	0.4	0.5	0.7	0.7	0.8	0.8	0.9	1.0	1.2	2.3	0.3	0.4	0.5	0.5	0.4	0.2	0.4	0.5
			%CV	1.5	1.8	2.2	1.5	1.9	2.0	2.0	2.0	3.1	3.2	3.1	3.1	3.2	3.3	4.0	7.1	0.7	1.1	1.4	1.4	1.0	0.6	1.1	1.8

(c) Dynamic Modulus (| E* |) Results at 103.5 kPa Confining Pressure

Mixture	Asphalt Cement	Coarse Agg		|E*| - Dynamic Modulus (Mpa)																									
			Temp	10C								25C								54.4C									
			Freq (Hz)	*25*	*20*	*10*	*5*	*2*	*1*	*0.5*	*0.1*	*25*	*20*	*10*	*5*	*2*	*1*	*0.5*	*0.1*	*25*	*20*	*10*	*5*	*2*	*1*	*0.5*	*0.1*
D	PG 64-22	*Gravel*	Avg.	15818	15400	14185	12988	11413	10243	9102	6674	7629	7279	6259	5305	4146	3355	2658	1437	1047	837	591	411	252	179	128	67
			STD	1584	1538	1520	1508	1467	1402	1319	1104	175	181	166	151	131	110	89	60	145	164	135	107	79	58	40	17
			%CV	10.0	10.0	10.7	11.6	12.9	13.7	14.5	16.5	2.3	2.5	2.6	2.8	3.2	3.3	3.4	4.2	13.8	19.6	22.8	26.1	31.3	32.7	30.9	26.2
		Limestone	Avg.	15746	15241	13681	12163	10225	8805	7479	4763	7751	7298	5965	4759	3411	2555	1881	900	635	467	329	230	138	103	81	51
			STD	432	423	389	329	273	256	231	137	398	362	307	268	218	176	131	62	48	43	37	31	22	18	13	7
			%CV	2.7	2.8	2.8	2.7	2.7	2.9	3.1	2.9	5.1	5.0	5.2	5.6	6.4	6.9	7.0	6.9	7.5	9.2	11.4	13.3	16.3	17.1	16.5	13.9
		Granite	Avg.	12929	12562	11440	10339	8907	7879	6876	4793	6035	5712	4776	3925	2942	2297	1762	868	650	521	366	250	146	101	75	35
			STD	352	341	334	307	273	251	231	169	305	308	289	254	201	166	135	73	54	37	38	36	30	28	16	6
			%CV	2.7	2.7	2.9	3.0	3.1	3.2	3.4	3.5	5.1	5.4	6.1	6.5	6.8	7.2	7.7	8.4	8.3	7.1	10.3	14.4	20.8	27.5	21.6	16.9
	PG 70-22	*Gravel*	Avg.	15160	14777	13592	12429	10923	9799	8744	6421	8248	7891	6829	5822	4612	3783	3045	1696	1178	1047	819	647	486	407	339	223
			STD	586	588	578	563	539	513	462	404	244	245	232	229	189	166	136	71	112	105	92	82	71	59	46	64
			%CV	3.9	4.0	4.3	4.5	4.9	5.2	5.3	6.3	3.0	3.1	3.4	3.9	4.1	4.4	4.5	4.2	9.5	10.0	11.2	12.8	14.7	14.5	13.6	28.5
		Limestone	Avg.	15630	15232	13984	12745	11140	9925	8712	6038	7065	6680	5551	4542	3383	2647	2051	1127	920	820	620	481	348	274	229	139
			STD	146	146	139	144	151	155	156	136	146	132	98	87	75	66	55	32	35	38	27	21	15	19	12	9
			%CV	0.936	0.96	0.994	1.128	1.357	1.566	1.788	2.25	2.07	1.97	1.77	1.91	2.23	2.49	2.7	2.8	3.82	4.65	4.35	4.42	4.44	6.77	5.43	6.24
	PG 76-22	*Gravel*	Avg.	12068	11767	10826	9823	8642	7743	6869	4907	6144	5847	4995	4207	3275	2707	2114	1170	767	632	481	354	240	190	155	100
			STD	547	529	475	444	364	317	281	187	450	434	387	345	282	206	198	118	42	36	19	24	19	14	11	8
			%CV	4.5	4.5	4.4	4.5	4.2	4.1	4.1	3.8	7.3	7.4	7.7	8.2	8.6	7.6	9.4	10.1	5.5	5.7	3.9	6.8	7.8	7.6	7.1	7.6
		Limestone	Avg.	18242	17761	16320	14907	13044	11652	10270	7294	8879	8481	7198	6014	4599	3673	2900	1677	1238	1145	910	736	569	471	402	258
			STD	1029	1007	948	895	791	712	643	498	208	212	198	199	179	158	129	56	31	40	32	28	26	25	24	22
			%CV	5.6	5.7	5.8	6.0	6.1	6.1	6.3	6.8	2.3	2.5	2.8	3.3	3.9	4.3	4.4	3.3	2.5	3.5	3.5	3.9	4.6	5.3	5.9	8.5

(d) Phase Angle (δ) Test Results at 103.5 kPa Confining Pressure

Mixture	Asphalt Cement	Coarse Agg	δ - Phase Angle																									
			Temp	10C								25C								54.4C								
			Freq (Hz)	25	20	10	5	2	1	0.5	0.1	25	20	10	5	2	1	0.5	0.1	25	20	10	5	2	1	0.5	0.1
D	PG 64-22	Gravel	Avg.	10.8	11.0	12.1	13.2	14.7	16.0	17.4	21.2	21.4	21.9	23.6	25.3	27.4	28.9	30.2	33.5	37.1	42.0	41.8	41.3	41.1	39.3	39.1	35.8
			STD	0.9	1.2	1.2	1.3	1.5	1.5	1.6	1.7	0.6	0.6	0.6	0.6	0.6	0.5	0.4	0.1	2.2	3.9	4.2	4.4	5.4	4.8	5.6	6.6
			%CV	8.6	10.8	10.0	10.1	9.9	9.6	9.4	8.1	3.0	2.8	2.7	2.4	2.1	1.6	1.4	0.4	5.8	9.2	10.1	10.6	13.1	12.1	14.4	18.6
		Limestone	Avg.	14.0	14.4	16.0	17.6	20.0	21.9	23.9	28.6	25.4	26.1	28.2	30.2	32.4	34.1	35.3	36.6	35.1	41.2	39.6	38.3	37.1	34.4	32.1	26.8
			STD	0.1	0.1	0.1	0.1	0.1	0.1	0.1	0.1	0.4	0.5	0.3	0.3	0.3	0.3	0.3	0.7	0.4	1.1	1.4	1.7	1.9	1.7	1.4	0.4
			%CV	0.8	0.8	0.9	0.6	0.6	0.6	0.5	0.4	1.7	1.8	1.2	1.1	0.9	0.9	0.8	1.8	1.1	2.7	3.5	4.3	5.1	5.0	4.4	1.3
		Granite	Avg.	11.7	11.8	13.2	14.5	16.3	17.8	19.5	23.9	23.0	23.6	25.4	27.3	29.6	31.2	32.7	36.0	37.3	42.8	42.0	41.5	41.2	39.8	38.8	37.5
			STD	0.2	0.4	0.2	0.2	0.2	0.1	0.1	0.4	0.5	0.5	0.6	0.7	0.7	0.8	0.7	0.4	0.9	1.8	1.6	1.9	2.3	1.9	1.7	4.9
			%CV	2.0	3.2	1.5	1.3	1.0	0.8	0.5	1.5	2.0	2.1	2.3	2.4	2.4	2.4	2.2	1.1	2.5	4.2	3.7	4.6	5.5	4.7	4.3	13.1
	PG 70-22	Gravel	Avg.	10.5	10.8	11.8	12.9	14.4	15.4	16.8	20.7	19.5	20.0	21.6	23.3	25.5	27.0	28.5	31.9	34.4	35.7	33.6	31.4	28.4	25.9	24.0	21.7
			STD	0.4	0.4	0.5	0.5	0.4	0.5	0.5	0.3	0.3	0.4	0.4	0.3	0.3	0.3	0.4	0.2	1.3	2.2	2.7	3.0	3.1	2.9	2.7	4.1
			%CV	4.0	3.9	4.1	3.6	3.0	2.9	3.2	1.6	1.8	1.9	1.8	1.5	1.3	1.2	1.3	0.7	3.7	6.2	8.0	9.5	10.9	11.2	11.1	19.0
		Limestone	Avg.	10.7	11.1	12.2	13.4	15.3	16.9	18.6	23.3	23.6	24.1	26.1	27.9	30.0	31.3	32.2	33.2	34.6	36.3	34.9	32.8	30.5	28.7	27.1	25.4
			STD	0.3	0.2	0.3	0.3	0.3	0.4	0.4	0.3	0.1	0.1	0.1	0.1	0.2	0.3	0.4	0.4	0.4	0.5	0.9	0.9	0.8	0.8	0.6	0.5
			%CV	2.7	2.0	2.3	2.2	2.1	2.1	2.1	1.4	0.5	0.5	0.3	0.3	0.6	0.9	1.1	1.1	1.1	1.5	2.6	2.6	2.6	2.8	2.1	1.8
	PG 76-22	Gravel	Avg.	11.0	11.3	12.3	13.8	15.1	16.5	18.0	21.9	21.0	21.6	23.3	24.9	27.0	28.5	29.7	32.3	35.0	38.6	37.7	36.2	34.7	32.8	31.1	27.8
			STD	0.2	0.2	0.2	0.4	0.3	0.3	0.3	0.3	0.3	0.3	0.4	0.4	0.4	0.4	0.4	0.3	0.9	1.0	1.1	1.1	1.0	0.9	0.7	0.7
			%CV	1.4	1.7	1.9	3.0	1.7	1.7	1.6	1.3	1.2	1.4	1.5	1.4	1.3	1.3	1.3	1.0	2.5	2.6	3.0	3.1	3.0	2.9	2.3	2.6
		Limestone	Avg.	10.8	11.1	12.4	13.7	15.6	17.1	18.7	23.2	22.2	22.5	24.3	26.0	27.9	29.3	30.3	31.3	31.9	32.7	30.8	28.9	26.7	25.2	23.8	22.6
			STD	0.1	0.1	0.1	0.1	0.3	0.3	0.3	0.4	0.7	0.7	0.7	0.7	0.6	0.6	0.5	0.6	0.1	0.2	0.2	0.2	0.4	0.5	0.6	1.0
			%CV	1.3	1.0	0.9	1.1	1.8	1.6	1.6	1.9	3.2	3.3	2.8	2.6	2.2	2.0	1.7	1.8	0.2	0.5	0.5	0.8	1.4	2.2	2.7	4.4

(e) Dynamic Modulus (| E* |) Results at 207 kPa Confining Pressure

Mixture	Asphalt Cement	Coarse Agg		|E*| - Dynamic Modulus (Mpa)																									
			Temp	10C								25C								54.4C									
			Freq (Hz)	25	20	10	5	2	1	0.5	0.1	25	20	10	5	2	1	0.5	0.1	25	20	10	5	2	1	0.5	0.1
D	PG 64-22	Gravel	Avg.	15624	15220	13996	12777	11201	10054	8931	6526	7713	7433	6393	5407	4202	3382	2668	1444	985	788	551	382	235	169	123	66
			STD	1446	1417	1412	1395	1343	1284	1246	1090	250	241	224	194	165	140	120	79	130	129	102	77	53	37	25	12
			%CV	9.3	9.3	10.1	10.9	12.0	12.8	13.9	16.7	3.2	3.2	3.5	3.6	3.9	4.1	4.5	5.5	13.2	16.3	18.5	20.2	22.4	21.8	20.3	17.3
		Limestone	Avg.	15973	15454	13885	12373	10412	8994	7647	4894	7549	7072	5766	4594	3282	2462	1827	921	630	446	306	207	118	83	66	43
			STD	329	343	316	268	209	169	132	74	392	371	309	266	212	174	135	72	26	21	21	18	14	16	13	10
			%CV	2.1	2.2	2.3	2.2	2.0	1.9	1.7	1.5	5.2	5.3	5.4	5.8	6.5	7.1	7.4	7.8	4.1	4.8	7.0	8.5	11.8	19.3	20.2	24.1
		Granite	Avg.	13048	12665	11544	10436	9016	7980	6988	4894	6107	5776	4821	3992	2995	2333	1779	876	759	493	343	234	139	94	68	35
			STD	396	400	384	342	302	279	236	167	378	361	293	275	224	185	147	79	236	83	63	48	32	26	15	6
			%CV	3.0	3.2	3.3	3.3	3.4	3.5	3.4	3.4	6.2	6.3	6.1	6.9	7.5	7.9	8.2	9.0	31.1	16.9	18.5	20.4	22.7	27.5	22.1	18.1
	PG 70-22	Gravel	Avg.	15249	14873	13739	12556	11047	9939	8851	6504	8392	8004	6915	5876	4665	3829	3083	1731	1381	1300	1063	883	708	610	520	335
			STD	448	461	464	492	458	418	410	356	257	244	226	192	171	154	130	73	18	35	48	61	78	95	125	171
			%CV	2.9	3.1	3.4	3.9	4.1	4.2	4.6	5.5	3.1	3.1	3.3	3.3	3.7	4.0	4.2	4.2	1.3	2.7	4.5	7.0	11.0	15.6	24.0	51.1
		Limestone	Avg.	15394	15002	13759	12525	10891	9693	8507	5900	7203	6824	5708	4695	3531	2794	2201	1285	1034	930	721	566	410	302	217	118
			STD	275	264	243	211	186	172	155	124	107	103	98	89	78	70	59	34	139	156	148	137	115	71	32	13
			%CV	1.8	1.8	1.8	1.7	1.7	1.8	1.8	2.1	1.5	1.5	1.7	1.9	2.2	2.5	2.7	2.6	13.5	16.7	20.5	24.1	28.1	23.4	14.8	11.2
	PG 76-22	Gravel	Avg.	11934	11632	10695	9750	8531	7624	6740	4835	6123	5828	4975	4187	3254	2638	2112	1201	945	793	591	442	303	235	188	116
			STD	570	544	482	420	359	338	303	212	461	442	393	335	278	232	189	108	192	171	124	92	63	44	32	13
			%CV	4.8	4.7	4.5	4.3	4.2	4.4	4.5	4.4	7.5	7.6	7.9	8.0	8.5	8.8	8.9	9.0	20.3	21.5	21.0	20.7	20.6	18.6	17.1	11.3
		Limestone	Avg.	17945	17291	15968	14548	12697	11376	10040	7157	9000	8587	7297	6092	4693	3788	3050	1904	1231	1110	860	679	506	407	340	212
			STD	1185	1152	1082	1029	928	850	750	565	164	152	77	119	105	93	75	52	73	86	78	73	66	62	51	32
			%CV	6.6	6.7	6.8	7.1	7.3	7.5	7.5	7.9	1.8	1.8	1.1	1.9	2.2	2.4	2.5	2.7	6.0	7.8	9.1	10.8	13.1	15.1	15.0	15.0

(f) Phase Angle (δ) Test Results at 207 kPa Confining Pressure

Mixture	Asphalt Cement	Coarse Agg	δ - Phase Angle																									
			Temp	10C								25C								54.4C								
			Freq (Hz)	*25*	*20*	*10*	*5*	*2*	*1*	*0.5*	*0.1*	*25*	*20*	*10*	*5*	*2*	*1*	*0.5*	*0.1*	*25*	*20*	*10*	*5*	*2*	*1*	*0.5*	*0.1*
D	PG 64-22	*Gravel*	Avg.	10.7	11.1	12.2	13.3	14.9	16.2	17.5	21.3	21.5	21.8	23.3	25.0	27.1	28.5	30.0	33.2	37.3	42.1	41.9	41.4	40.5	38.6	36.9	32.0
			STD	1.0	1.1	1.2	1.4	1.5	1.6	1.6	1.7	0.6	0.7	0.5	0.5	0.4	0.5	0.4	0.4	1.1	1.9	2.1	2.2	2.6	2.3	2.0	0.8
			%CV	9.4	10.2	10.1	10.2	10.0	9.7	9.0	7.9	3.0	3.3	2.3	2.0	1.6	1.7	1.5	1.2	2.8	4.4	5.1	5.4	6.4	6.1	5.3	2.6
		Limestone	Avg.	14.0	14.3	15.9	17.4	19.8	21.6	23.5	28.2	25.8	26.4	28.4	30.3	32.4	33.8	34.9	35.5	35.2	42.3	41.1	40.0	39.3	37.3	34.4	31.8
			STD	0.1	0.1	0.1	0.1	0.0	0.1	0.1	0.1	0.7	0.6	0.6	0.5	0.5	0.5	0.5	1.0	0.3	1.1	1.4	1.5	2.0	2.9	2.5	6.9
			%CV	0.6	0.5	0.3	0.3	0.2	0.5	0.6	0.4	2.6	2.4	2.0	1.5	1.4	1.4	1.4	2.7	0.9	2.5	3.4	3.8	5.2	7.8	7.2	21.7
		Granite	Avg.	11.7	12.0	13.2	14.5	16.3	17.8	19.5	23.7	22.8	23.4	25.4	27.0	29.2	30.9	32.5	35.8	37.3	42.6	42.6	41.8	41.4	40.4	39.1	35.2
			STD	0.0	0.1	0.1	0.1	0.2	0.2	0.2	0.2	0.5	0.5	0.5	0.7	0.7	0.6	0.6	0.4	0.7	3.1	3.2	2.9	2.7	3.1	2.9	3.2
			%CV	0.3	0.7	0.8	0.6	0.9	0.9	0.8	0.7	2.1	2.2	2.0	2.4	2.3	2.1	1.8	1.0	2.0	7.2	7.6	6.9	6.6	7.7	7.4	9.0
	PG 70-22	*Gravel*	Avg.	10.3	10.7	11.7	12.8	14.3	15.5	16.9	20.6	19.3	19.7	21.4	23.0	25.0	26.5	28.0	31.1	30.6	30.3	27.9	25.5	22.5	20.5	19.4	19.5
			STD	0.3	0.4	0.4	0.5	0.5	0.5	0.5	0.6	0.3	0.3	0.4	0.3	0.4	0.3	0.3	0.3	1.6	1.8	2.1	2.3	2.4	2.7	3.4	6.2
			%CV	3.3	3.5	3.8	3.7	3.4	3.0	3.0	3.0	1.6	1.7	1.8	1.5	1.5	1.2	1.1	1.0	5.2	5.8	7.4	8.9	10.9	13.4	17.7	31.6
		Limestone	Avg.	10.1	10.5	11.6	12.9	14.7	16.4	18.1	23.0	24.4	24.9	27.0	28.9	31.2	32.8	33.8	35.7	38.0	41.7	41.1	40.0	38.9	37.5	35.3	31.4
			STD	0.3	0.3	0.3	0.4	0.4	0.4	0.5	0.5	0.1	0.1	0.0	0.1	0.1	0.2	0.3	0.4	0.6	0.8	0.7	0.9	1.2	1.2	1.0	1.5
			%CV	2.9	2.7	3.0	2.9	2.8	2.7	2.6	2.0	0.6	0.4	0.1	0.2	0.5	0.7	0.8	1.0	1.6	1.8	1.8	2.2	3.1	3.2	2.7	4.8
	PG 76-22	*Gravel*	Avg.	11.3	11.5	12.6	13.7	15.4	16.8	18.2	22.0	21.0	21.6	23.2	24.8	26.7	28.0	29.2	31.3	34.7	38.0	37.2	36.0	34.5	33.0	31.7	29.0
			STD	0.2	0.2	0.2	0.2	0.2	0.2	0.2	0.1	0.3	0.3	0.4	0.4	0.4	0.3	0.3	0.2	1.5	1.7	1.8	1.9	2.0	2.0	1.8	1.2
			%CV	1.5	1.7	1.7	1.5	1.3	1.2	1.0	0.5	1.2	1.5	1.5	1.6	1.4	1.2	1.0	0.6	4.3	4.4	4.9	5.4	5.8	6.0	5.8	4.1
		Limestone	Avg.	12.0	11.8	12.8	14.1	16.0	17.5	19.2	23.2	21.9	22.3	23.8	25.5	27.3	28.3	29.0	28.9	32.0	33.1	31.6	29.9	27.9	26.3	25.1	24.1
			STD	1.2	0.6	0.2	0.3	0.4	0.5	0.6	0.6	0.5	0.5	0.3	0.5	0.4	0.4	0.4	0.7	0.5	0.7	0.8	0.9	1.0	1.2	1.3	1.3
			%CV	10.1	4.7	1.7	1.9	2.4	2.6	3.0	2.5	2.3	2.0	1.4	1.8	1.5	1.6	1.5	2.5	1.4	2.0	2.4	2.9	3.7	4.7	5.1	5.6

Variations of the dynamic moduli values were observed to behave as expected for the limestone aggregate "D" mixes. Figure 4.1 shows that as the asphalt cement PG grade progresses from PG64-22 to PG70-22 to PG76-22 there is a steady increase in the average dynamic modulus due the increase in relative stiffness of each mixture.

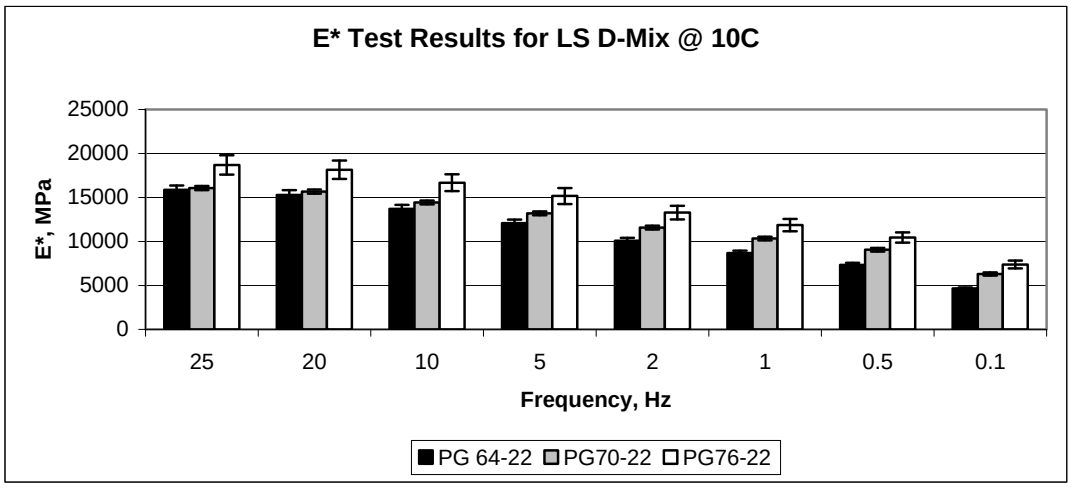

(a) 10 °C

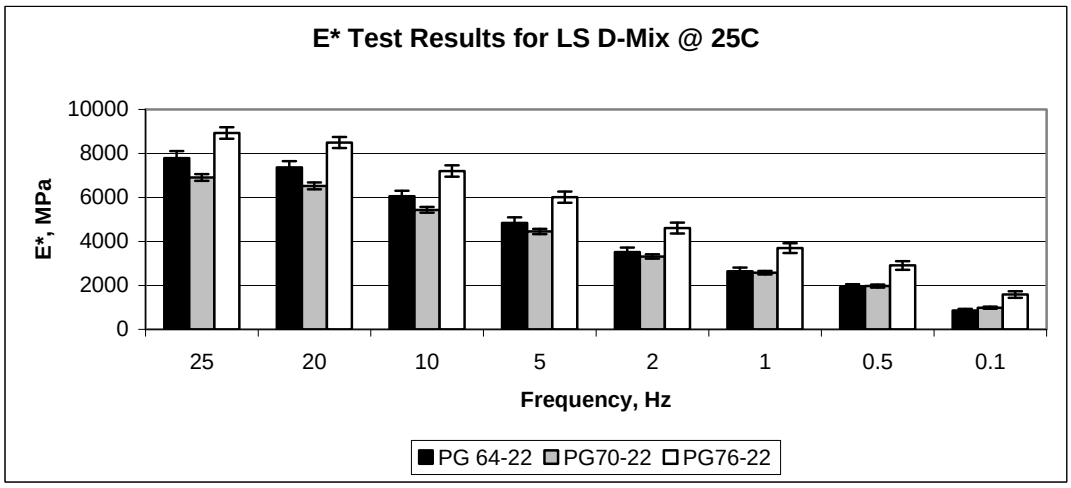

(b) 25 °C

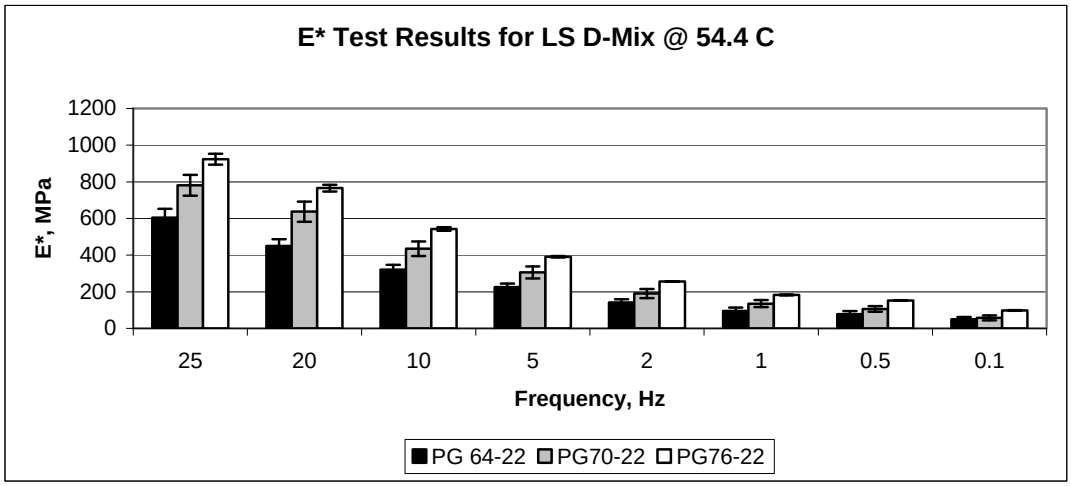

(c) 54.4 °C

Figure 4-1 |E*| Results for 411-D Limestone Mixtures

The effect of applied confining stress is sporadic. At 25 ºC and 54.4 ºC the additional confining pressure generally resulted in an increased dynamic modulus and decreased phase angle. For the highest temperature test this change is only most readily apparent in the transition between 0 kPa and 103.5 kPa confining stress. This may be due to the duration of the test sequence. The test samples are progressed in succession from 0 to 103.5 to 207.0 kPa at constant temperature. The asphalt sample may have had time to adequately soften by the time the low-end frequencies of the third test have been initiated, resulting in a lower dynamic modulus and higher phase angle than expected. Low temperature (10ºC) testing was affected in a reverse manner than expected by applied confining stress. Modulus values typically decreased. This could be attributed to the nature of the SPT test machine. Warmer room temperature air is introduced into the pressure cell as the confining stress is applied. This warm air may significantly warm, and therefore soften, the asphalt mixture. Figure 4-2 examines more closely the

temperature and confining pressure effects on a PG76-22 Limestone mixture at low frequency.

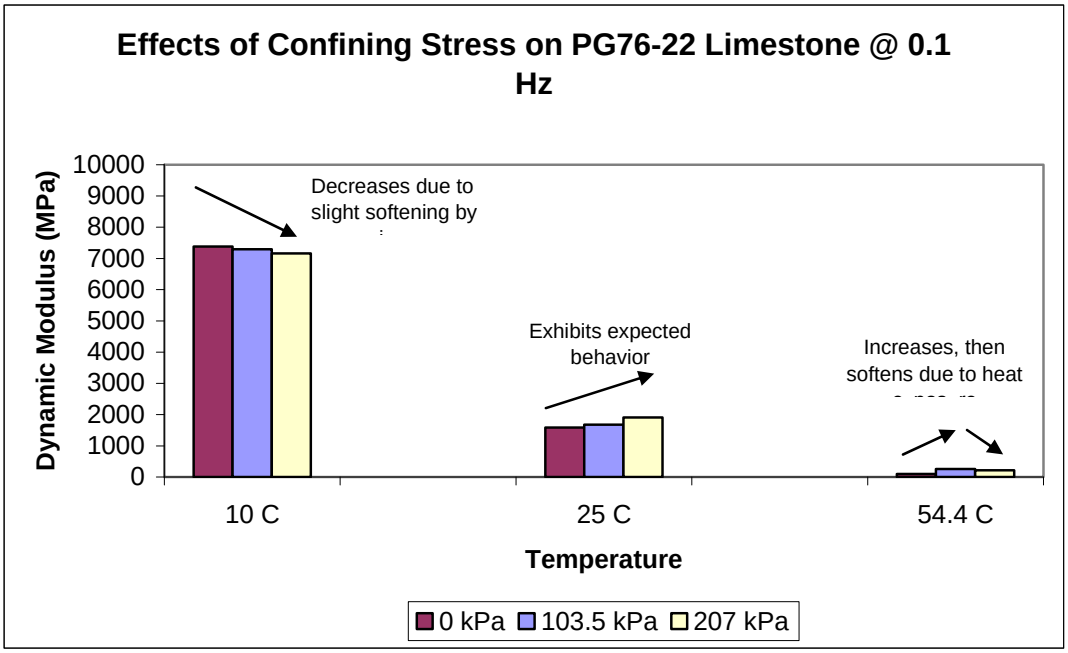

Figure 4-2 Effects of Confining Stress on PG76-22 Limestone Mixture at 0.1 Hz

Figure 4-3 presents the dynamic modulus test results for "D" gravel mixtures. These mixtures behaved predictably in only that as the temperature increased the average dynamic modulus decreased. Test results indicate no change or an actual decrease in modulus value when increasing the performance grade of the asphalt cement. Again it should be noted that the mixes were collected from a variety of aggregate sources with no attempt to match gradation or other various aggregate properties. However, these tests did produce highly repeatable results with low standard deviations and coefficients of variability.

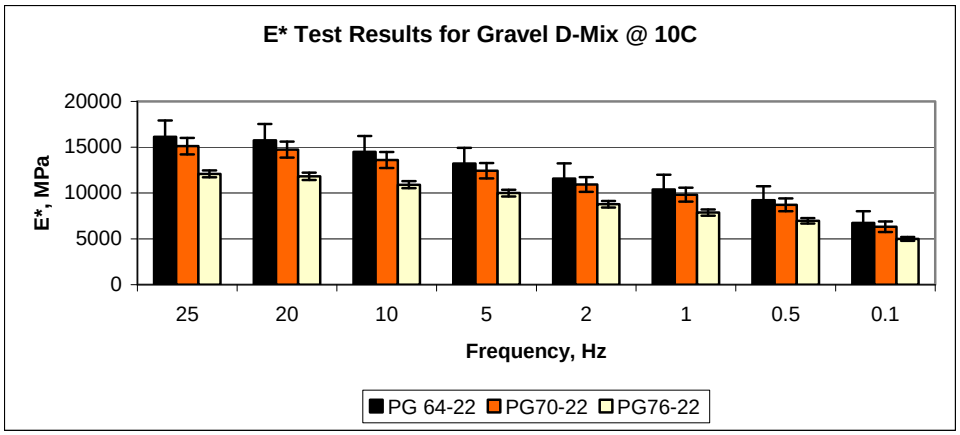

(a) 10 °C

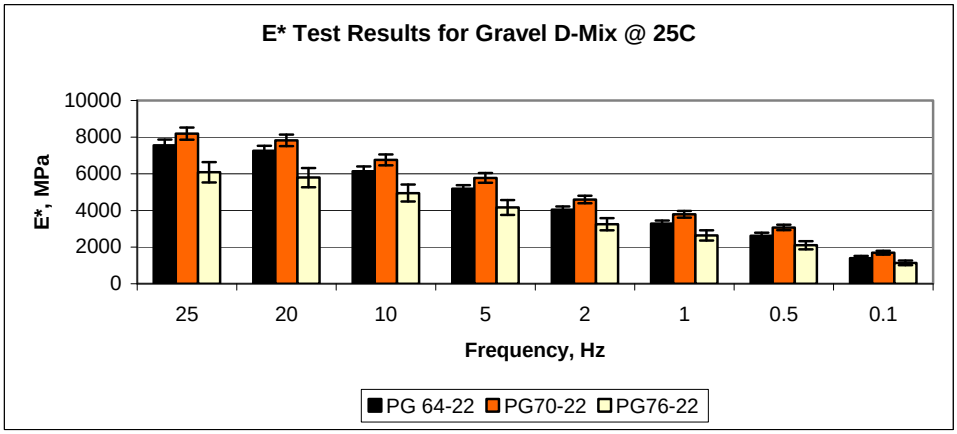

(b) 25 °C

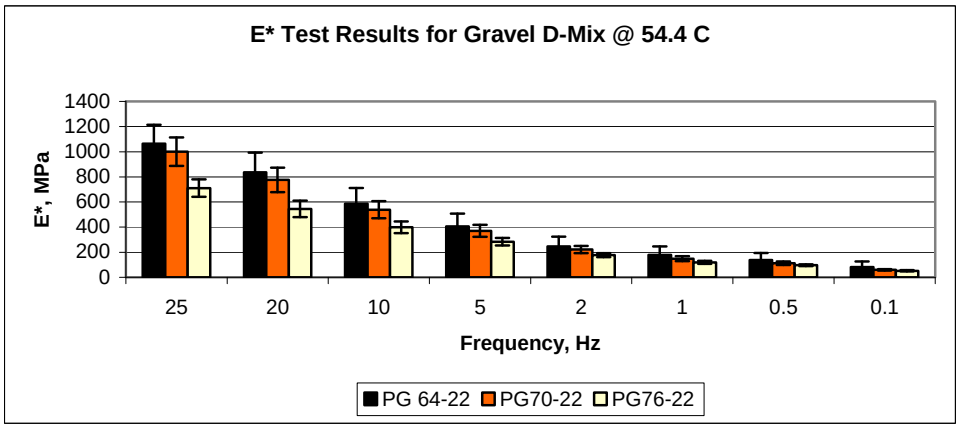

(c) 54.4 °C

Figure 4-3 |E*| Results for 411-D Gravel Mixtures

4.2.2 307 BM-2 Mixtures

BM-2 asphalt pavement is a dense mix similar to D mix with stronger aggregate structure intended for use in shoulder construction or as binder and intermediate mixes. The asphalt cement content is approximately equal to that of a typical D mix. The trend of test results for the BM-2 mixtures behaved comparably to the limestone D mixes particularly in the progression from un-modified PG64-22 asphalt cement to slightly modified PG70-22 asphalt cement. With an increase in binder performance grade the dynamic modulus increases. Also, with the addition of confining stress the dynamic modulus increases while the phase angle decreases, except for the same phenomena at the cold temperature testing discussed previously. The only gravel based BM-2 mixture behaves very similarly to the gravel based surface mixtures, performing more reliably at the high temperature level. Table 4-2 presents complete test results of the BM-2 testing.

Table 4-2 Summary of Dynamic Modulus Tests for 307 BM-2 Mixtures

(a) Dynamic Modulus (|E*|) Results at 0 kPa Confining Pressure

Mixture	Asphalt Cement	Coarse Agg	|E*| - Dynamic Modulus (Mpa)																							
			Temp	10C								25C								54.4C						
			Freq (Hz)	25	20	10	5	2	1	0.5	0.1	25	20	10	5	2	1	0.5	0.1	25	20	10	5	2	1	0.5	0.1
BM-2	PG 64-22	Limestone	Avg.	21903	21477	20245	18960	17116	15791	14304	10874	10392	9976	8628	7361	5780	4709	3736	1980	1157	992	684	469	279	189	146	76
			STD	1015	1072	1082	1089	1175	1055	1058	862	788	744	663	597	504	439	349	186	69	58	40	27	17	13	11	15
			%CV	4.6	5.0	5.3	5.7	6.9	6.7	7.4	7.9	7.6	7.5	7.7	8.1	8.7	9.3	9.4	9.4	5.9	5.9	5.9	5.7	6.2	6.7	7.3	20.1
	PG 70-22	Limestone	Avg.	26491	25865	24060	22367	20066	18203	16325	12034	12194	11751	10150	8601	6759	5510	4362	2309	1361	1148	804	563	352	247	188	109
			STD	400	377	414	404	420	409	385	379	330	343	326	263	236	234	210	151	186	162	121	82	51	37	23	13
			%CV	1.5	1.5	1.7	1.8	2.1	2.2	2.4	3.2	2.7	2.9	3.2	3.1	3.5	4.3	4.8	6.5	13.7	14.1	15.0	14.6	14.5	14.9	12.1	12.4
	PG 76-22	Limestone	Avg.	20281	19851	18348	16986	15070	13640	12207	8894	9323	8890	7595	6371	4923	3954	3118	1650	1171	965	688	484	299	215	168	102
			STD	672	703	493	503	455	390	316	232	145	146	137	100	85	71	57	36	120	104	77	57	37	28	20	12
			%CV	3.3	3.5	2.7	3.0	3.0	2.9	2.6	2.6	1.6	1.6	1.8	1.6	1.7	1.8	1.8	2.2	10.3	10.8	11.1	11.9	12.3	13.0	11.8	11.5
	PG 82-22	Gravel	Avg.	13709	13289	12078	10890	9340	8206	7138	4919	7067	6696	5668	4706	3589	2852	2222	1143	1222	951	686	498	326	233	186	112
			STD	969	925	834	754	646	573	505	370	551	531	472	388	301	248	197	107	141	129	93	68	39	33	22	12
			%CV	7.1	7.0	6.9	6.9	6.9	7.0	7.1	7.5	7.8	7.9	8.3	8.3	8.4	8.7	8.9	9.3	11.6	13.6	13.5	13.6	12.0	14.1	11.9	10.5

(b) Phase Angle (δ) Test Results at 0 kPa Confining Pressure

Mixture	Asphalt Cement	Coarse Agg	δ - Phase Angle																							
			Temp	10C								25C								54.4C						
			Freq (Hz)	25	20	10	5	2	1	0.5	0.1	25	20	10	5	2	1	0.5	0.1	25	20	10	5	2	1	0.5	0.1
BM-2	PG 64-22	Limestone	Avg.	7.2	7.4	8.5	9.5	11.0	12.2	13.5	17.7	20.0	20.4	22.4	24.4	27.2	29.2	31.1	34.9	39.3	41.7	41.1	40.3	39.5	39.4	36.6	33.6
			STD	0.6	0.5	0.2	0.2	0.4	0.3	0.3	0.6	0.6	0.6	0.6	0.6	0.5	0.4	0.2	0.5	0.3	0.5	0.6	0.4	0.2	0.5	1.0	2.8
			%CV	7.9	6.9	2.7	2.6	3.7	2.6	2.4	3.5	2.8	2.7	2.7	2.4	2.0	1.5	0.8	1.3	0.9	1.3	1.4	1.1	0.6	1.2	2.7	8.3
	PG 70-22	Limestone	Avg.	8.0	8.4	9.4	10.3	11.9	13.3	14.8	19.1	20.6	20.8	22.6	24.2	26.5	28.1	29.6	32.3	36.1	38.2	37.1	36.0	34.9	34.1	32.3	27.6
			STD	0.7	0.6	0.6	0.5	0.5	0.5	0.5	0.7	0.3	0.3	0.3	0.4	0.4	0.4	0.4	0.5	0.5	0.6	0.7	0.7	0.8	1.0	0.3	0.4
			%CV	9.0	7.4	6.3	5.0	4.3	3.8	3.6	3.5	1.6	1.4	1.5	1.6	1.5	1.4	1.3	1.4	1.4	1.6	1.9	1.9	2.2	2.9	0.8	1.5
	PG 76-22	Limestone	Avg.	9.2	9.3	10.5	11.6	13.3	14.8	16.2	20.7	21.5	22.0	24.0	26.0	28.6	30.4	32.2	35.1	38.0	41.1	39.9	38.7	37.6	36.0	34.0	28.9
			STD	0.2	0.2	0.2	0.3	0.2	0.3	0.3	0.1	0.3	0.3	0.4	0.4	0.5	0.5	0.5	0.7	0.6	0.9	0.9	1.0	1.1	1.4	1.4	1.4
			%CV	1.7	2.5	1.8	2.3	1.9	1.8	1.7	0.6	1.3	1.3	1.6	1.7	1.6	1.6	1.7	2.0	1.6	2.3	2.3	2.6	3.0	3.8	4.0	5.0
	PG 82-22	Gravel	Avg.	12.3	12.7	13.9	15.3	17.3	18.8	20.5	24.6	22.6	23.2	25.0	26.7	28.8	30.3	31.5	34.2	37.3	41.8	40.8	39.7	38.1	37.3	35.3	31.1
			STD	0.1	0.3	0.3	0.4	0.5	0.6	0.6	0.8	0.6	0.6	0.7	0.7	0.8	0.7	0.7	0.6	0.5	0.1	0.2	0.6	1.3	0.6	0.8	1.0
			%CV	1.1	2.7	2.3	2.7	2.9	3.1	3.1	3.1	2.6	2.5	2.8	2.6	2.6	2.4	2.1	1.8	1.3	0.2	0.6	1.5	3.4	1.7	2.3	3.1

(c) Dynamic Modulus (| E* |) Results at 103.5 kPa Confining Pressure

Mixture	Asphalt Cement	Coarse Agg	|E*| - Dynamic Modulus (Mpa)																									
			Temp	10C								25C								54.4C								
			Freq (Hz)	25	20	10	5	2	1	0.5	0.1	25	20	10	5	2	1	0.5	0.1	25	20	10	5	2	1	0.5	0.1
BM-2	PG 64-22	*Limestone*	Avg.	21478	21018	19677	18328	16520	15118	13680	10336	10537	10110	8737	7416	5821	4737	3702	1953	1428	1327	1010	781	564	440	320	153
			STD	1090	1092	1048	1023	985	945	881	729	549	548	509	480	426	381	287	167	65	73	79	81	83	81	72	25
			%CV	5.1	5.2	5.3	5.6	6.0	6.2	6.4	7.1	5.2	5.4	5.8	6.5	7.3	8.0	7.7	8.6	4.6	5.5	7.8	10.4	14.8	18.5	22.6	16.5
	PG 70-22	*Limestone*	Avg.	25058	24457	22716	21021	18805	17086	15332	11264	12094	11651	10012	8465	6600	5308	4171	2271	1573	1442	1097	850	628	509	429	295
			STD	557	548	532	521	499	511	526	543	340	310	287	276	262	241	207	143	206	197	154	119	89	74	64	51
			%CV	2.2	2.2	2.3	2.5	2.7	3.0	3.4	4.8	2.8	2.7	2.9	3.3	4.0	4.5	5.0	6.3	13.1	13.7	14.0	14.0	14.1	14.5	14.9	17.4
	PG 76-22	*Limestone*	Avg.	19891	19398	17940	16488	14607	13176	11738	8494	9542	9104	7800	6590	5088	4104	3252	1813	1268	1103	821	615	425	335	273	182
			STD	394	369	279	252	234	213	178	153	264	256	240	201	196	181	187	226	117	114	95	83	75	76	76	78
			%CV	2.0	1.9	1.6	1.5	1.6	1.6	1.5	1.8	2.8	2.8	3.1	3.0	3.8	4.4	5.8	12.5	9.2	10.3	11.6	13.4	17.6	22.7	27.9	42.6
	PG 82-22	*Gravel*	Avg.	13742	13333	12140	10954	9422	8303	7239	4995	6994	6620	5586	4629	3526	2807	2212	1235	1376	1194	929	729	545	455	396	299
			STD	829	769	682	604	534	478	424	320	505	482	426	368	285	227	174	87	107	103	82	65	46	37	35	26
			%CV	6.0	5.8	5.6	5.5	5.7	5.8	5.9	6.4	7.2	7.3	7.6	8.0	8.1	8.1	7.8	7.1	7.8	8.7	8.8	8.9	8.5	8.0	8.8	8.7

(d) Phase Angle (δ) Test Results at 103.5 kPa Confining Pressure

Mixture	Asphalt Cement	Coarse Agg	δ - Phase Angle																									
			Temp	10C								25C								54.4C								
			Freq (Hz)	*25*	*20*	*10*	*5*	*2*	*1*	*0.5*	*0.1*	*25*	*20*	*10*	*5*	*2*	*1*	*0.5*	*0.1*	*25*	*20*	*10*	*5*	*2*	*1*	*0.5*	*0.1*
BM-2	PG 64-22	*Limestone*	Avg.	7.9	8.2	9.1	10.1	11.5	12.7	14.1	18.1	19.4	19.8	21.7	23.7	26.2	28.2	30.3	33.9	34.8	35.0	33.5	31.7	29.4	27.8	27.7	27.9
			STD	0.2	0.2	0.2	0.2	0.3	0.3	0.4	0.5	0.5	0.5	0.5	0.5	0.5	0.4	0.3	0.4	0.3	0.6	0.8	1.1	1.5	1.7	2.4	2.3
			%CV	2.2	2.1	2.2	2.5	2.6	2.5	2.9	2.8	2.4	2.4	2.4	2.2	1.8	1.4	1.1	1.1	0.9	1.7	2.5	3.4	5.0	6.2	8.6	8.4
	PG 70-22	*Limestone*	Avg.	8.8	9.0	10.1	11.1	12.6	13.9	15.4	19.6	20.5	20.7	22.3	24.0	26.2	27.7	29.1	31.5	33.6	34.2	32.9	31.3	29.0	27.2	25.5	22.4
			STD	0.5	0.5	0.5	0.5	0.5	0.6	0.6	0.7	0.3	0.3	0.3	0.3	0.3	0.3	0.4	0.4	0.3	0.4	0.4	0.4	0.4	0.5	0.6	0.7
			%CV	6.0	5.4	4.8	4.4	4.3	4.3	4.1	3.8	1.6	1.3	1.5	1.2	1.3	1.1	1.3	1.1	0.8	1.2	1.2	1.1	1.5	1.9	2.3	3.1
	PG 76-22	*Limestone*	Avg.	9.7	9.9	11.0	12.1	13.7	15.2	16.7	20.9	20.8	21.4	23.3	25.0	27.4	29.0	30.3	32.5	35.6	37.6	36.1	34.4	32.3	30.3	28.7	25.1
			STD	0.1	0.1	0.1	0.1	0.1	0.2	0.2	0.1	0.8	0.8	0.9	1.0	1.1	1.3	1.6	2.7	1.2	1.9	2.3	2.7	3.4	4.1	4.8	5.9
			%CV	0.7	0.6	0.8	1.0	1.0	1.3	1.2	0.7	3.8	3.5	4.0	4.1	4.1	4.4	5.1	8.3	3.3	5.1	6.2	7.9	10.7	13.4	16.7	23.4
	PG 82-22	*Gravel*	Avg.	12.4	12.7	13.8	15.1	17.0	18.6	20.2	24.1	22.5	23.1	24.7	26.3	28.1	29.4	30.3	31.6	33.9	35.9	34.0	32.2	29.7	27.7	25.9	22.9
			STD	0.1	0.3	0.3	0.3	0.3	0.3	0.3	0.3	0.4	0.4	0.5	0.5	0.5	0.4	0.4	0.6	0.8	0.7	0.7	0.7	0.7	0.7	0.4	0.1
			%CV	1.0	2.0	1.9	2.0	1.9	1.7	1.7	1.4	1.9	1.9	2.0	1.9	1.7	1.5	1.3	2.0	2.4	1.9	1.9	2.1	2.2	2.4	1.6	0.2

(e) Dynamic Modulus (| E* |) Results at 207 kPa Confining Pressure

Mixture	Asphalt Cement	Coarse Agg		|E*| - Dynamic Modulus (Mpa)																							
			Temp	10C								25C								54.4C							
			Freq (Hz)	25	20	10	5	2	1	0.5	0.1	25	20	10	5	2	1	0.5	0.1	25	20	10	5	2	1	0.5	0.1
BM-2	PG 64-22	*Limestone*	Avg.	20979	20514	19168	17801	15968	14598	13194	9959	10601	10164	8781	7462	5835	4702	3694	1939	1532	1429	1120	892	671	530	394	164
			STD	1085	1074	1035	977	926	863	803	674	514	497	460	423	364	324	269	138	335	368	352	330	297	258	191	64
			%CV	5.2	5.2	5.4	5.5	5.8	5.9	6.1	6.8	4.8	4.9	5.2	5.7	6.2	6.9	7.3	7.1	21.9	25.8	31.4	36.9	44.3	48.6	48.5	39.0
	PG 70-22	*Limestone*	Avg.	24267	23674	21928	20233	18031	16351	14651	10759	12064	11585	9944	8394	6509	5243	4140	2373	1708	1572	1208	947	705	568	474	317
			STD	615	607	606	638	645	654	626	560	376	352	340	306	280	247	211	142	271	259	207	164	122	96	82	59
			%CV	2.5	2.6	2.8	3.2	3.6	4.0	4.3	5.2	3.1	3.0	3.4	3.6	4.3	4.7	5.1	6.0	15.9	16.5	17.1	17.3	17.3	17.0	17.3	18.5
	PG 76-22	*Limestone*	Avg.	19415	18949	17498	16028	14110	12703	11294	8220	9480	9053	7736	6508	5018	4015	3146	1700	1251	1079	790	580	390	283	213	123
			STD	444	443	429	408	341	323	295	199	174	170	147	130	101	81	68	38	117	126	112	93	72	48	29	14
			%CV	2.3	2.3	2.5	2.5	2.4	2.5	2.6	2.4	1.8	1.9	1.9	2.0	2.0	2.0	2.2	2.2	9.3	11.7	14.2	16.1	18.6	16.9	13.7	11.6
	PG 82-22	*Gravel*	Avg.	13857	13475	12281	11096	9555	8430	7353	5084	7027	6657	5632	4678	3582	2883	2315	1400	1514	1342	1074	871	674	571	501	384
			STD	723	702	641	585	506	451	402	300	508	488	431	360	282	232	190	130	103	97	76	60	47	38	36	30
			%CV	5.2	5.2	5.2	5.3	5.3	5.4	5.5	5.9	7.2	7.3	7.6	7.7	7.9	8.1	8.2	9.3	6.8	7.2	7.1	6.9	7.0	6.7	7.2	7.8

(f) Phase Angle (δ) Test Results at 207 kPa Confining Pressure

Mixture	Asphalt Cement	Coarse Agg		δ - Phase Angle																							
			Temp	10C								25C								54.4C							
			Freq (Hz)	*25*	*20*	*10*	*5*	*2*	*1*	*0.5*	*0.1*	*25*	*20*	*10*	*5*	*2*	*1*	*0.5*	*0.1*	*25*	*20*	*10*	*5*	*2*	*1*	*0.5*	*0.1*
BM-2	PG 64-22	*Limestone*	Avg.	8.2	8.5	9.5	10.5	12.0	13.3	14.6	18.8	19.6	20.0	21.9	23.9	26.4	28.4	30.2	33.9	33.3	33.6	32.1	30.4	28.4	27.5	26.4	26.8
			STD	0.2	0.2	0.2	0.2	0.3	0.4	0.4	0.5	0.8	0.8	0.9	0.9	1.0	1.0	0.8	0.4	4.4	5.7	6.2	6.8	7.7	8.2	6.7	3.5
			%CV	2.8	2.3	2.2	2.3	2.8	3.0	3.0	2.8	4.0	4.0	4.0	3.9	3.9	3.5	2.8	1.1	13.3	16.8	19.3	22.4	26.9	29.8	25.6	13.2
	PG 70-22	*Limestone*	Avg.	9.4	9.7	10.7	11.8	13.4	14.6	16.1	20.1	20.6	20.7	22.4	24.0	26.0	27.5	28.8	30.3	32.1	32.7	31.5	29.9	27.8	26.2	24.5	21.8
			STD	0.7	0.7	0.8	0.8	0.9	0.8	0.9	0.9	0.3	0.3	0.4	0.4	0.5	0.4	0.4	0.3	1.0	1.1	1.1	0.9	0.7	0.6	0.7	0.7
			%CV	7.6	7.3	7.1	6.6	6.4	5.8	5.3	4.7	1.4	1.3	1.8	1.9	1.8	1.6	1.4	0.9	3.1	3.5	3.3	2.9	2.6	2.5	2.8	3.2
	PG 76-22	*Limestone*	Avg.	10.0	11.3	11.5	12.7	14.4	15.8	17.3	21.5	21.1	21.6	23.4	25.1	27.4	29.1	30.7	33.5	35.5	38.0	37.1	36.0	34.7	33.5	32.2	28.4
			STD	0.1	0.0	0.1	0.1	0.2	0.2	0.2	0.3	0.2	0.1	0.2	0.2	0.2	0.2	0.2	0.3	1.2	1.8	2.1	2.2	2.6	2.3	2.3	2.2
			%CV	0.8	0.5	1.0	1.1	1.4	1.5	1.3	1.5	0.7	0.7	0.7	0.7	0.6	0.7	0.6	0.9	3.4	4.7	5.6	6.1	7.6	6.9	7.0	7.7
	PG 82-22	*Gravel*	Avg.	12.3	12.7	13.9	15.1	16.9	18.5	20.0	23.8	22.3	22.8	24.4	25.8	27.3	28.3	28.8	29.0	32.4	33.7	31.6	29.6	27.3	25.5	24.2	21.8
			STD	0.0	0.2	0.1	0.2	0.1	0.1	0.2	0.2	0.4	0.4	0.4	0.4	0.5	0.6	0.9	1.6	1.0	1.1	1.4	1.5	1.5	1.3	0.8	0.2
			%CV	0.2	1.4	1.0	1.0	0.8	0.8	0.9	0.9	1.9	1.8	1.5	1.5	1.8	2.3	3.1	5.5	3.1	3.3	4.4	5.0	5.5	5.0	3.3	0.8

4.2.3 307A and 307A-S Mixtures

Asphalt concrete mixtures in the TDOT Construction Specifications meeting the criteria of A or A-S (includes RAP) mix possess larger aggregate sizes, lower asphalt contents, and are intended for use as a base layer. Dynamic modulus values for these mixtures proved to be much higher than standard surface mixtures due to the strong influence of the aggregate structure. Little variation in modulus value is identifiable between the results of the tested mixtures, regardless of PG grade or aggregate source. However, the A and A-S mixes produced the most consistent increase in dynamic modulus value when subjected to increased confining stress. This is most likely due to the open aggregate structure of the mix. By applying confining stress to the sample the mixtures were able to develop greater aggregate interlock and therefore greater shear capacity required to resist the strain imposed by the dynamic modulus test. Table 4-3 presents dynamic modulus and corresponding phase angle data of A and A-S type mixes.

Table 4-3 Summary of Dynamic Modulus Tests for 307 A and 307 A-S Mixtures

(a) Dynamic Modulus (|E*|) Results at 0 kPa Confining Pressure

Mixture	Asphalt Cement	Coarse Agg	|E*| - Dynamic Modulus (Mpa)																							
			Temp	10C								25C								54.4C							
			Freq (Hz)	25	20	10	5	2	1	0.5	0.1	25	20	10	5	2	1	0.5	0.1	25	20	10	5	2	1	0.5	0.1
A	PG 70-22	Limestone (East)	Avg.	19209	18665	17041	56570	13401	11876	10421	7314	9895	9503	8157	6905	5352	4337	3458	1926	1112	867	619	432	261	175	132	67
			STD	2959	2931	2793	56914	2331	2148	1947	1468	1444	1397	1257	1154	923	791	679	516	163	137	103	73	43	27	18	7
			%CV	15.4	15.7	16.4	100.6	17.4	18.1	18.7	20.1	14.6	14.7	15.4	16.7	17.3	18.2	19.6	26.8	14.6	15.8	16.6	16.9	16.4	15.3	13.9	9.9
		Limestone (Middle)	Avg.	23625	23175	21855	20477	18566	17052	15489	11669	11552	11133	9599	8125	6344	5120	4016	2090	1773	1557	1135	842	582	453	379	265
			STD	520	499	432	378	335	251	222	243	919	922	811	690	531	421	324	156	289	304	266	238	210	196	175	150
			%CV	2.2	2.2	2.0	1.8	1.8	1.5	1.4	2.1	8.0	8.3	8.4	8.5	8.4	8.2	8.1	7.5	16.3	19.5	23.4	28.3	36.1	43.4	46.3	56.6
	PG 76-22	Limestone	Avg.	20635	20168	18870	17563	15729	14277	12795	9350	11437	10970	9534	8161	6444	5258	4194	2153	1540	1236	869	603	381	266	209	122
			STD	1372	1371	1346	1310	1249	1213	1163	949	727	672	614	565	503	426	305	213	162	144	105	73	50	32	29	26
			%CV	6.7	6.8	7.1	7.5	7.9	8.5	9.1	10.2	6.4	6.1	6.4	6.9	7.8	8.1	7.3	9.9	10.5	11.6	12.1	12.1	13.1	12.1	13.8	21.2

(b) Phase Angle (δ) Test Results at 0 kPa Confining Pressure

Mixture	Asphalt Cement	Coarse Agg	δ - Phase Angle																							
			Temp	10C								25C								54.4C							
			Freq (Hz)	25	20	10	5	2	1	0.5	0.1	25	20	10	5	2	1	0.5	0.1	25	20	10	5	2	1	0.5	0.1
A	PG 70-22	Limestone (East)	Avg.	11.9	12.2	13.6	14.9	16.9	18.5	20.2	24.4	23.1	23.2	24.6	25.7	28.0	29.3	30.3	31.9	35.0	38.9	37.8	36.8	36.3	36.7	34.4	30.4
			STD	1.0	1.0	1.1	1.1	1.2	1.2	1.3	1.3	0.7	0.5	0.5	0.7	0.3	0.4	0.5	1.0	1.9	2.1	2.0	2.0	1.9	2.2	1.6	2.9
			%CV	8.6	8.4	8.2	7.5	7.0	6.7	6.3	5.4	3.0	2.3	2.0	2.8	1.2	1.4	1.7	3.0	5.5	5.3	5.2	5.5	5.4	5.9	4.7	9.5
		Limestone (Middle)	Avg.	7.6	7.7	8.6	9.5	11.1	12.5	14.0	18.3	20.5	20.9	22.9	25.0	27.7	29.6	31.2	33.5	35.3	36.3	35.0	33.4	31.2	29.9	27.5	23.7
			STD	0.5	0.7	0.7	0.7	0.8	0.8	0.9	0.9	0.3	0.3	0.4	0.5	0.8	1.0	1.3	1.9	1.8	2.8	3.2	3.7	4.4	5.2	5.1	4.9
			%CV	6.8	8.8	7.6	7.5	7.3	6.8	6.2	5.1	1.2	1.3	1.8	2.1	2.8	3.2	4.0	5.6	5.0	7.8	9.2	11.1	14.1	17.4	18.4	20.7
	PG 76-22	Limestone	Avg.	8.7	9.1	10.2	11.4	13.3	14.9	16.6	21.2	19.6	20.0	22.1	24.1	26.7	28.7	30.5	34.1	37.9	41.0	40.0	38.8	37.3	36.7	34.7	28.9
			STD	0.5	0.5	0.6	0.6	0.6	0.7	0.7	0.8	0.6	0.5	0.5	0.5	0.4	0.5	0.4	0.8	0.4	0.7	0.7	0.7	0.9	1.2	1.8	0.7
			%CV	6.2	6.0	5.5	5.4	4.7	4.6	4.4	3.7	2.9	2.6	2.3	2.0	1.7	1.6	1.3	2.5	1.1	1.8	1.9	1.8	2.5	3.3	5.1	2.5

(c) Dynamic Modulus (|E*|) Results at 15 kPa Confining Pressure

Mixture	Asphalt Cement	Coarse Agg	|E*| - Dynamic Modulus (Mpa)																									
			Temp	10C							25C								54.4C									
			Freq (Hz)	*25*	*20*	*10*	*5*	*2*	*1*	*0.5*	*0.1*	*25*	*20*	*10*	*5*	*2*	*1*	*0.5*	*0.1*	*25*	*20*	*10*	*5*	*2*	*1*	*0.5*	*0.1*
A	PG 70-22	*Limestone (East)*	Avg.	18865	18361	16799	15282	13257	11790	10365	7282	9645	9185	7779	6542	5028	4031	3163	1682	1163	938	680	486	311	228	174	96
			STD	2693	2616	2456	2304	2089	1921	1761	1340	1225	1201	1114	935	764	664	555	342	178	169	133	98	63	46	34	18
			%CV	14.3	14.2	14.6	15.1	15.8	16.3	17.0	18.4	12.7	13.1	14.3	14.3	15.2	16.5	17.5	20.3	15.3	18.0	19.5	20.1	20.2	20.0	19.5	18.5
		Limestone (Middle)	Avg.	23007	22593	21261	19948	18103	16630	15107	11330	11882	11427	9818	8286	6419	5141	4020	2200	1858	1689	1273	986	733	604	526	394
			STD	474	450	395	373	366	399	439	385	912	892	762	642	475	362	262	131	167	156	119	87	64	57	58	65
			%CV	2.1	2.0	1.9	1.9	2.0	2.4	2.9	3.4	7.7	7.8	7.8	7.7	7.4	7.0	6.5	5.9	9.0	9.3	9.4	8.9	8.8	9.4	11.0	16.5
	PG 76-22	*Limestone*	Avg.	20725	20282	18881	17455	15595	14142	12667	9204	11497	11069	9565	8136	6353	5130	4020	2126	1647	1402	1028	764	403	423	368	260
			STD	1408	1375	1301	1230	1143	1116	1080	963	272	307	310	327	325	305	271	188	239	246	195	158	275	99	101	77
			%CV	6.8	6.8	6.9	7.0	7.3	7.9	8.5	10.5	2.4	2.8	3.2	4.0	5.1	5.9	6.7	8.9	14.5	17.5	19.0	20.7	68.2	23.3	27.5	29.4

(d) Phase Angle (δ) Test Results at 15 kPa Confining Pressure

Mixture	Asphalt Cement	Coarse Agg	δ - Phase Angle																									
			Temp	10C							25C								54.4C									
			Freq (Hz)	*25*	*20*	*10*	*5*	*2*	*1*	*0.5*	*0.1*	*25*	*20*	*10*	*5*	*2*	*1*	*0.5*	*0.1*	*25*	*20*	*10*	*5*	*2*	*1*	*0.5*	*0.1*
A	PG 70-22	*Limestone (East)*	Avg.	12.1	12.4	13.6	14.7	16.6	18.2	19.8	23.8	22.1	22.5	24.3	25.6	27.5	28.8	30.0	32.1	33.8	37.0	36.2	35.4	34.7	33.4	32.3	29.4
			STD	0.7	0.7	0.7	0.7	0.8	0.9	1.0	1.0	0.4	0.3	0.5	0.2	0.1	0.2	0.2	0.2	1.7	1.7	1.9	1.8	1.9	1.9	2.0	2.3
			%CV	5.9	5.4	5.3	4.7	5.0	4.9	4.9	4.4	1.9	1.5	2.0	0.9	0.5	0.7	0.6	0.7	5.0	4.7	5.1	5.1	5.5	5.8	6.1	7.7
		Limestone (Middle)	Avg.	8.0	8.3	9.2	10.1	11.7	13.0	14.4	18.7	20.1	20.5	22.5	24.5	27.0	28.8	30.3	32.0	34.0	34.5	33.1	31.3	28.6	26.4	24.2	20.5
			STD	0.6	0.7	0.7	0.7	0.7	0.7	0.7	0.7	0.3	0.3	0.4	0.5	0.8	1.0	1.3	1.7	0.4	0.4	0.5	0.7	0.9	0.9	1.0	0.8
			%CV	7.3	8.2	7.1	6.9	6.3	5.4	4.6	4.0	1.5	1.4	1.8	2.1	3.0	3.5	4.1	5.3	1.3	1.1	1.6	2.3	3.2	3.5	4.1	3.8
	PG 76-22	*Limestone*	Avg.	9.1	9.5	10.6	11.8	13.6	15.1	16.7	21.4	19.6	20.0	22.0	24.0	26.5	28.4	30.1	33.1	35.8	37.8	36.4	34.7	32.5	30.7	28.5	24.8
			STD	0.5	0.4	0.5	0.6	0.6	0.6	0.7	0.8	0.4	0.4	0.4	0.3	0.3	0.2	0.1	0.4	0.4	0.8	0.8	1.0	1.3	1.1	1.7	2.0
			%CV	5.0	4.7	5.1	5.1	4.7	4.3	4.2	3.6	1.9	2.1	1.8	1.4	1.0	0.5	0.5	1.1	1.2	2.1	2.1	2.8	3.9	3.7	6.0	8.1

(e) Dynamic Modulus (|E*|) Results at 207 kPa Confining Pressure

Mixture	Asphalt Cement	Coarse Agg	|E*| - Dynamic Modulus (Mpa)																									
			Temp	10C							25C								54.4C									
			Freq (Hz)	25	20	10	5	2	1	0.5	0.1	25	20	10	5	2	1	0.5	0.1	25	20	10	5	2	1	0.5	0.1
A	PG 70-22	Limestone (East)	Avg.	18729	18238	60640	15146	13157	11711	10293	7260	9227	8779	7455	6212	4761	3784	2956	1582	1200	957	698	499	319	235	177	96
			STD	2549	2486	60779	2178	1952	1794	1643	1273	1191	1154	1022	903	736	616	506	306	160	161	129	93	60	43	27	12
			%CV	13.6	13.6	100.2	14.4	14.8	15.3	16.0	17.5	12.9	13.1	13.7	14.5	15.4	16.3	17.1	19.3	13.3	16.9	18.5	18.6	18.6	18.3	15.1	12.4
		Limestone (Middle)	Avg.	22701	22263	20953	19610	17995	16445	14770	10965	11989	11508	9926	8397	6510	5219	4119	2391	1980	1818	1399	1111	850	709	626	486
			STD	744	716	665	682	693	689	698	556	821	796	672	605	458	355	265	139	185	185	150	130	118	116	117	120
			%CV	3.3	3.2	3.2	3.5	3.9	4.2	4.7	5.1	6.8	6.9	6.8	7.2	7.0	6.8	6.4	5.8	9.4	10.2	10.8	11.7	13.9	16.4	18.6	24.7
	PG 76-22	Limestone	Avg.	20627	20171	18703	17199	15436	14009	12535	9146	11485	11009	9476	8020	6243	5018	3942	2146	1794	1560	1167	891	648	528	457	342
			STD	1261	1267	1110	953	1140	1107	1091	1045	326	354	358	366	366	331	288	212	348	346	283	236	195	173	159	134
			%CV	6.1	6.3	5.9	5.5	7.4	7.9	8.7	11.4	2.8	3.2	3.8	4.6	5.9	6.6	7.3	9.9	19.4	22.2	24.3	26.5	30.1	32.7	34.8	39.1

(f) Phase Angle (δ) Test Results at 207 kPa Confining Pressure

Mixture	Asphalt Cement	Coarse Agg	δ - Phase Angle																									
			Temp	10C							25C								54.4C									
			Freq (Hz)	25	20	10	5	2	1	0.5	0.1	25	20	10	5	2	1	0.5	0.1	25	20	10	5	2	1	0.5	0.1
A	PG 70-22	Limestone (East)	Avg.	12.2	12.5	13.7	15.0	16.8	18.3	19.7	23.7	22.4	22.7	24.2	25.7	27.6	28.9	30.0	32.0	33.0	37.4	36.1	35.3	34.3	33.1	41.9	29.0
			STD	0.5	0.5	0.6	0.6	0.7	0.7	0.8	0.9	0.1	0.2	0.2	0.3	0.5	0.5	0.5	0.3	1.7	0.8	1.2	1.1	1.2	1.3	13.5	1.7
			%CV	4.3	4.1	4.3	4.1	3.9	4.0	4.0	3.7	0.7	0.7	1.0	1.3	1.7	1.7	1.6	0.9	5.1	2.1	3.2	3.0	3.6	3.9	32.3	5.8
		Limestone (Middle)	Avg.	8.5	8.6	9.8	10.7	12.3	13.7	15.2	19.4	20.0	20.3	22.3	24.2	26.7	28.3	29.6	30.5	32.4	32.6	31.2	29.2	26.5	24.2	22.1	18.7
			STD	0.4	0.4	0.5	0.5	0.5	0.4	0.3	0.4	0.4	0.4	0.5	0.6	0.8	1.0	1.2	1.5	0.7	0.9	1.2	1.6	1.8	1.7	1.6	1.2
			%CV	4.4	5.0	5.1	4.7	3.7	2.7	2.1	1.8	2.2	2.1	2.2	2.6	3.2	3.6	4.1	5.0	2.1	2.8	4.0	5.4	6.7	7.0	7.4	6.4
	PG 76-22	Limestone	Avg.	9.2	9.6	10.7	12.0	13.8	15.2	16.8	21.3	19.6	20.2	22.3	24.1	26.7	28.4	30.0	32.2	34.7	36.1	34.7	33.0	30.4	28.3	26.2	22.5
			STD	0.5	0.5	0.5	0.5	0.7	0.7	0.8	1.0	0.5	0.5	0.5	0.5	0.4	0.3	0.2	0.3	0.8	1.2	1.3	1.6	1.9	2.1	2.4	2.5
			%CV	5.2	4.8	4.6	4.2	5.3	4.9	4.8	4.6	2.4	2.5	2.1	2.0	1.5	1.1	0.5	0.8	2.2	3.3	3.9	4.8	6.4	7.4	9.1	11.0

(g) Dynamic Modulus (| E* |) Results at 0 kPa Confining Pressure

Mixture	Asphalt Cement	Coarse Agg	|E*| - Dynamic Modulus (Mpa)																									
			Temp	10C								25C								54.4C								
			Freq (Hz)	25	20	10	5	2	1	0.5	0.1	25	20	10	5	2	1	0.5	0.1	25	20	10	5	2	1	0.5	0.1
A-S	PG 70-22	Limestone (East)	Avg.	22953	22640	21453	20170	18345	16880	15328	11542	11653	11264	9827	8469	6778	5592	4497	2464	1497	1246	890	638	408	266	215	123
			STD	2493	2129	1815	1620	1445	1313	1192	896	806	812	691	595	466	352	258	134	175	151	105	70	41	26	15	3
			%CV	10.9	9.4	8.5	8.0	7.9	7.8	7.8	7.8	6.9	7.2	7.0	7.0	6.9	6.3	5.7	5.5	11.7	12.1	11.8	11.1	10.1	9.6	7.1	2.2
		Limestone (Middle)	Avg.	23606	23068	21692	20340	18525	17065	15572	12089	12287	11983	10543	8930	7077	5683	4403	2225	1513	1265	865	595	364	238	185	103
			STD	1986	1973	1943	1856	1750	1626	1481	1167	1367	1360	1283	1169	1109	1056	952	622	372	348	243	165	93	52	38	23
			%CV	8.4	8.6	9.0	9.1	9.4	9.5	9.5	9.7	11.1	11.4	12.2	13.1	15.7	18.6	21.6	27.9	24.6	27.5	28.1	27.6	25.5	22.0	20.7	22.0

(h) Phase Angle (δ) Test Results at 0 kPa Confining Pressure

Mixture	Asphalt Cement	Coarse Agg	δ - Phase Angle																									
			Temp	10C								25C								54.4C								
			Freq (Hz)	25	20	10	5	2	1	0.5	0.1	25	20	10	5	2	1	0.5	0.1	25	20	10	5	2	1	0.5	0.1
A-S	PG 70-22	Limestone (East)	Avg.	7.9	8.2	8.9	9.8	11.3	12.7	14.2	18.5	19.9	20.1	21.7	23.3	25.5	27.0	28.4	31.1	33.0	35.0	33.7	32.1	30.5	31.9	28.5	26.3
			STD	0.4	0.4	0.3	0.3	0.3	0.3	0.4	0.3	0.2	0.2	0.3	0.3	0.4	0.4	0.5	0.8	0.8	0.7	0.9	1.1	1.2	1.0	1.5	1.9
			%CV	4.9	4.5	3.0	2.8	2.4	2.4	2.9	1.9	0.9	1.1	1.3	1.3	1.5	1.6	1.8	2.6	2.4	2.1	2.7	3.5	4.0	3.3	5.4	7.3
		Limestone (Middle)	Avg.	6.8	7.0	8.0	8.9	10.6	12.0	13.6	18.0	19.9	19.9	21.4	23.9	26.3	28.4	30.3	33.4	36.7	38.9	37.7	36.1	34.1	34.5	31.6	28.1
			STD	0.6	0.7	0.7	0.6	0.6	0.6	0.5	0.8	1.0	1.0	1.0	1.6	1.5	1.6	1.7	1.5	1.5	2.3	1.8	1.4	1.0	1.6	1.5	1.3
			%CV	8.7	9.3	8.4	6.8	5.5	4.8	3.9	4.3	4.9	5.2	4.8	6.5	5.7	5.8	5.8	4.6	4.1	5.9	4.9	3.8	3.0	4.5	4.7	4.7

(i) Dynamic Modulus (| E* |) Results at 103.5 kPa Confining Pressure

Mixture	Asphalt Cement	Coarse Agg	|E*| - Dynamic Modulus (Mpa)																									
			Temp	10C								25C								54.4C								
			Freq (Hz)	25	20	10	5	2	1	0.5	0.1	25	20	10	5	2	1	0.5	0.1	25	20	10	5	2	1	0.5	0.1
A-S	PG 70-22	Limestone (East)	Avg.	22583	22178	20846	19501	17634	16180	14656	10950	11949	11492	9981	8532	6751	5510	4390	2399	1665	1469	1096	833	585	449	374	238
			STD	1591	1578	1493	1386	1269	1183	1051	823	760	725	611	508	380	290	217	133	176	168	125	94	67	53	45	25
			%CV	7.0	7.1	7.2	7.1	7.2	7.3	7.2	7.5	6.4	6.3	6.1	6.0	5.6	5.3	4.9	5.5	10.5	11.5	11.4	11.3	11.5	11.8	12.0	10.3
		Limestone (Middle)	Avg.	21928	21491	20278	19089	17483	16235	14909	11524	12546	12144	10579	8993	6984	5542	4272	2202	1605	1398	1003	734	499	380	311	206
			STD	2026	1992	1884	1771	1629	1476	1345	1150	1469	1440	1337	1253	1160	1071	942	592	382	355	271	204	145	106	93	70
			%CV	9.2	9.3	9.3	9.3	9.3	9.1	9.0	10.0	11.7	11.9	12.6	13.9	16.6	19.3	22.0	26.9	23.8	25.4	27.0	27.8	29.0	28.0	30.0	34.2

(j) Phase Angle (δ) Test Results at 103.5 kPa Confining Pressure

Mixture	Asphalt Cement	Coarse Agg	δ - Phase Angle																									
			Temp	10C								25C								54.4C								
			Freq (Hz)	25	20	10	5	2	1	0.5	0.1	25	20	10	5	2	1	0.5	0.1	25	20	10	5	2	1	0.5	0.1
A-S	PG 70-22	Limestone (East)	Avg.	8.6	8.8	9.7	10.8	12.2	13.5	15.0	19.1	19.3	19.5	21.1	22.6	24.8	26.3	27.7	30.6	31.4	32.7	31.2	29.5	27.7	26.6	24.6	21.9
			STD	0.3	0.3	0.3	0.3	0.4	0.4	0.5	0.5	0.3	0.4	0.4	0.4	0.5	0.5	0.6	0.9	0.6	0.6	0.5	0.5	0.3	0.2	0.1	0.3
			%CV	4.0	3.0	3.0	3.1	3.2	2.8	3.2	2.5	1.4	1.9	1.9	1.9	2.1	1.9	2.1	2.9	2.0	1.8	1.7	1.6	0.9	0.7	0.3	1.5
		Limestone (Middle)	Avg.	7.6	7.8	8.9	9.9	11.4	12.7	14.2	18.6	19.3	19.5	21.4	23.4	26.2	28.3	30.3	33.2	35.6	37.3	36.2	34.5	32.3	30.3	28.1	23.8
			STD	0.1	0.2	0.3	0.3	0.3	0.3	0.3	0.5	1.0	1.0	1.1	1.3	1.5	1.8	1.9	1.7	2.0	2.6	2.4	2.2	2.2	1.9	2.0	2.0
			%CV	1.3	2.2	2.9	3.1	2.9	2.5	2.4	2.5	4.9	5.3	5.3	5.5	5.7	6.2	6.2	5.0	5.5	6.9	6.7	6.5	6.8	6.4	7.2	8.3

(k) Dynamic Modulus (| E* |) Results at 207 kPa Confining Pressure

Mixture	Asphalt Cement	Coarse Agg	|E*| - Dynamic Modulus (Mpa)																							
			Temp	10C								25C								54.4C							
			Freq (Hz)	25	20	10	5	2	1	0.5	0.1	25	20	10	5	2	1	0.5	0.1	25	20	10	5	2	1	0.5	0.1
A-S	PG 70-22	Limestone (East)	Avg.	21958	21502	20098	18809	16843	15366	13872	10349	11914	11510	9994	8529	6737	5525	4380	2480	1711	1505	1123	846	593	447	369	227
			STD	1442	1408	1366	1456	1259	1134	1053	827	686	653	557	457	324	213	164	85	160	163	120	94	68	53	46	28
			%CV	6.6	6.5	6.8	7.7	7.5	7.4	7.6	8.0	5.8	5.7	5.6	5.4	4.8	3.9	3.7	3.4	9.3	10.8	10.7	11.1	11.5	12.0	12.5	12.5
		Limestone (Middle)	Avg.	22162	21802	20556	19345	17664	16306	14779	11350	12526	12212	10632	9045	6979	5539	4275	2263	1664	1451	1042	771	534	412	343	233
			STD	1919	1809	1729	1601	1477	1402	1287	1016	1401	1452	1346	1286	1169	1091	948	598	391	371	289	231	175	136	125	94
			%CV	8.7	8.3	8.4	8.3	8.4	8.6	8.7	9.0	11.2	11.9	12.7	14.2	16.8	19.7	22.2	26.4	23.5	25.6	27.7	29.9	32.7	33.1	36.5	40.3

(l) Phase Angle (δ) Test Results at 207 kPa Confining Pressure

Mixture	Asphalt Cement	Coarse Agg	δ - Phase Angle																							
			Temp	10C								25C								54.4C							
			Freq (Hz)	25	20	10	5	2	1	0.5	0.1	25	20	10	5	2	1	0.5	0.1	25	20	10	5	2	1	0.5	0.1
A-S	PG 70-22	Limestone (East)	Avg.	9.2	9.4	10.6	11.8	13.2	14.3	16.0	19.9	19.2	19.4	20.9	22.4	24.5	25.9	27.1	29.4	31.0	32.4	31.0	29.6	27.8	26.9	25.0	22.8
			STD	0.4	0.4	0.5	0.7	0.7	0.7	0.7	0.7	0.1	0.2	0.3	0.3	0.3	0.3	0.2	0.0	0.5	0.5	0.5	0.3	0.2	0.4	0.4	0.6
			%CV	4.4	4.6	4.6	6.0	5.3	5.0	4.4	3.5	0.6	1.3	1.3	1.1	1.2	1.0	0.9	0.1	1.7	1.5	1.5	1.1	0.8	1.5	1.7	2.6
		Limestone (Middle)	Avg.	7.8	8.1	9.2	10.2	11.8	13.2	14.7	18.9	19.7	19.2	21.3	23.4	26.1	28.3	30.2	32.8	35.0	36.8	35.9	34.3	31.9	29.8	27.5	23.0
			STD	0.2	0.2	0.2	0.2	0.2	0.3	0.3	0.2	0.3	1.3	1.0	1.2	1.5	1.7	1.9	1.8	2.3	3.0	3.1	3.2	3.3	2.9	3.0	2.3
			%CV	2.1	2.8	2.4	2.3	2.0	1.9	1.8	0.9	1.7	6.6	4.8	5.0	5.6	6.0	6.1	5.4	6.4	8.2	8.7	9.5	10.2	9.9	10.9	10.0

4.3 Flow Number (F_N) Test Results

The following section presents the average flow number (F_N) and failure strain results for TDOT mixtures tested at The University of Tennessee Asphalt Laboratory. Testing was performed at 54.4 ºC in an unconfined state (0kPa) and at 103.5 kPa confining stress. The applied deviatorical stress to the samples was 600 kPa. Resulting flow numbers proved to be highest among base mixtures in the confined stress state. Unlike the dynamic modulus testing, test results demonstrated higher flow numbers for all mixes with modified asphalt cement compared to their un-modified partners. Samples were deemed to meet failure criteria at 50,000 microstrains or 10,000 cycles. Figures 4-4 to 4-7 graphically present the results of the flow number test.

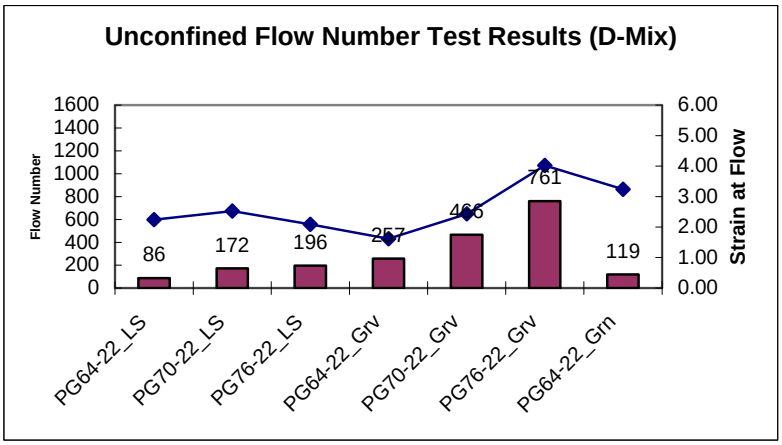

(a) Unconfined Test Results

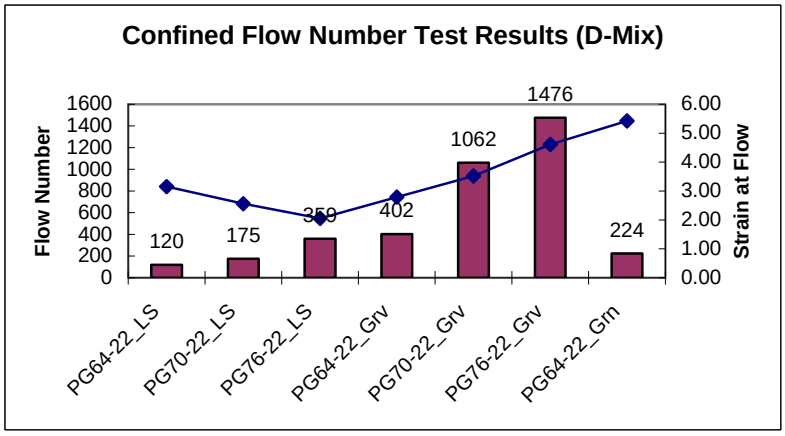

(b) Confined Test Results

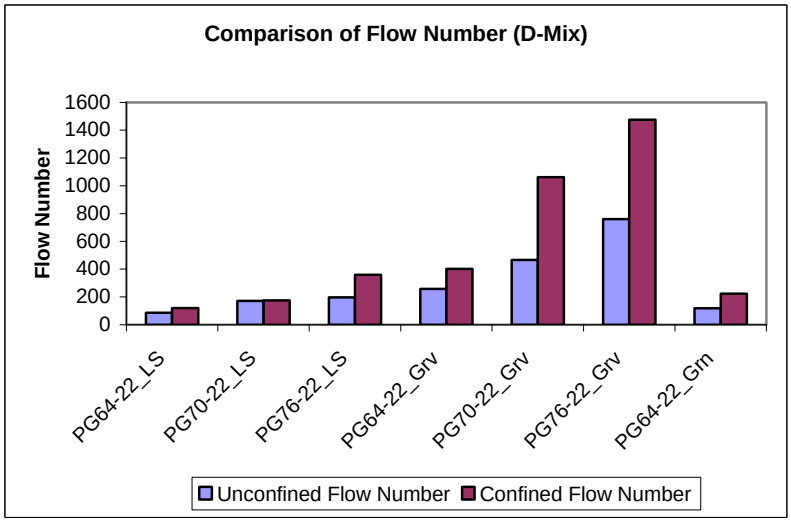

(c) Comparison between Unconfined and Confined Test Results

Figure 4-4 Flow Number Test Results for 411-D Mixtures

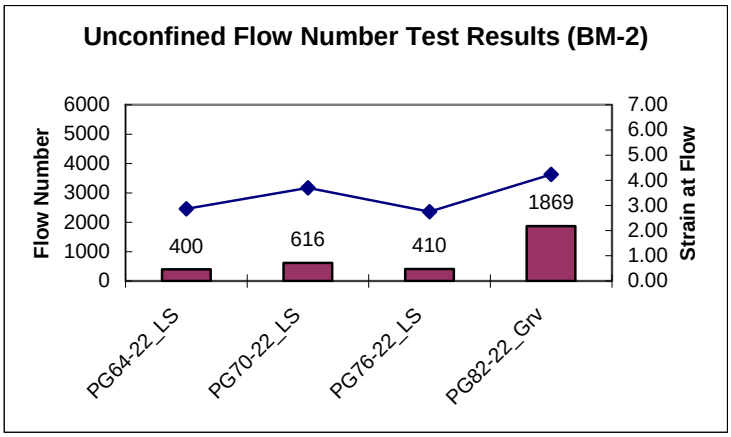

(a) Unconfined Test Results

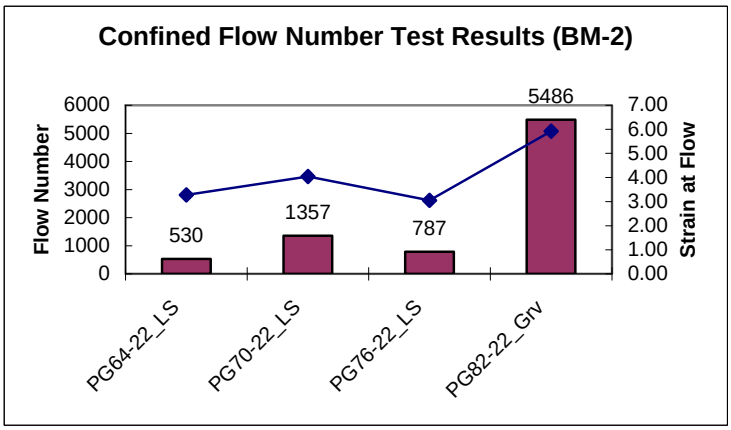

(b) Confined Test Results

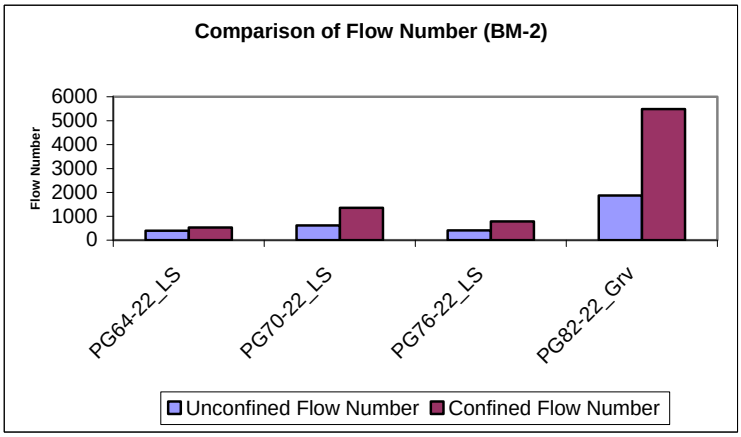

(c) Comparison between Unconfined and Confined Test Results

Figure 4-5 Flow Number Test Results for 307 BM-2 Mixtures

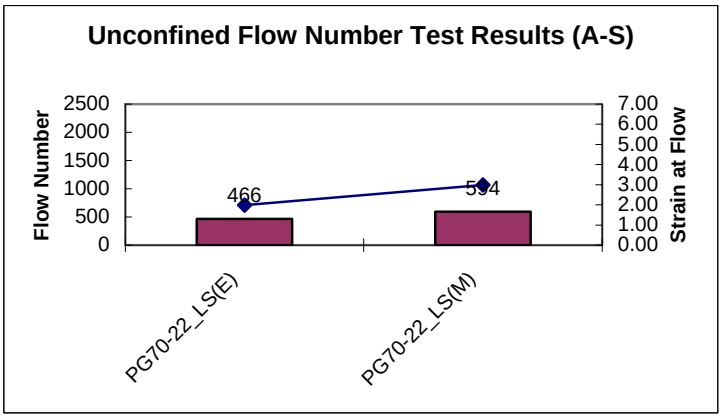

(a) Unconfined Test Results

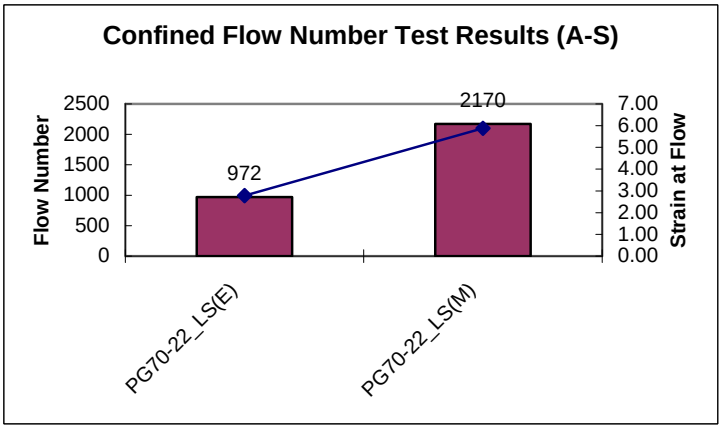

(b) Confined Test Results

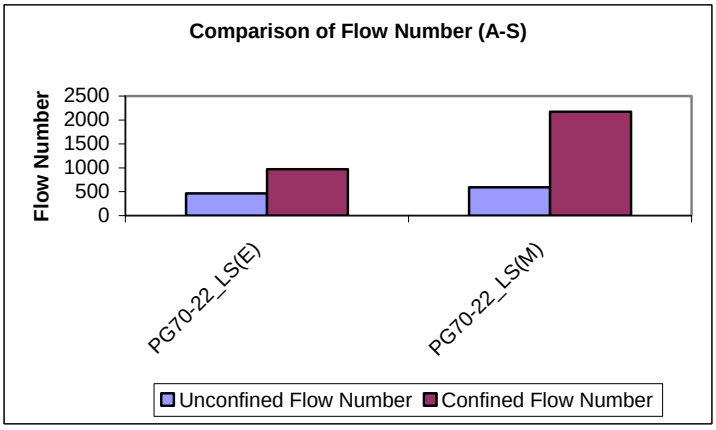

(c) Comparison between Unconfined and Confined Test Results

Figure 4-6 Flow Number Test Results for 307 A-S Mixtures

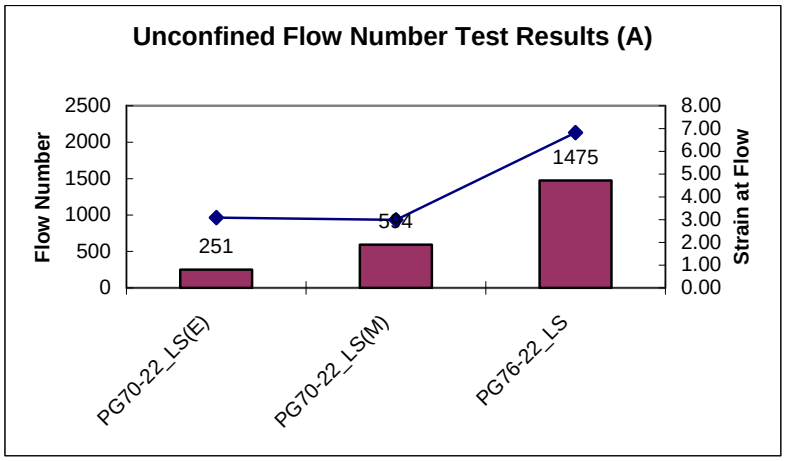

(a) Unconfined Test Results

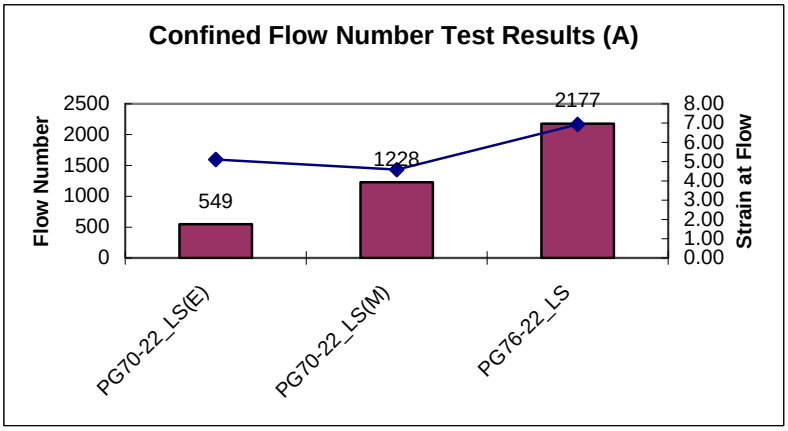

(b) Confined Test Results

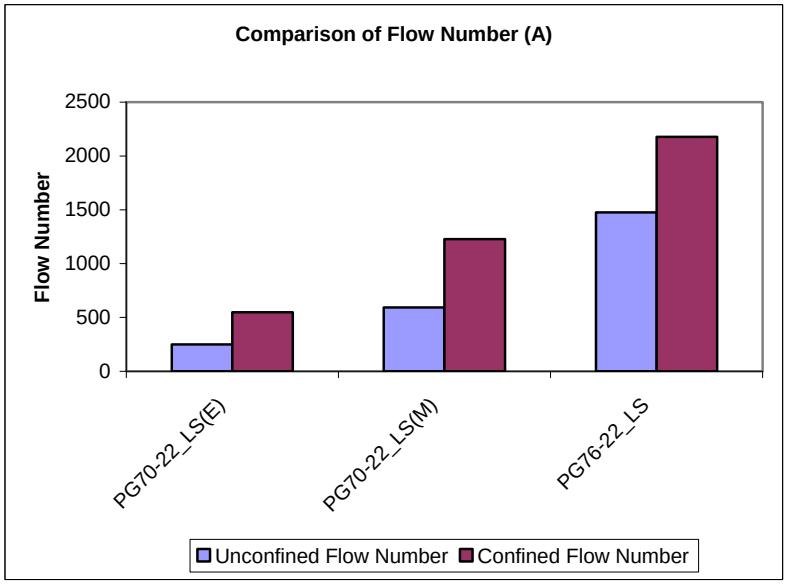

(c) Comparison between Unconfined and Confined Test Results

Figure 4-7 Flow Number Test Results for 307 A Mixtures

4.4 Asphalt Pavement Analyzer (APA) Test Results

The APA test was used as a proof torture test to evaluate the rutting susceptibility of the asphalt mixtures examined. After subjection to more than 8,000 cycles by a loaded wheel tester, modified asphalt mixtures showed lower rut depths than their un-modified partners for all mixture types regardless of aggregate source. Figure 4-8 presents the total rut depths experienced by each mixture. It can be seen that with the increase in the upper grade limit of asphalt binder, the mixture experienced less rut depth. This implied that HMA mixtures containing modified asphalt binder had higher rutting resistance compared to conventional non-modified asphalt mixtures.

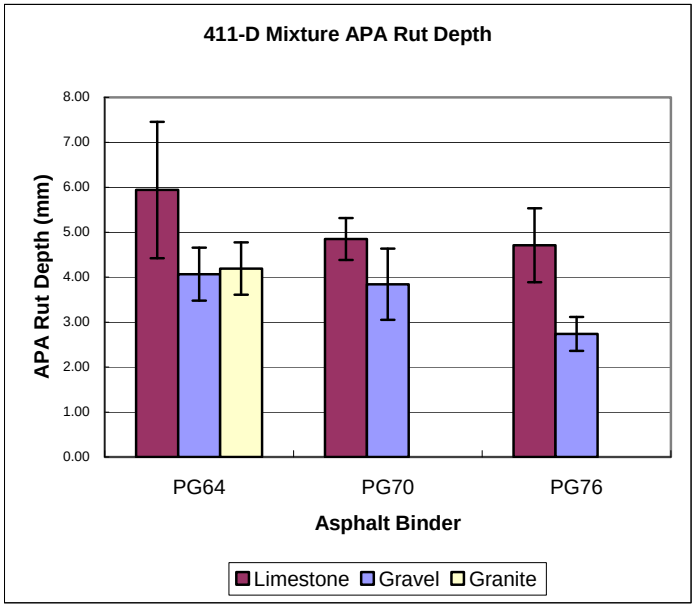

(a) 411-D Mixtures

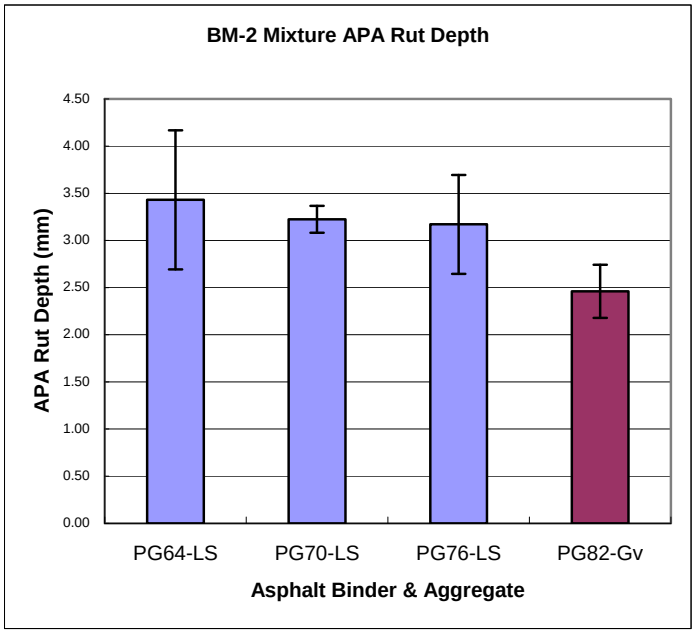

(b) 307 BM-2 Mixtures

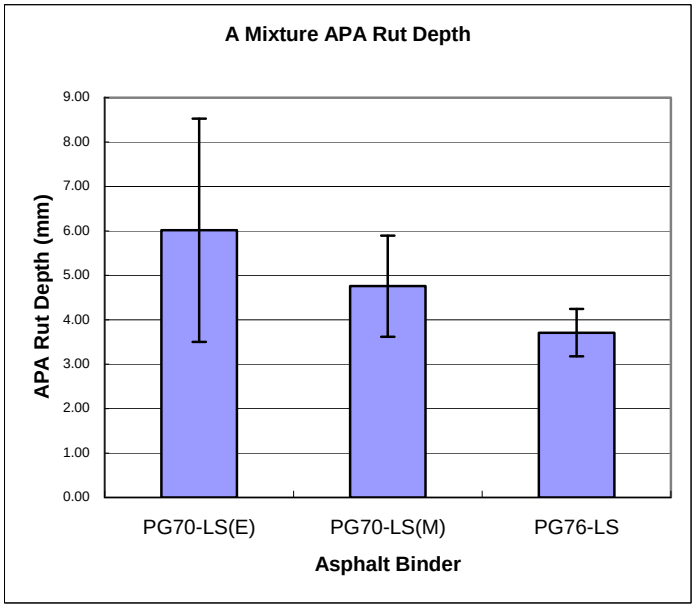

(c) 307 A Mixtures

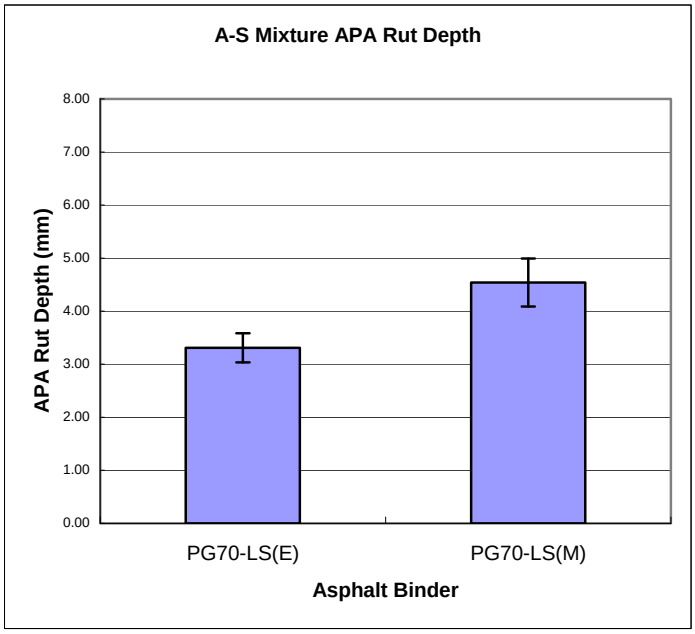

(d) 307 A-S Mixtures

Figure 4-8 APA Test Results

4.5 Results from Superpave IDT Tests

Results from the Superpave IDT tests can be used to characterize the fracture resistance properties of HMA mixtures. Figure 4-9 presents the indirect tensile resilient modulus results from the Superpave IDT resilient modulus test for each asphalt mixture. Generally, the higher the upper grade limit of asphalt binder, the higher the resilient modulus of asphalt mixture. This implied that use of modified asphalt binder could increase the resilient modulus of asphalt mixtures. From Figure 4-9(a), it is also observed that gravel mixtures generally exhibited higher resilient modulus value than limestone mixtures with same PG grade asphalt binder.

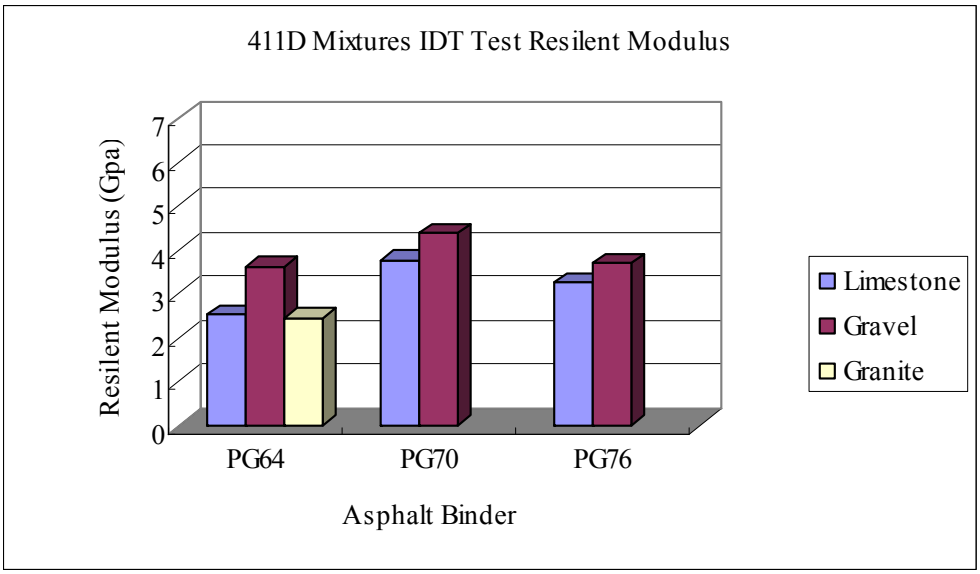

(a) 411-D Mixtures

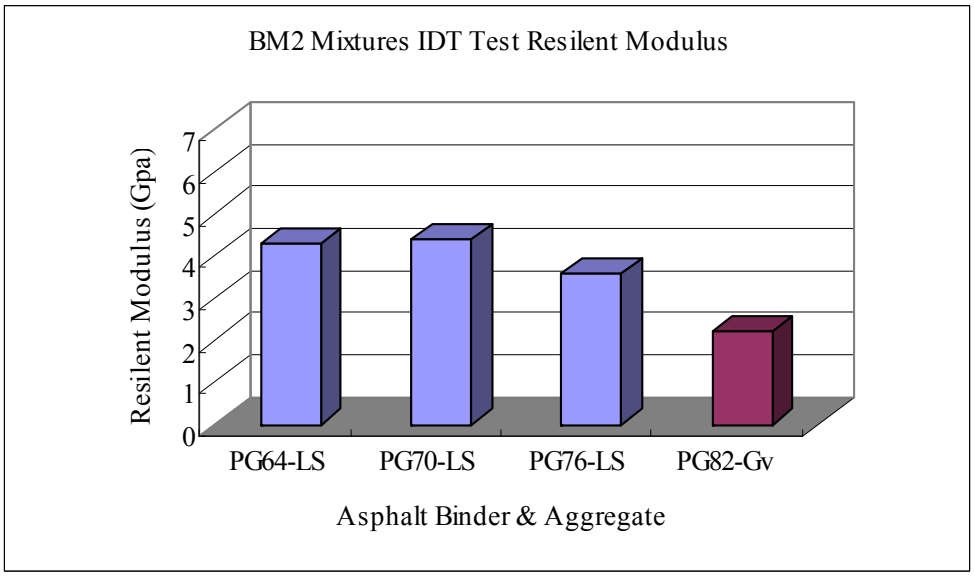

(b) 307 BM-2 Mixtures

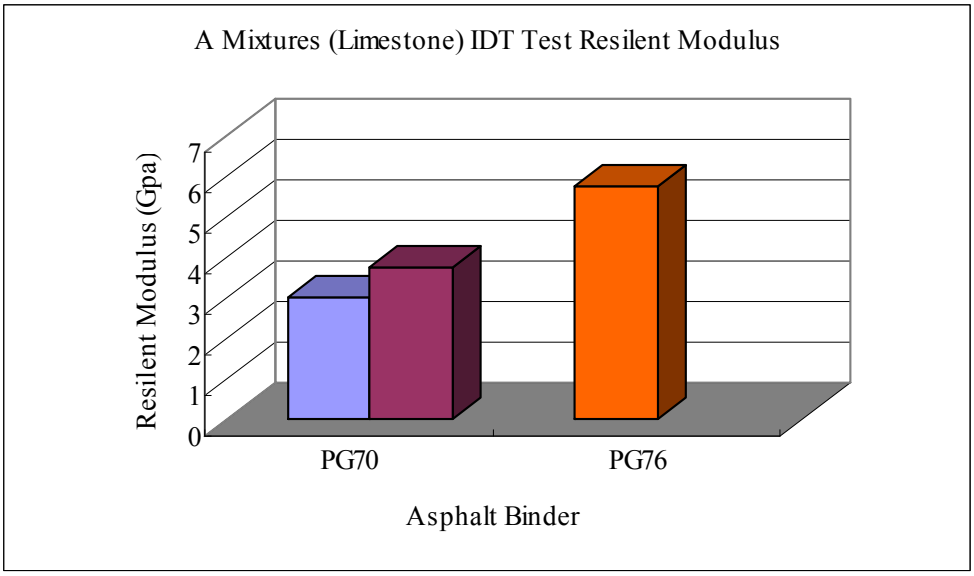

(c) 307 A Mixtures

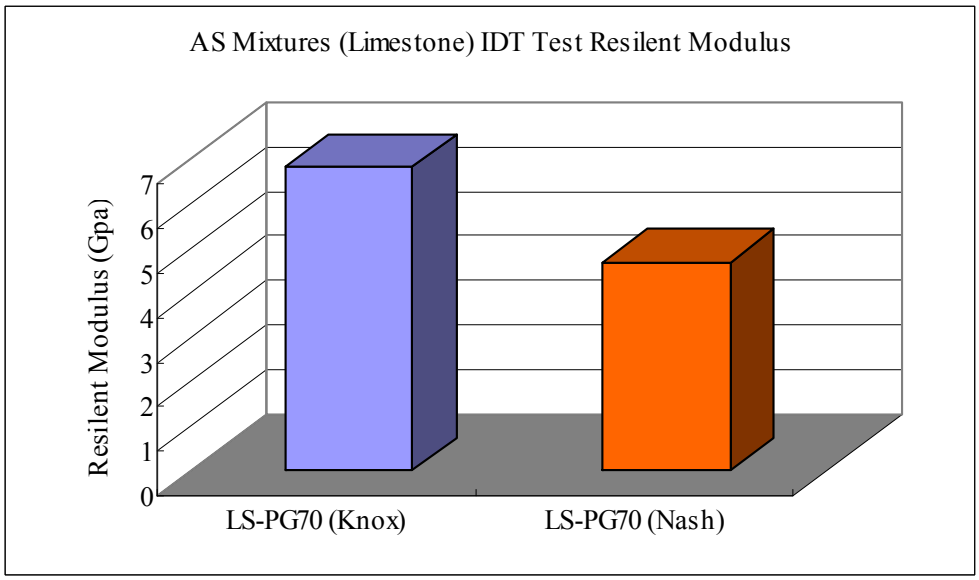

(d) 307 A-S Mixtures

Figure 4-9 Indirect Tensile Resilient Modulus Results

Figure 4-10 graphically presents the indirect tensile creep compliance results from

the Superpave IDT creep test for all the asphalt mixtures used for this study. Generally, use of asphalt binder with higher upper grade limit resulted in lower creep compliance of asphalt mixture, which was consistent with the findings from the resilient modulus test. Figure 4-10(a) shows that limestone mixtures had higher creep compliance than gravel mixtures containing same PG grade asphalt binder.

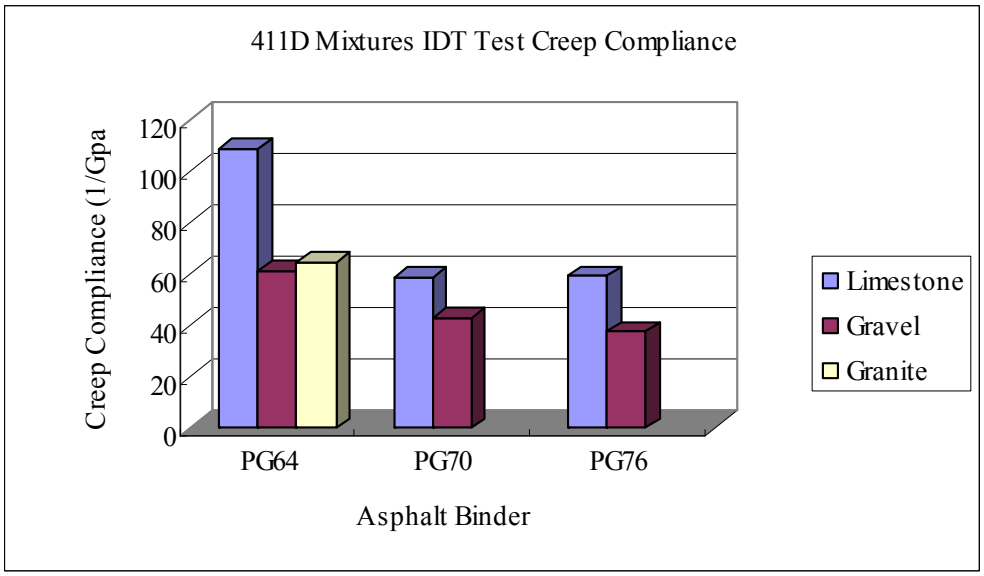

(a) 411-D Mixtures

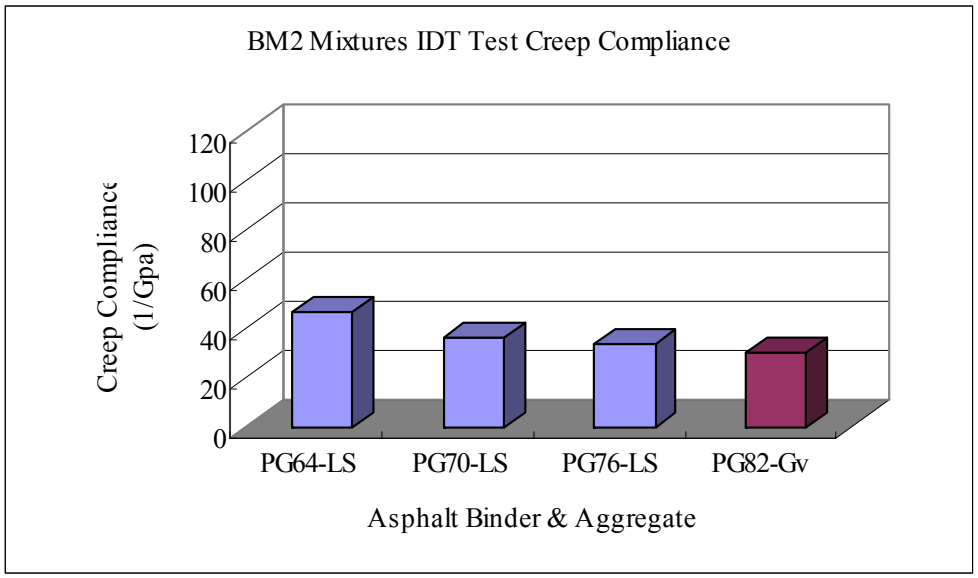

(b) 307 BM-2 Mixtures

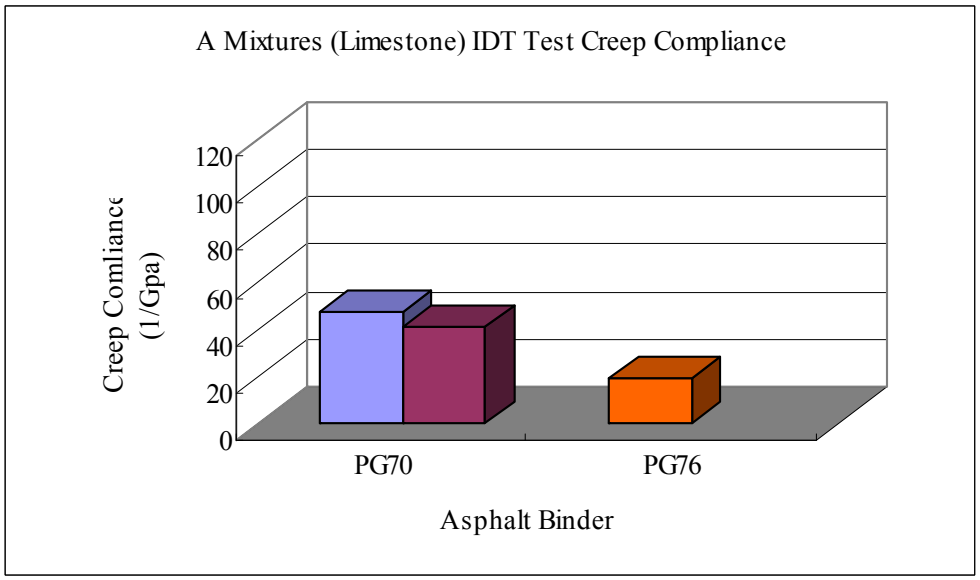

(c) 307 A Mixtures

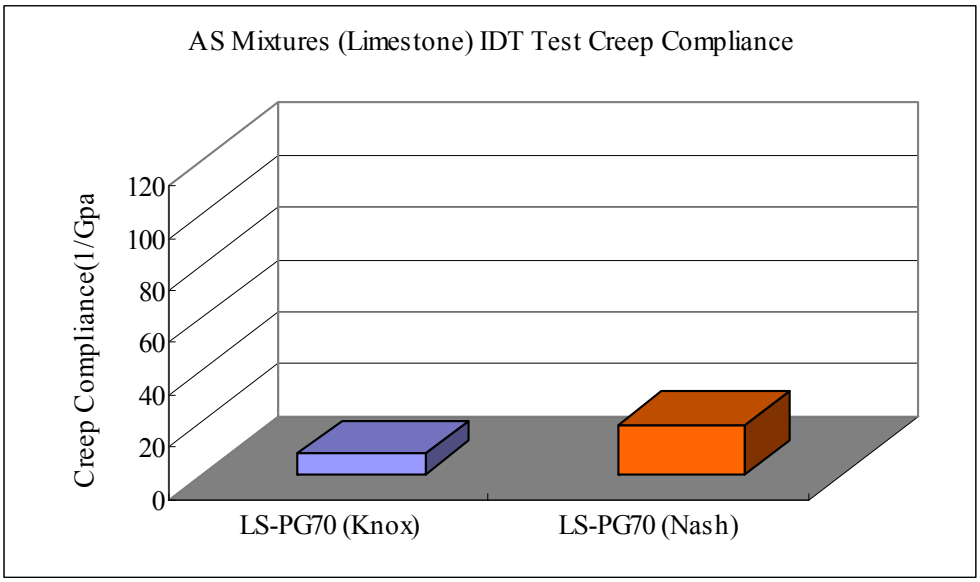

(d) 307 A-S Mixtures

Figure 4-10 Indirect Tensile Creep Compliance Results

Figure 4-11 shows the m-values obtained from the regressed equations for the creep compliances. The m-value is the exponent of the power function used to fit to the creep compliance data. The higher the m-value, the more flexible the asphalt mixture. From Figure 4-11, it can be seen that with the increase in the upper PG grade limit, asphalt mixtures showed lower m-values, which means mixtures became stiffer. This further confirmed the resilient modulus and creep compliance results.

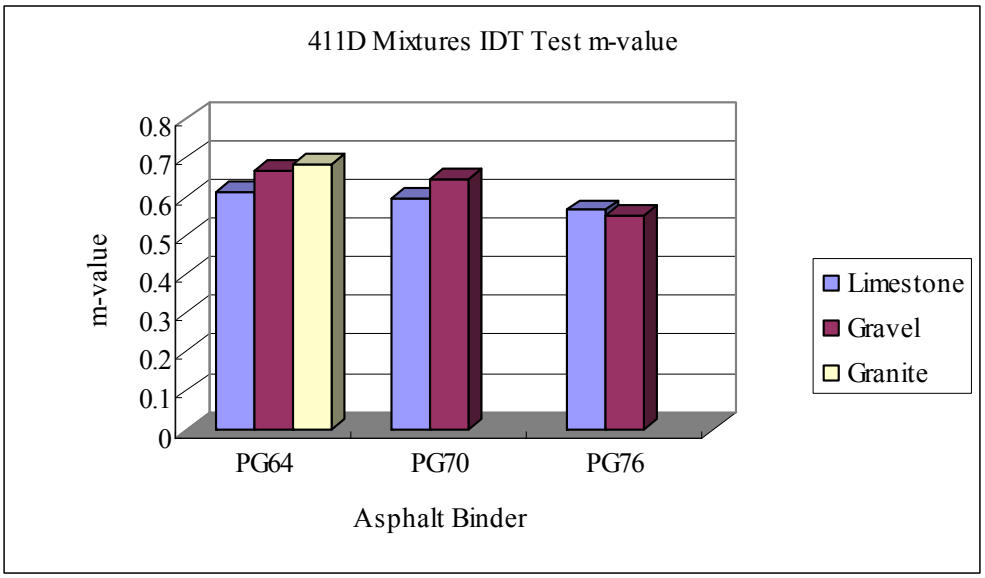

(a) 411-D Mixtures

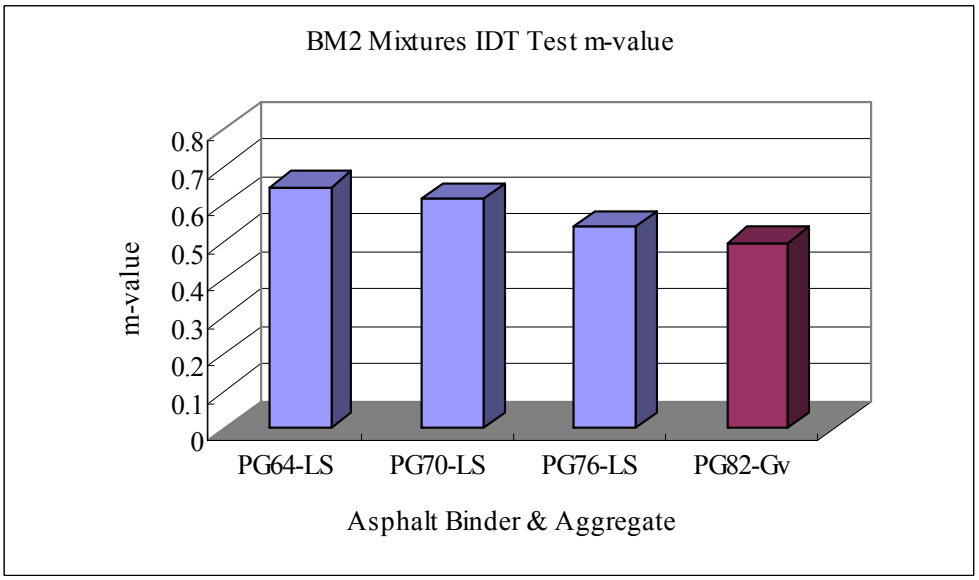

(b) 307 BM-2 Mixtures

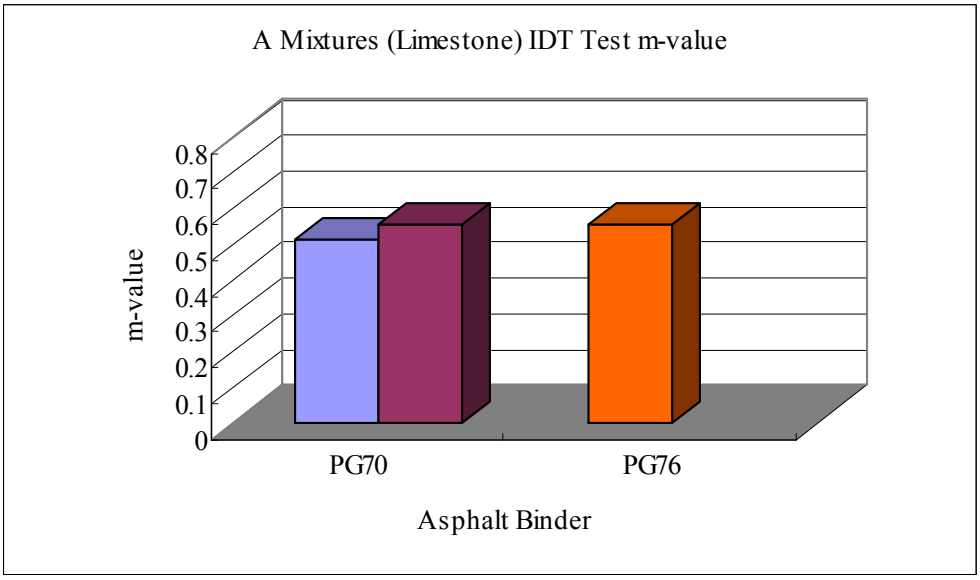

(c) 307 A Mixtures

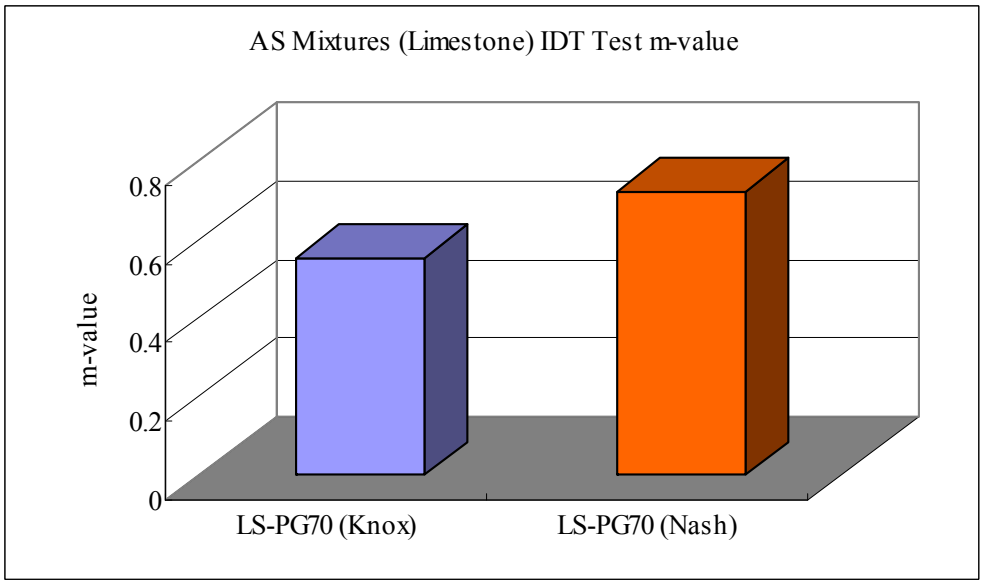

(d) 307 A-S Mixtures

Figure 4-11 m-Values from Creep Compliance Results

Figure 4-12 presents the indirect tensile strength results from the Superpave IDT

strength test for each asphalt mixture. Generally, the higher the upper grade limit of asphalt binder, the stronger the asphalt mixture. This means that use of modified asphalt binder can increase the strength of asphalt mixtures, and thus ultimately improve the bearing capacity of asphalt pavements.

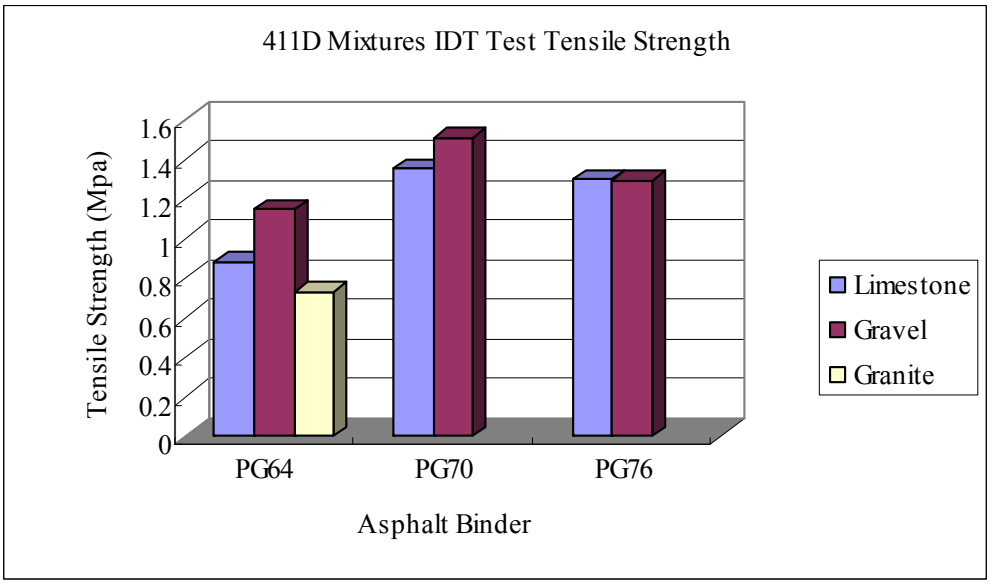

(a) 411-D Mixtures

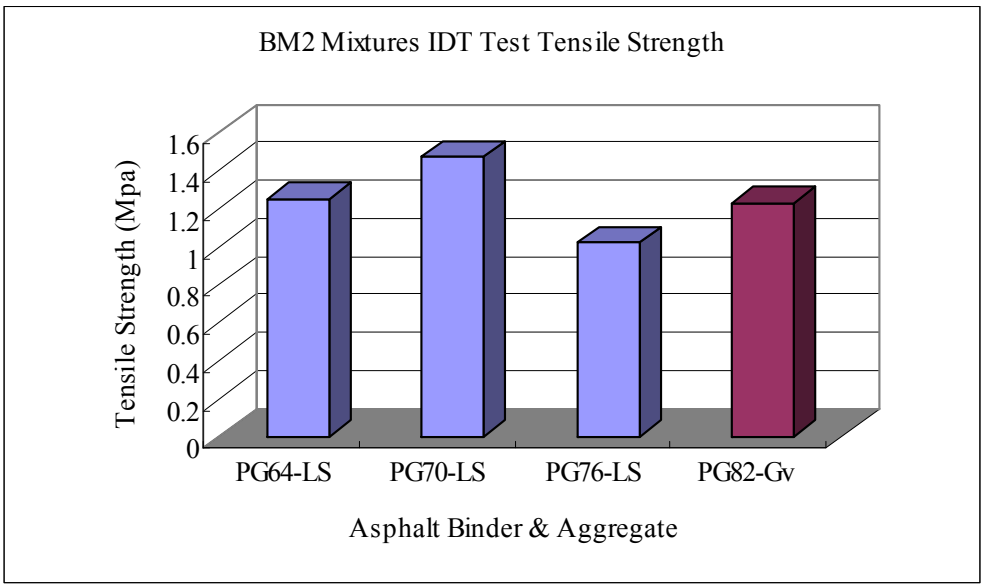

(b) 307 BM-2 Mixtures

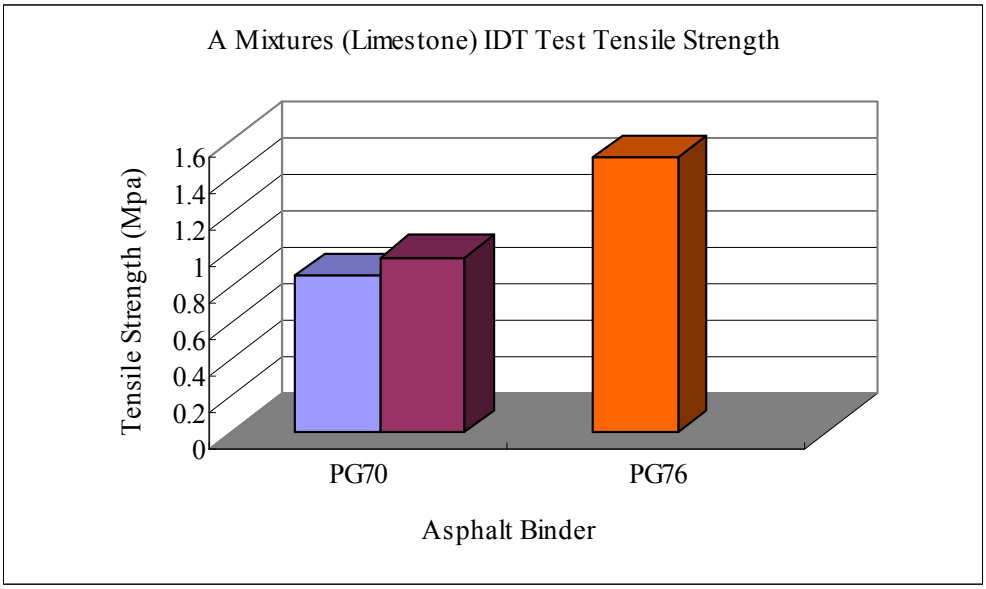

(c) 307 A Mixtures

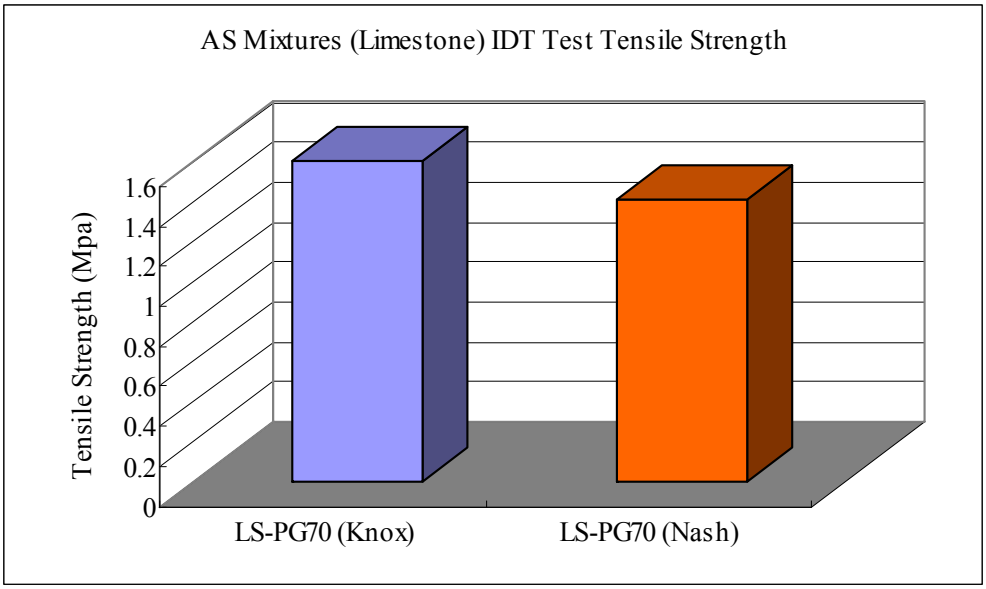

(d) 307 A-S Mixtures

Figure 4-12 Indirect Tensile Strength Results

Figure 4-13 presents the strain at the peak stress (failure strain) from the Superpave IDT strength test for each asphalt mixture. It is clearly observed that with the increase in the upper grade limit of asphalt binder, asphalt mixtures exhibited higher IDT strength. This implies that incorporation of modified asphalt binder could result in stronger asphalt mixtures. Therefore, use of modified asphalt binder could lead to dual advantages: increase in both the strength and the failure strain, which indicates that asphalt mixtures containing modified asphalt binder could absorb much more energy than the conventional asphalt binder mixtures. This will be confirmed later in this chapter with the fracture energy concept.

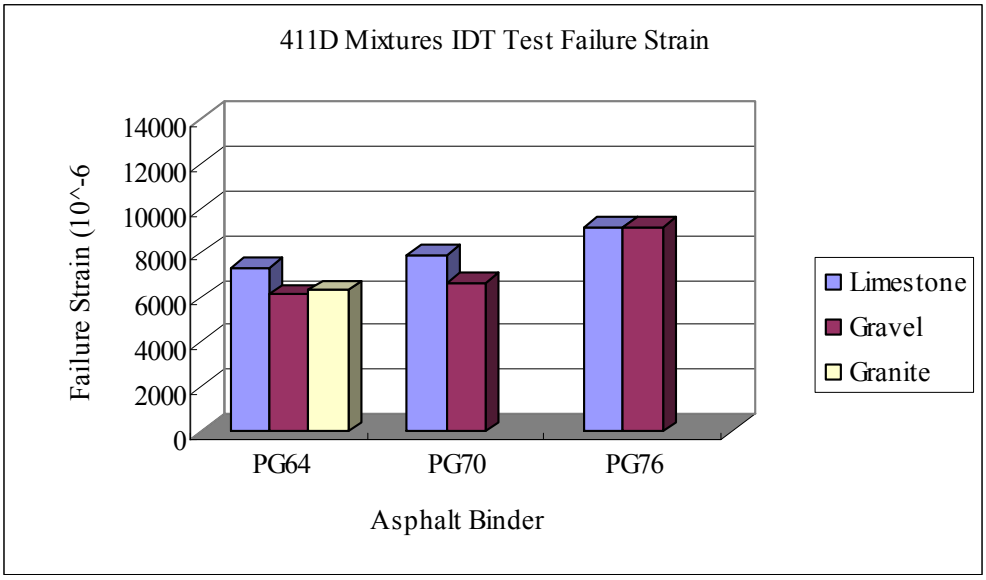

(a) 411-D Mixtures

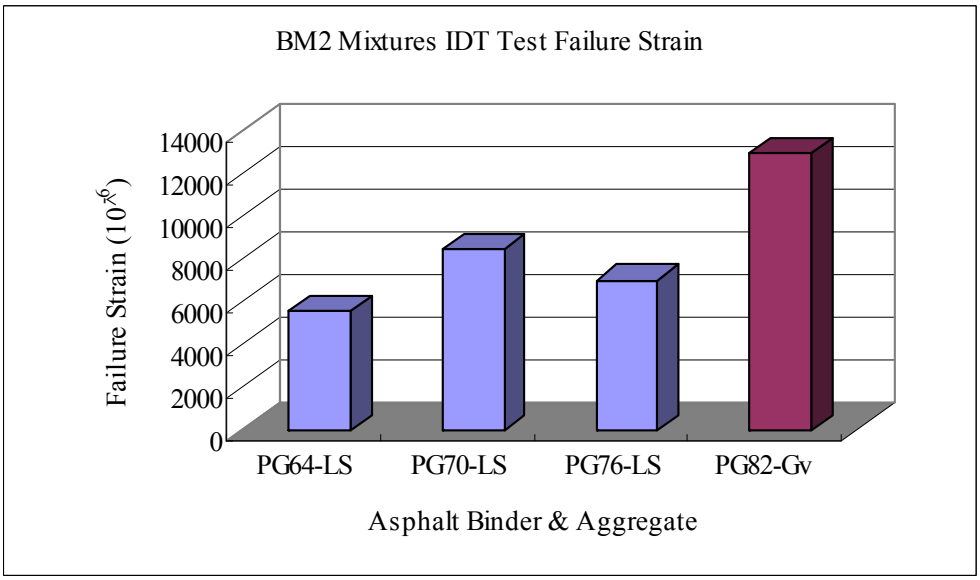

(b) 307 BM-2 Mixtures

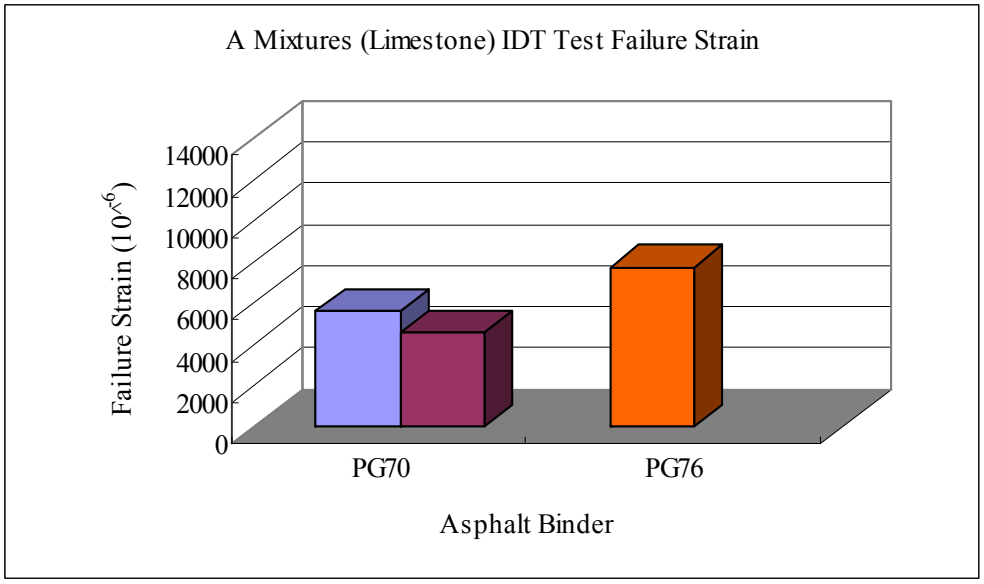

(c) 307 A Mixtures

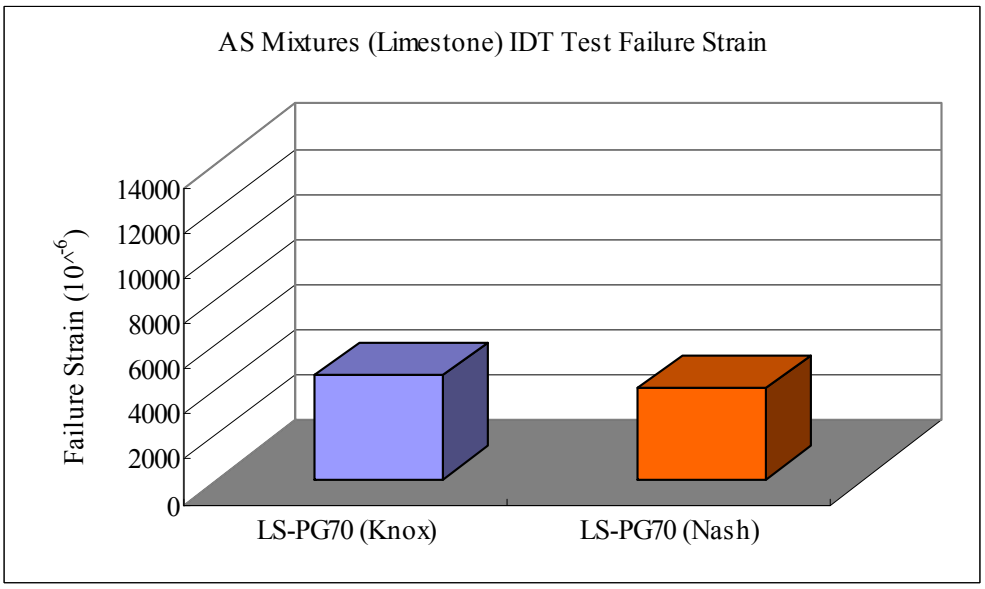

(d) 307 A-S Mixtures

Figure 4-13 IDT Failure Strain Results

Figure 4-14 presents the fracture energy results obtained from the Superpave IDT

tests for each asphalt mixture. Based on the previous analysis, use of modified asphalt binder could increase both the strength and the failure strain of asphalt mixtures, thus leading to the higher fracture energy value that asphalt mixtures could absorb. The improved energy absorbing capacity of asphalt mixtures is clearly confirmed in Figure 4-14. It is obvious that asphalt mixtures containing modified asphalt binder exhibited significantly higher fracture energy than conventional asphalt binder mixtures (PG 64-22 mixtures). The improved energy absorbing capacity of asphalt mixtures will help resist fatigue and fracture failure, thus leading to longer service life of asphalt pavements.

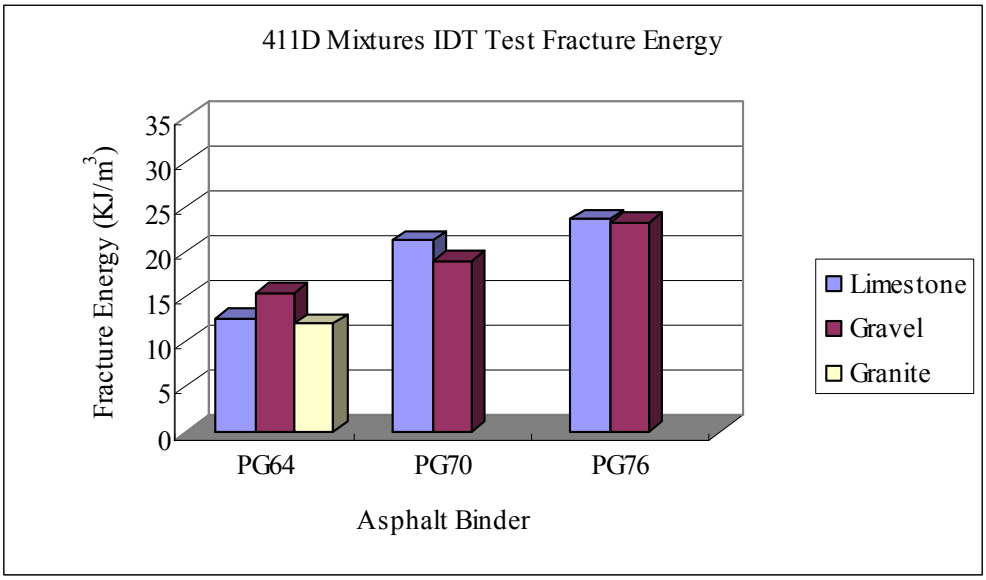

(a) 411-D Mixtures

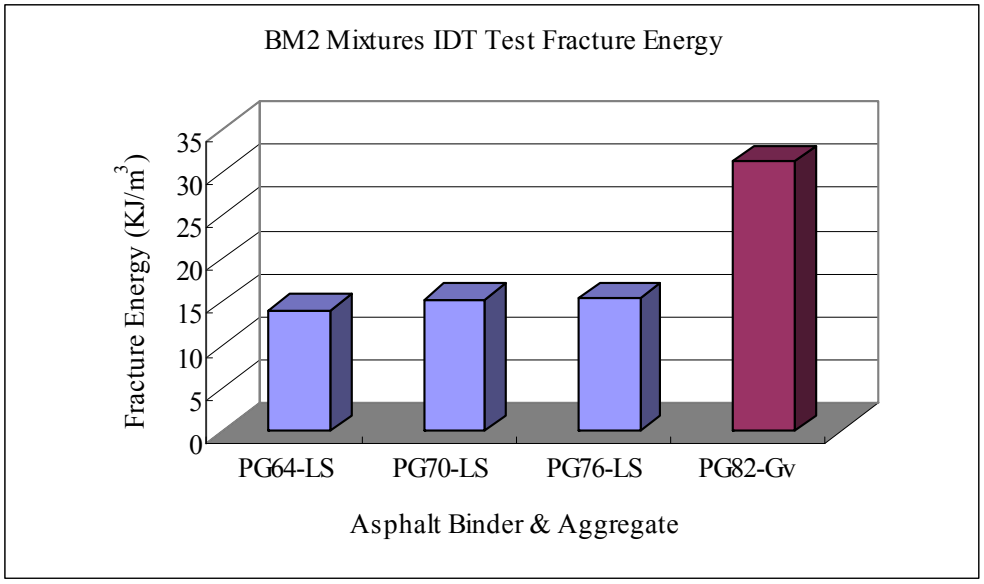

(b) 307 BM-2 Mixtures

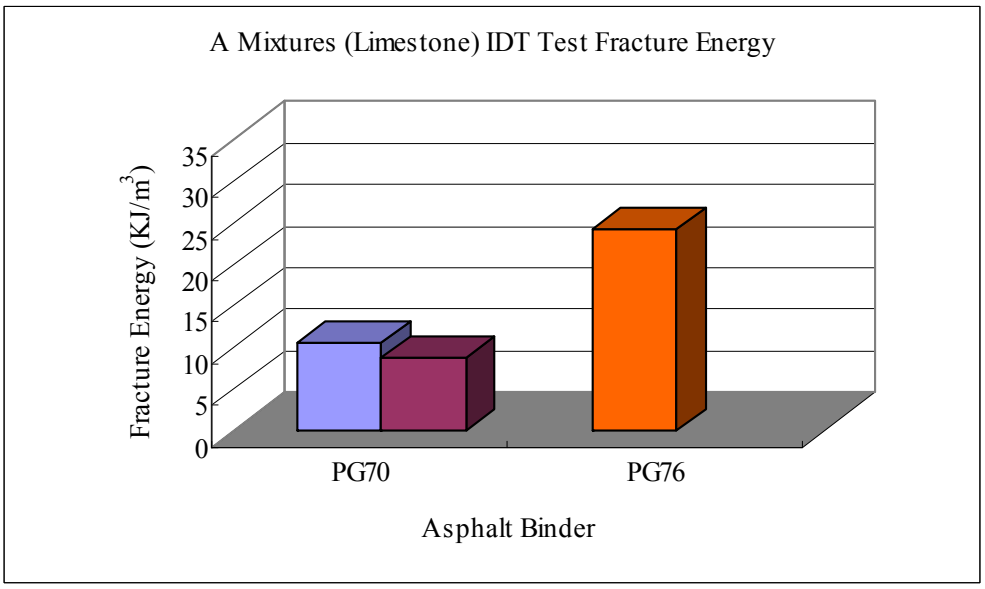

(c) 307 A Mixtures

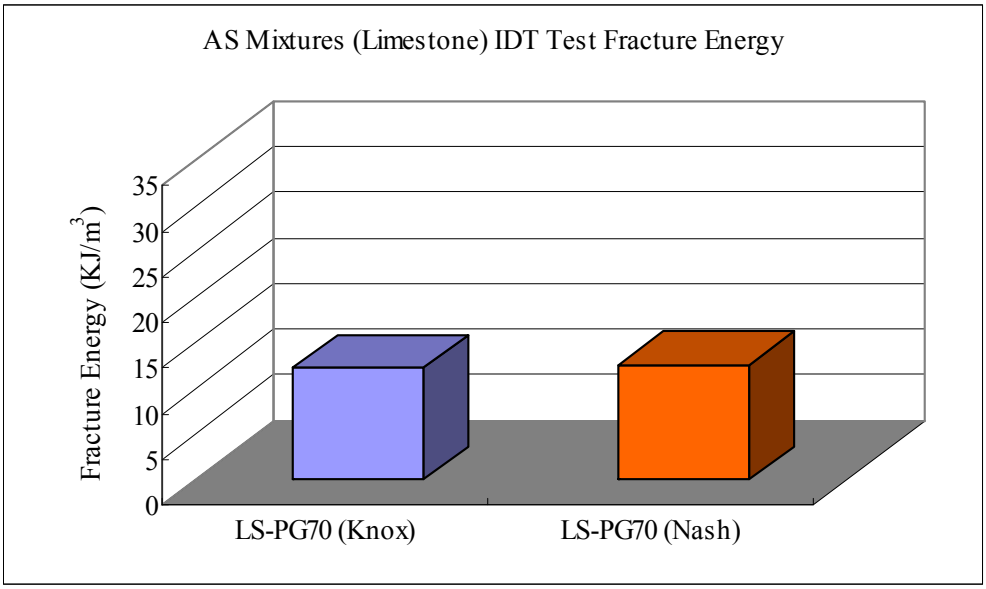

(d) 307 A-S Mixtures

Figure 4-14 IDT Fracture Energy Results

Figure 4-15 presents the dissipate creep strain energy threshold ($DCSE_f$) results from the Superpave IDT tests for each asphalt mixture. $DCSE_f$ is actually the part of fracture energy with the elastic energy excluded from the total fracture energy because the elastic energy does not contribute to the fatigue resistance of asphalt mixtures. From Figure 4-15, it is clearly observed that the $DCSE_f$ values of asphalt mixtures increased with the increase in the upper grade limit of asphalt binder, which implies that asphalt mixtures containing modified asphalt binder was potentially more resistant to fatigue or fracture failure than asphalt mixtures with conventional asphalt binder.

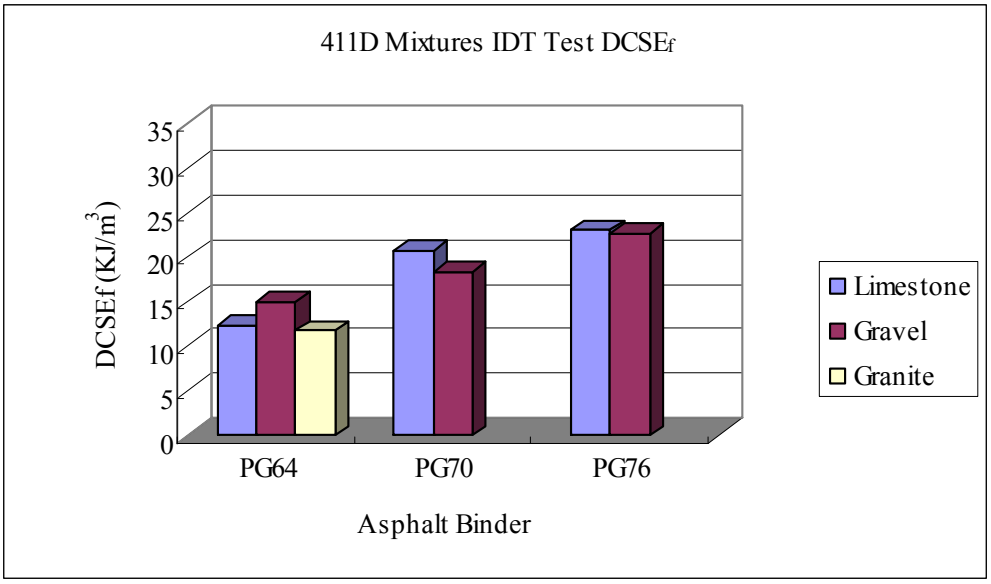

(a) 411-D Mixtures

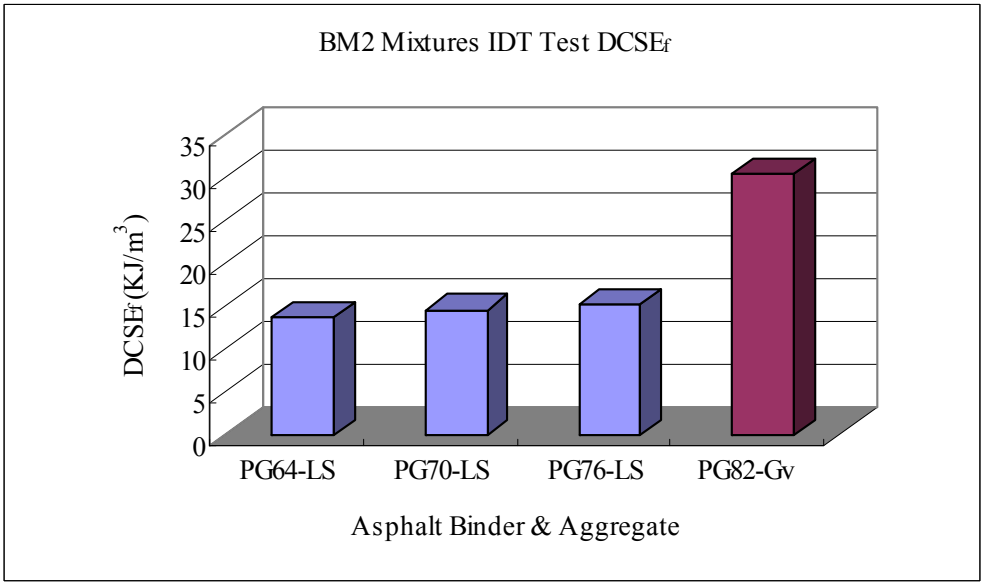

(b) 307 BM-2 Mixtures

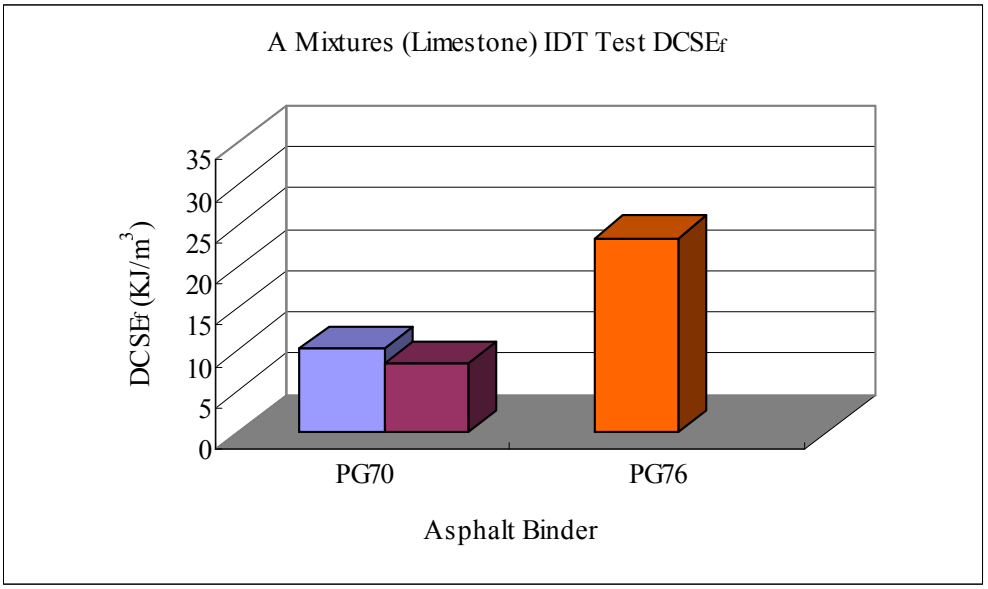

(c) 307 A Mixtures

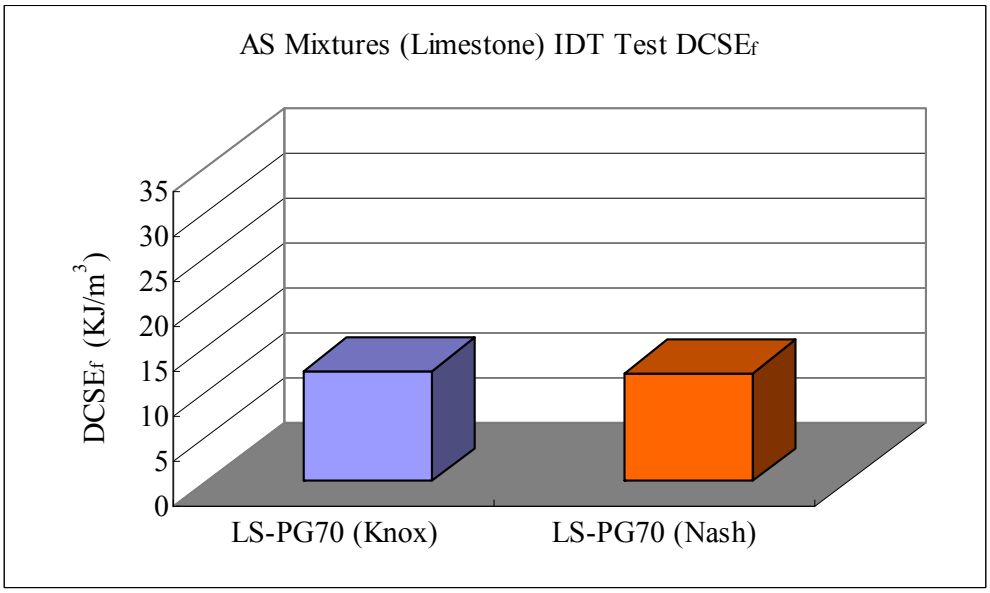

(d) 307 A-S Mixtures

Figure 4-15 Dissipated Creep Strain Energy Threshold ($DCSE_f$) Results

Figure 4-16 presents the energy ratio results from the Superpave IDT tests for

each asphalt mixture. The energy ratio concept proposed by Roque et al. (2004) is used to characterize the fatigue fracture resistance of asphalt mixtures. The larger the energy ratio, the higher the fatigue resistance of asphalt mixtures. From Figure 4-16, it can be seen that with the increase in the upper grade limit of asphalt binder, asphalt mixtures generally exhibited higher energy ratio value, which indicates higher resistance of asphalt mixtures to fatigue fracture. The improved energy ratio was significant for the 411-D surface mixtures (Figure 4-16a).

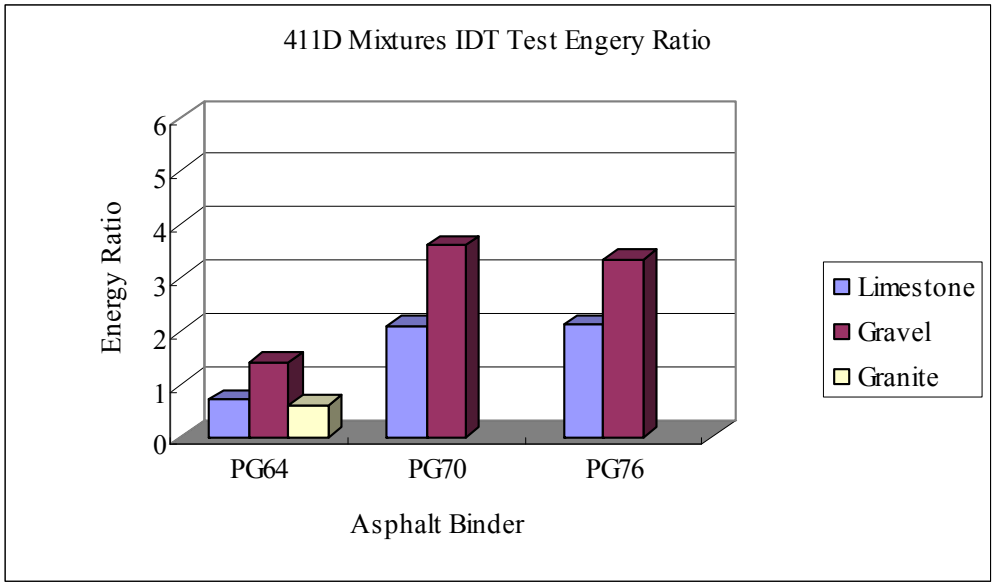

(a) 411-D Mixtures

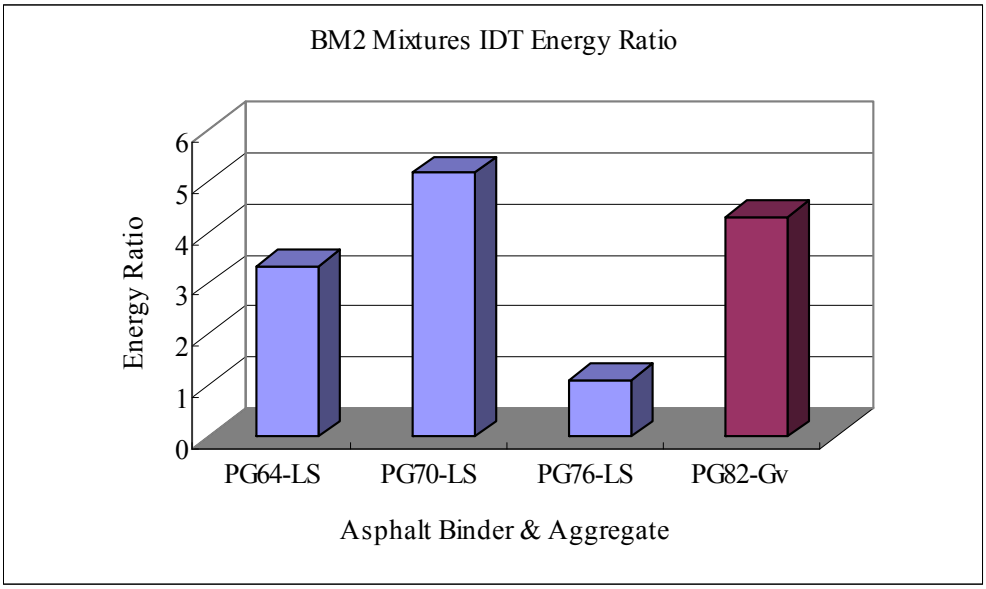

(b) 307 BM-2 Mixtures

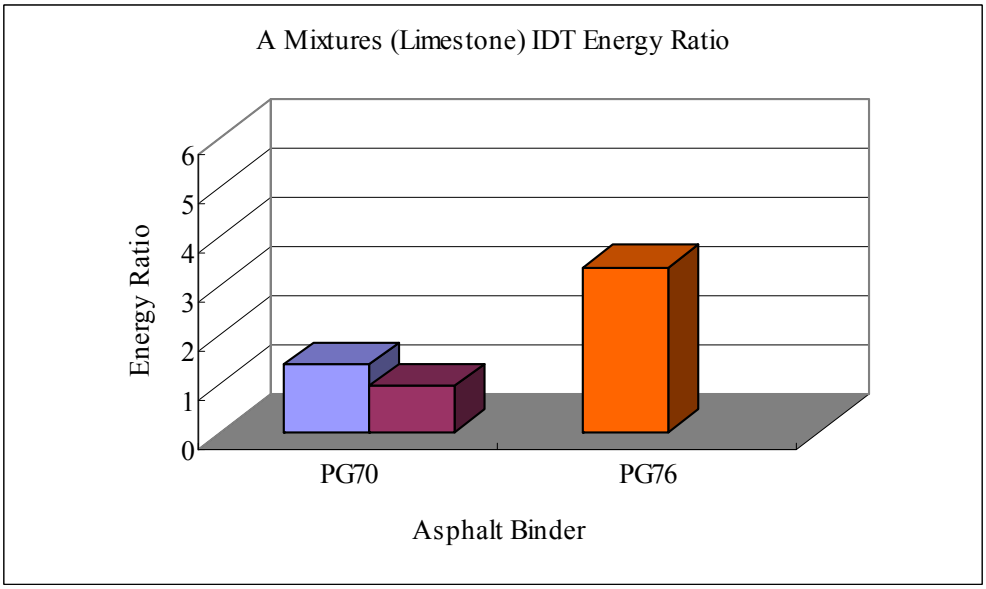

(c) 307 A Mixtures

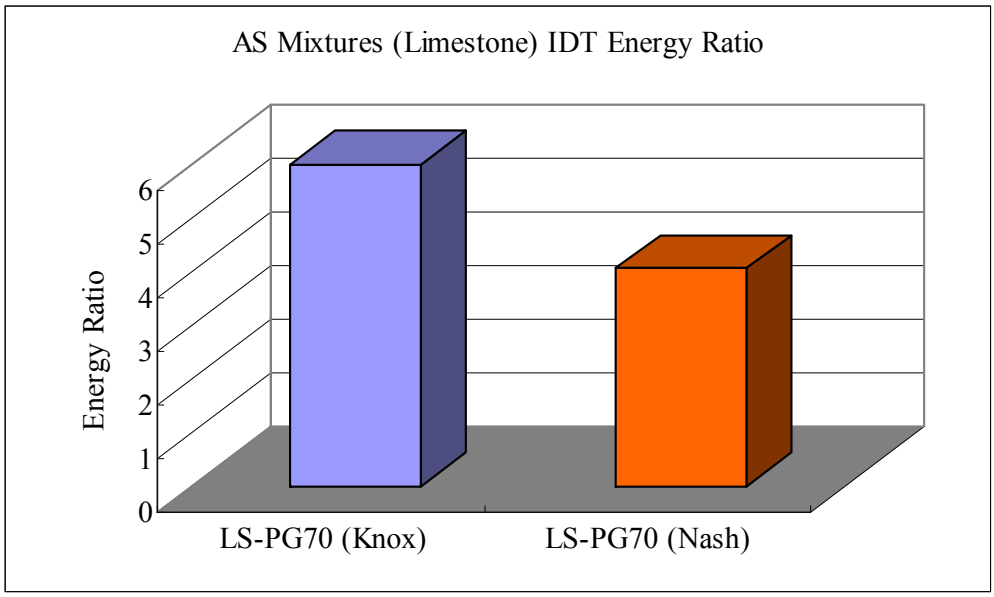

(d) 307 A-S Mixtures

Figure 4-16 Energy Ratio Results

4.6 Beam Fatigue Test Results

Figure 4-17 presents the fatigue life (load cycle to failure) results based on the 50% reduction in the initial stiffness from the beam fatigue test for each mixture. Figure 4-17 clearly shows that with the increase in the upper grade limit of asphalt binder, asphalt mixtures experienced much more load cycles, which indicates that asphalt mixtures were more fatigue resistant if produced with modified asphalt binder. The extended fatigue life due to modified asphalt binder can potentially lead to longer service life of asphalt pavements.

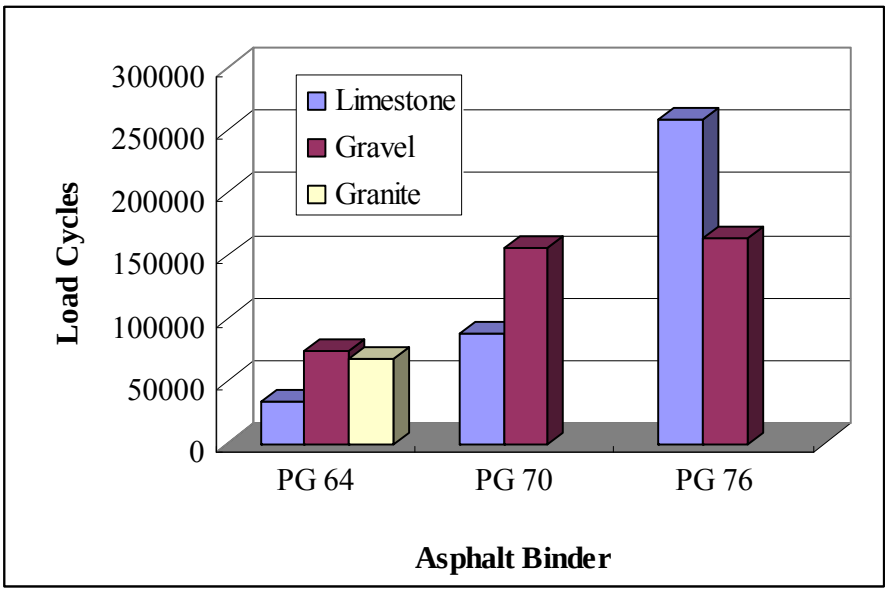

(a) 411-D Mixtures

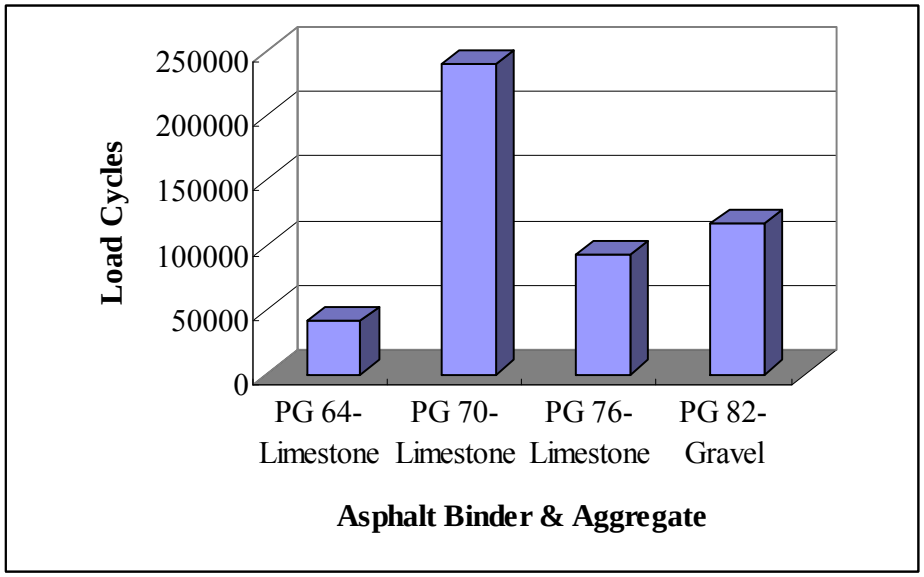

(b) 307 BM-2 Mixtures

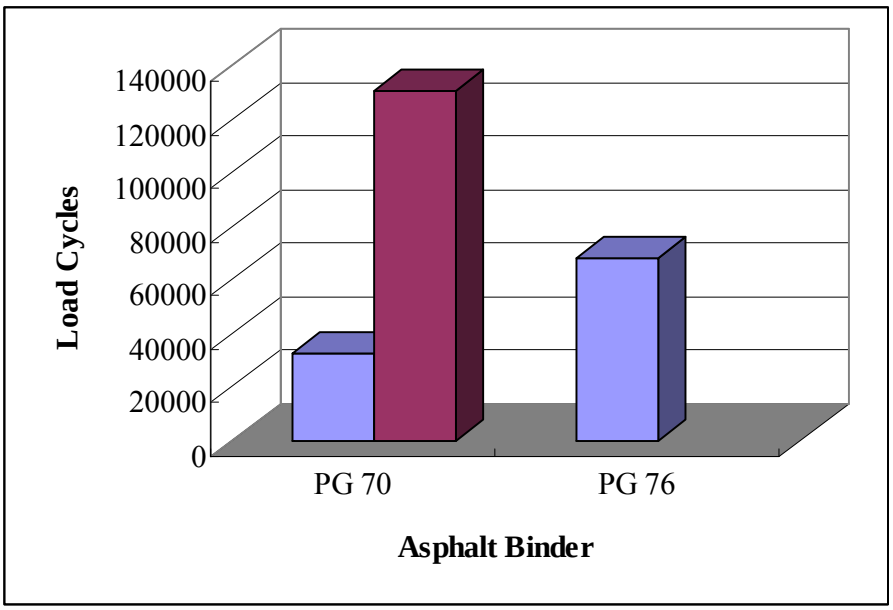

(c) 307 A Mixtures

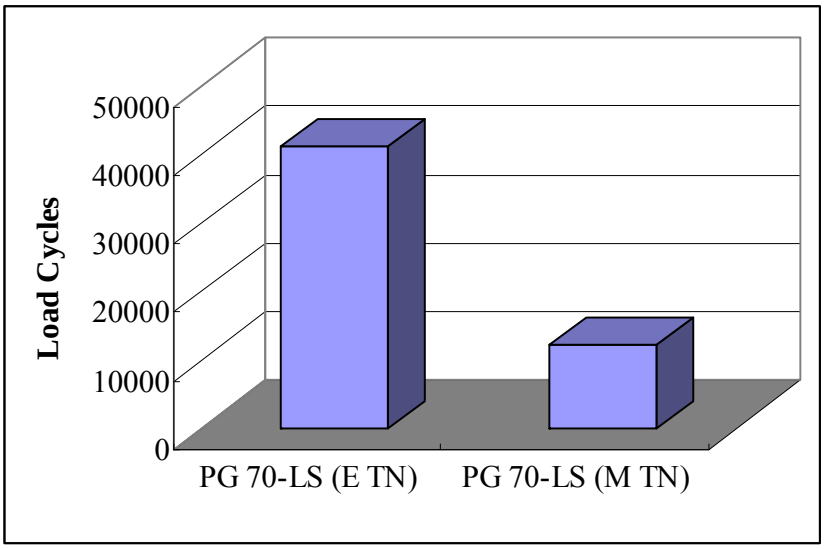

(d) 307 A-S Mixtures

Figure 4-17 Fatigue Life Results According to the 50% Stiffness Reduction

Figure 4-18 presents the plateau value results obtained from the beam fatigue test for each mixture based on the analysis method proposed by Shen and Carpenter (2005). The plateau value represents a period where there is a constant percent of input energy being turned into damage and thus can be used to characterize the fatigue life of HMA mixtures. For a strain-controlled test, the lower the PV, the longer the fatigue life for a specific HMA mixture (Shen and Carpenter, 2005).

From Figure 4-18, it can be clearly seen that with the increase in the upper grade limit of asphalt binder, asphalt mixtures exhibited significantly lower and lower plateau values. This implies that asphalt mixtures with modified asphalt binder could suffer less damage from loading than those mixtures with conventional asphalt binder and sustain more load cycles, thus leading to longer service life.

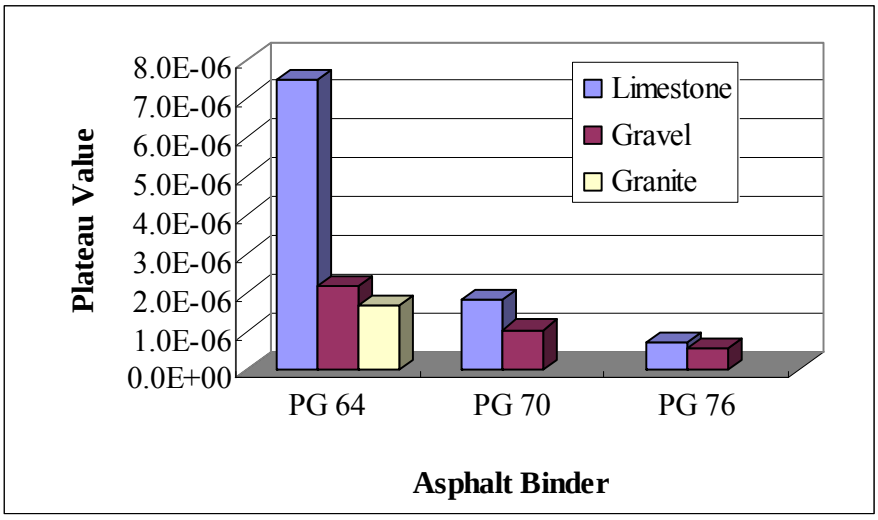

(a) 411-D Mixtures

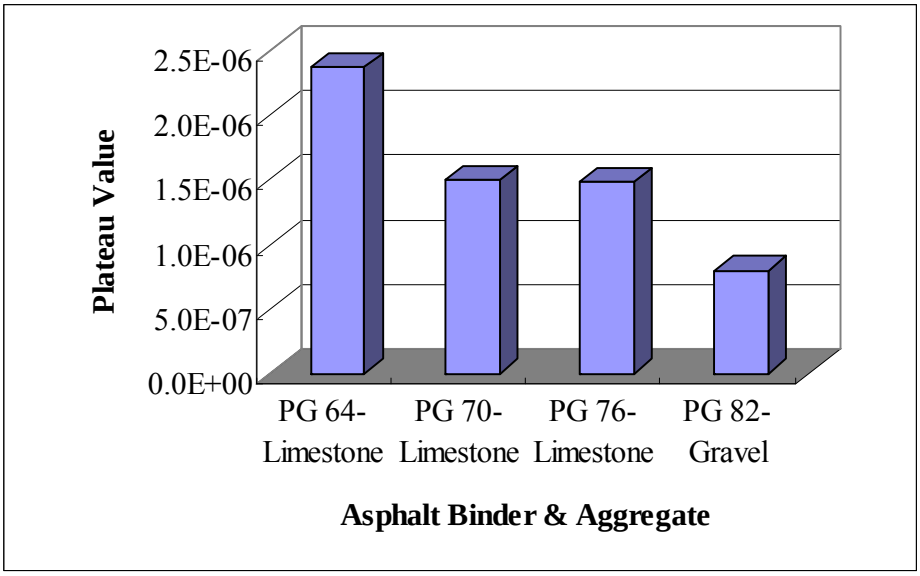

(b) 307 BM-2 Mixtures

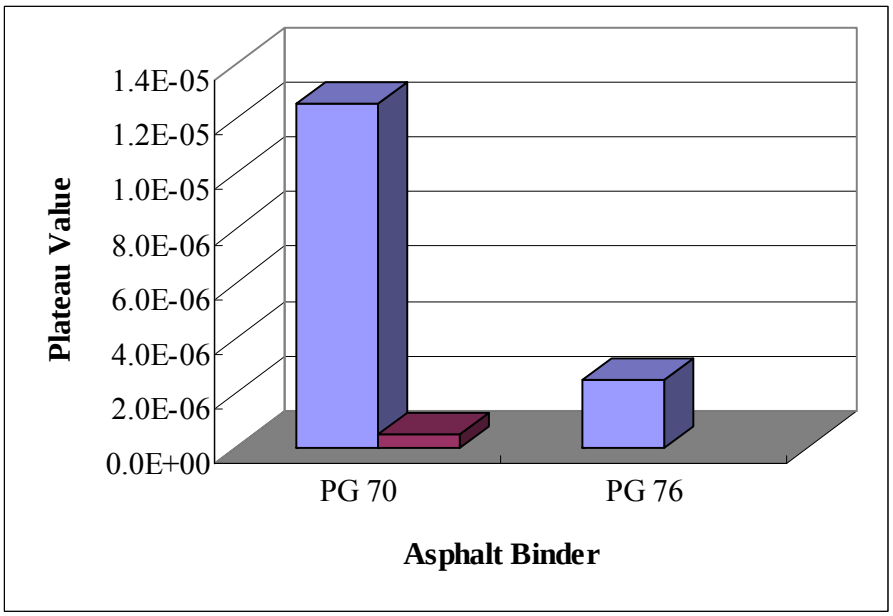

(c) 307 A Mixtures

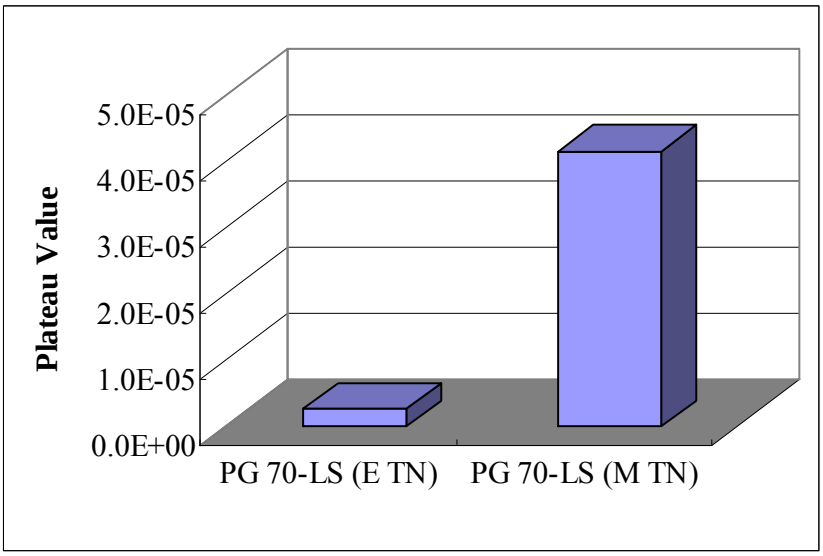

(d) 307 A-S Mixtures

Figure 4-18 Plateau Value Results

4.7 Semi-Circular Bending (SCB) Test Results

Figure 4-19 presents the semi-circular bending (SCB) strength results from the SCB strength test for each mixture. Generally, with the increase in the upper grade limit of asphalt binder, asphalt mixtures showed higher SCB strength. This means that use of modified asphalt binder could produce stronger asphalt mixtures, which would make asphalt pavements last longer. The SCB strength results were consistent with the IDT strength data.

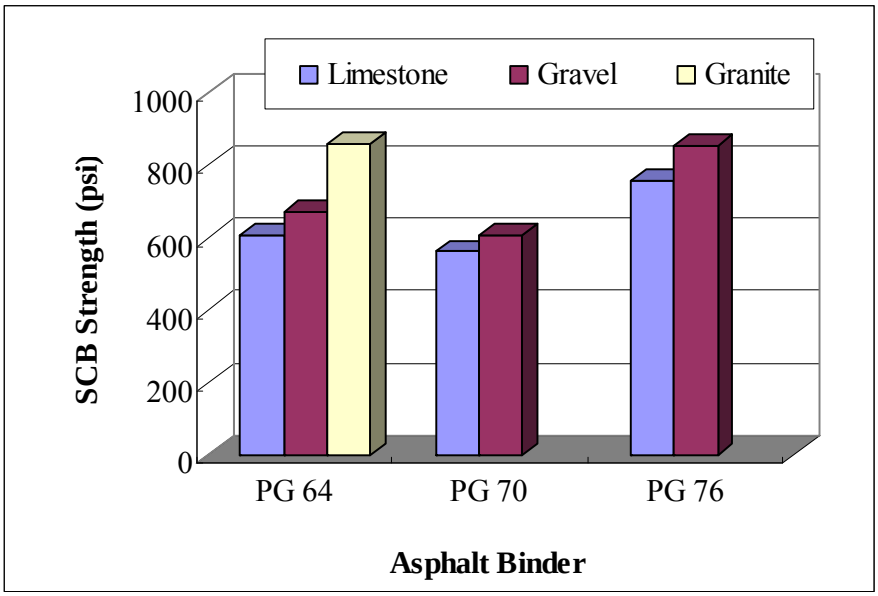

(a) 411-D Mixtures

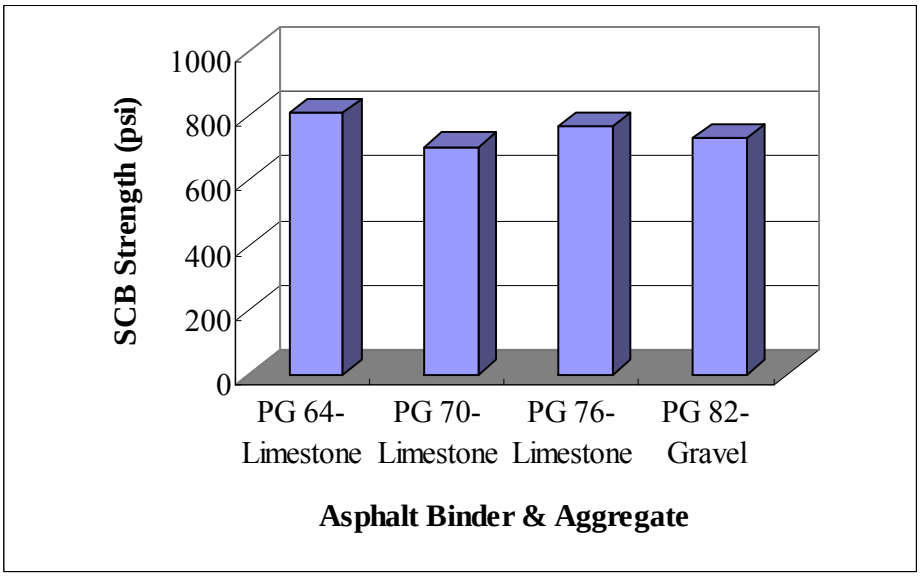

(b) 307 BM-2 Mixtures

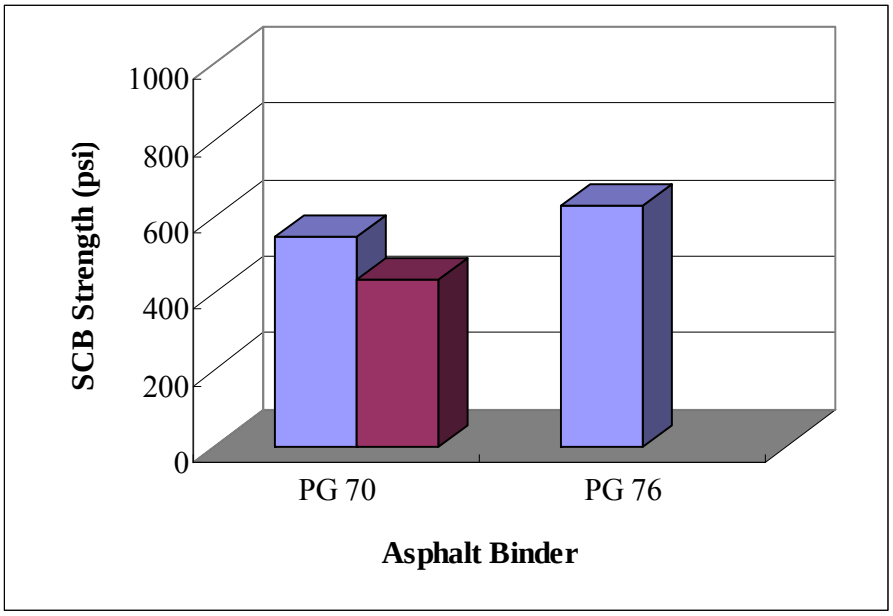

(c) 307 A Mixtures

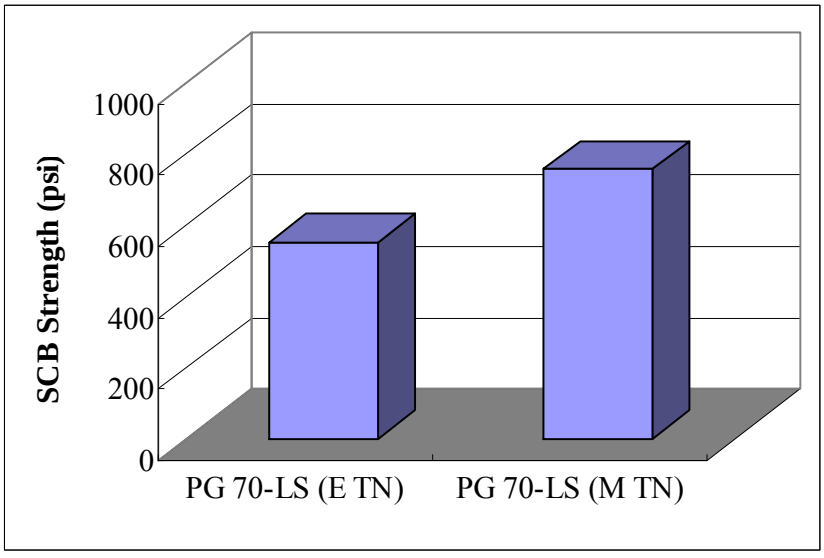

(d) 307 A-S Mixtures

Figure 4-19 SCB Strength Results

Figure 4-20 graphically presents the strain values at the peak SCB stress (failure strain) from the SCB strength test for each mixture. From Figure 4-20, no significant change in the failure strain was observed with the increase in the upper grade limit of asphalt binder. This implies the ductility of asphalt mixture did not compromise with the incorporation of modified asphalt binder. With the improved strength and similar failure strain, asphalt mixtures containing modified asphalt binder could absorb more energy those mixtures with conventional asphalt binder.

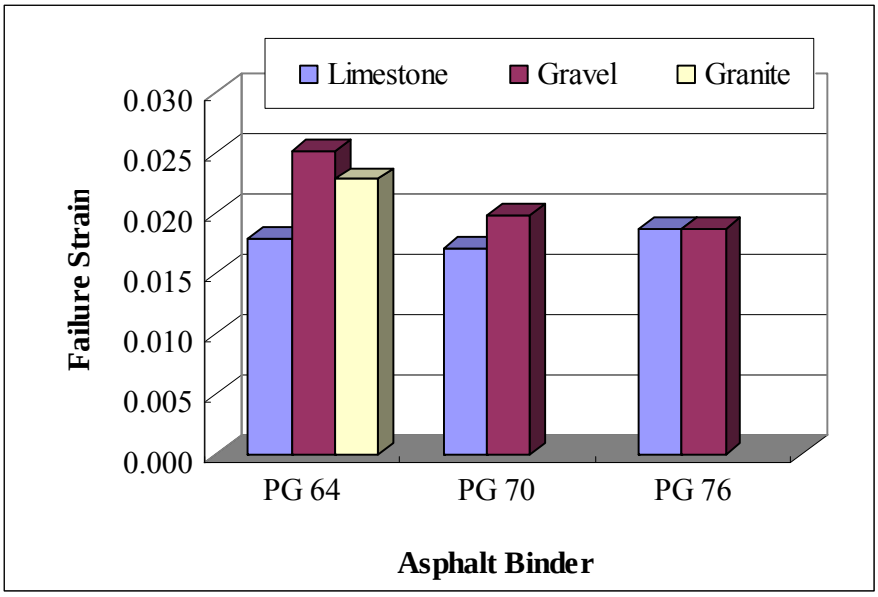

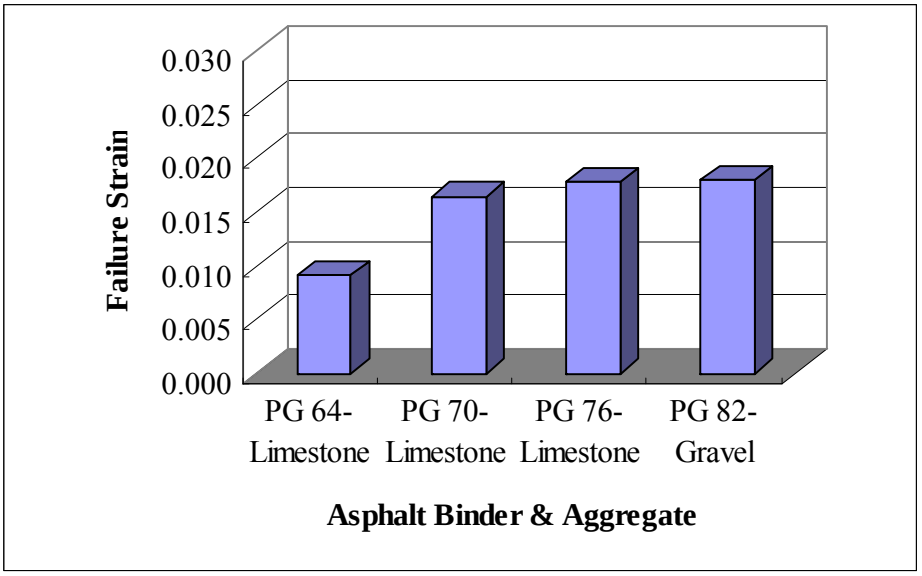

(b) 307 BM-2 Mixtures

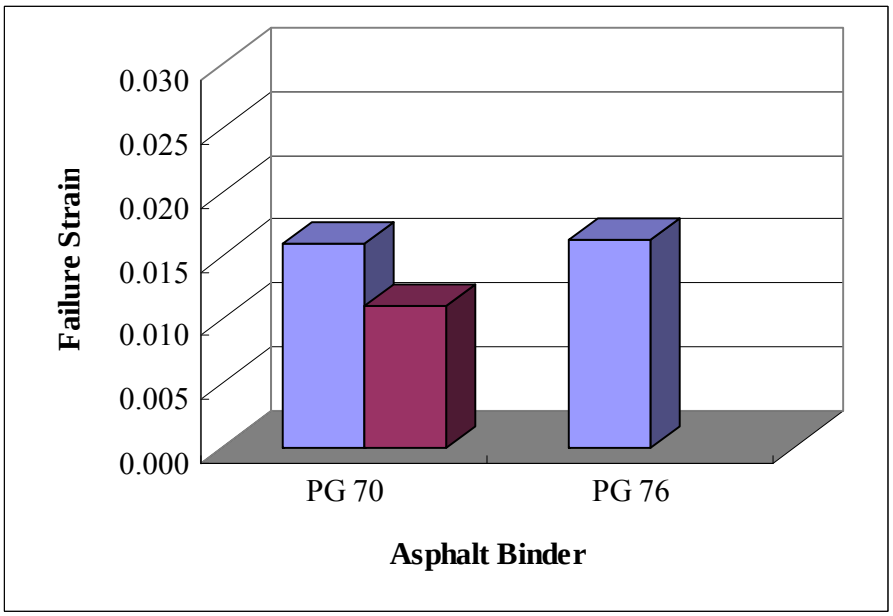

(c) 307 A Mixtures

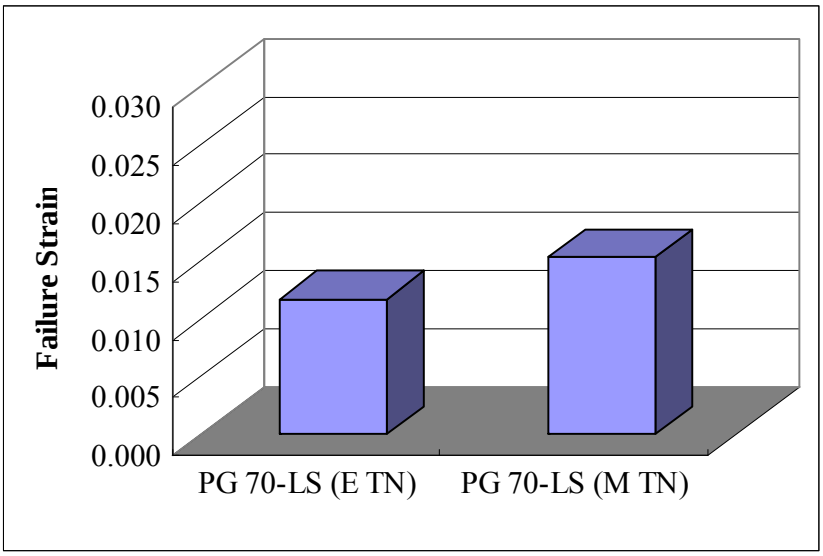

(d) 307 A-S Mixtures

Figure 4-20 SCB Failure Strain Results

The SCB fracture energy was evaluated for each mixture with the SCB notched test. The results from this test are presented in Figures 4-21 and 4-22. The fracture resistance of asphalt mixtures was evaluated at three notched depths: 0.5, 1.0, and 1.5 inches. The slope of the fracture energy vs. notch depth (Figure 4-21) represents the J-integral. The higher the J-integral, the more fracture-resistant the asphalt mixture.

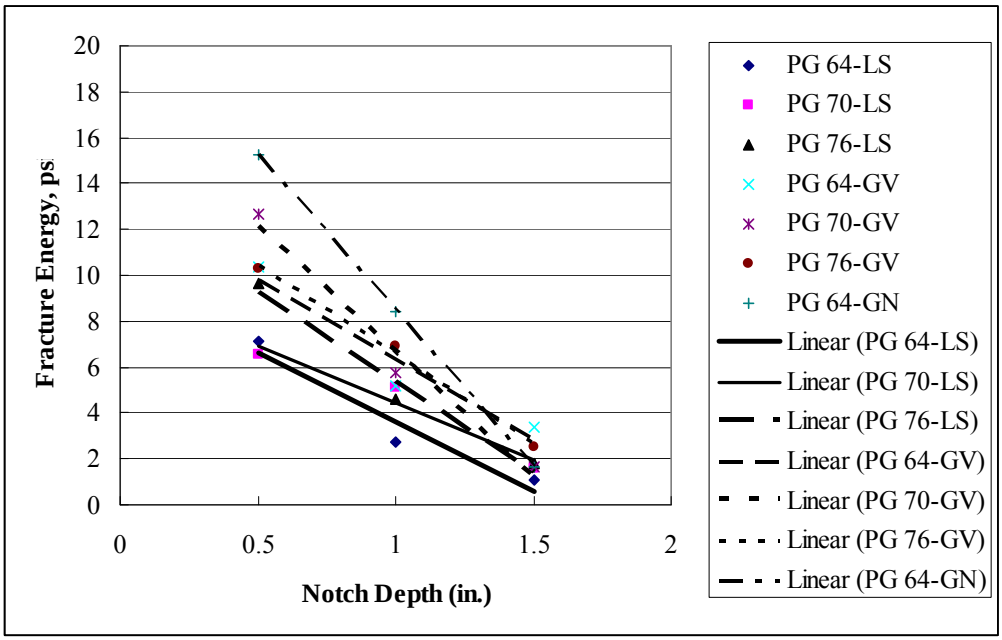

(a) 411-D Mixtures

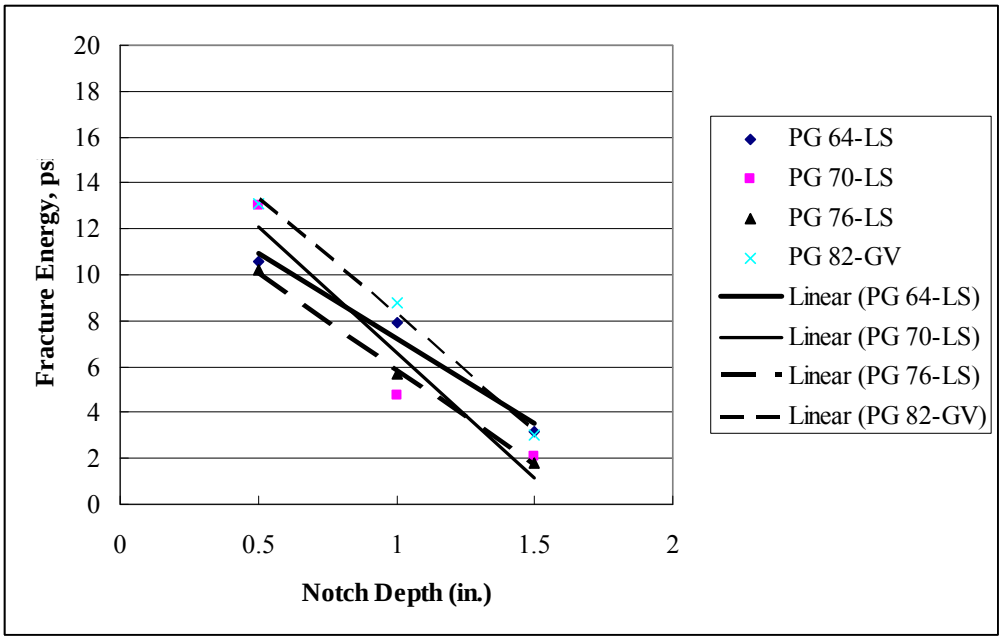

(b) 307 BM-2 Mixtures

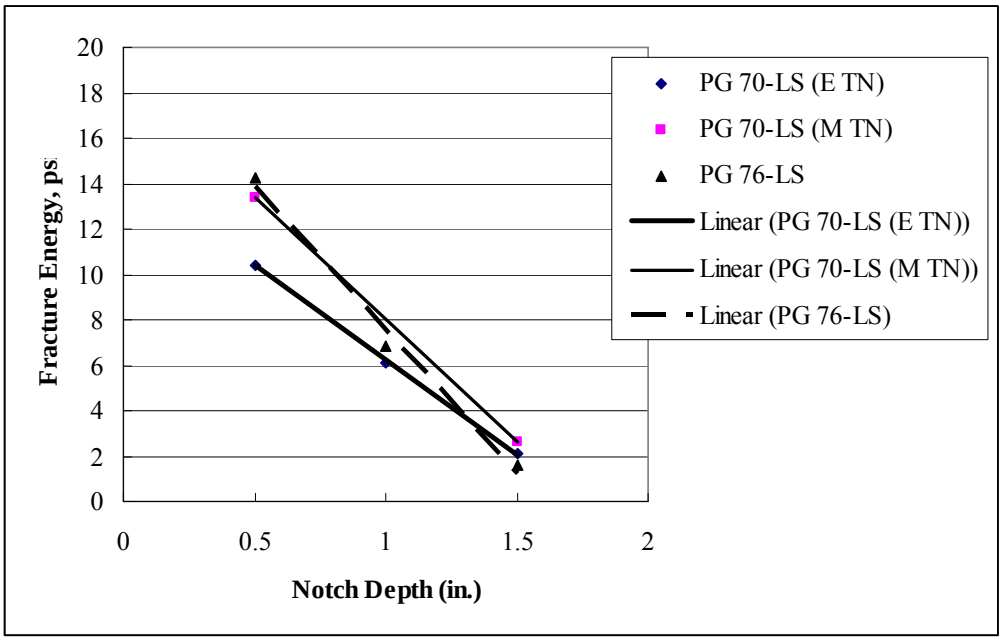

(c) 307 A Mixtures

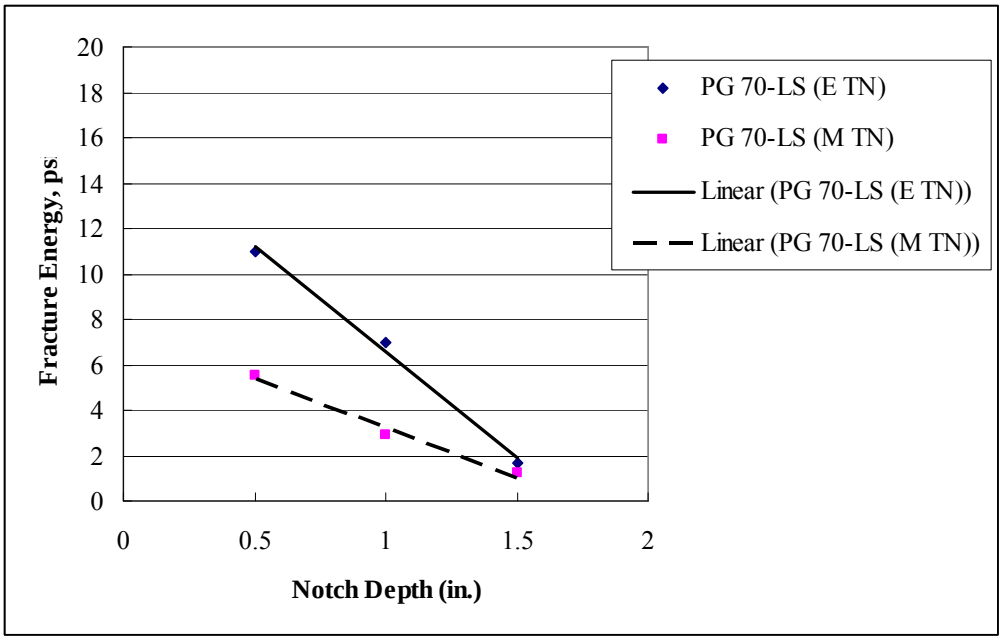

(d) 307 A-S Mixtures

Figure 4-21 SCB Notched Fracture Energy Results

A summary of the J-integral results for all mixtures is presented in Figure 4-22. Generally, the incorporation of modified asphalt binder slightly increased the J-integral values of asphalt mixtures, which means use of modified asphalt binder could improve the resistance of asphalt mixtures to fracture failure. This confirmed the findings from the Superpave IDT tests.

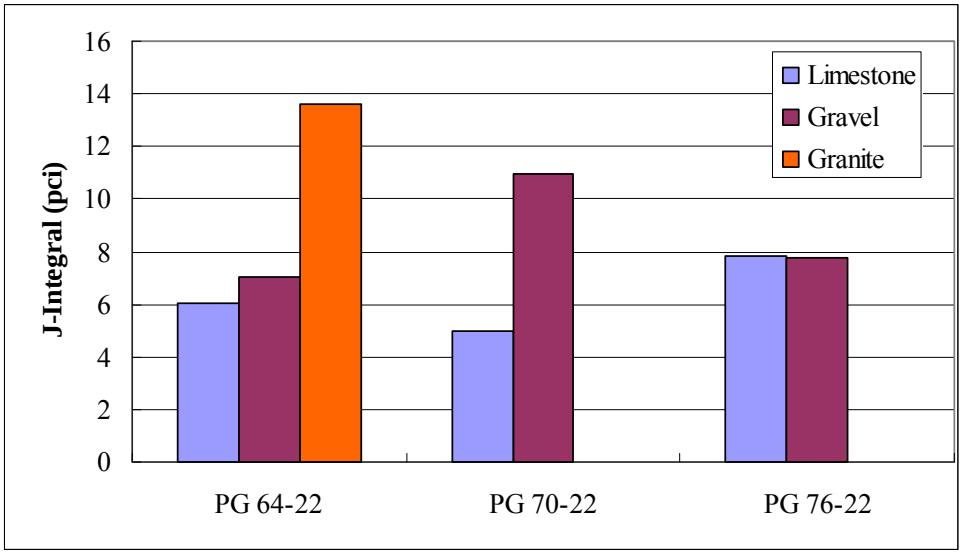

(a) 411-D Mixtures

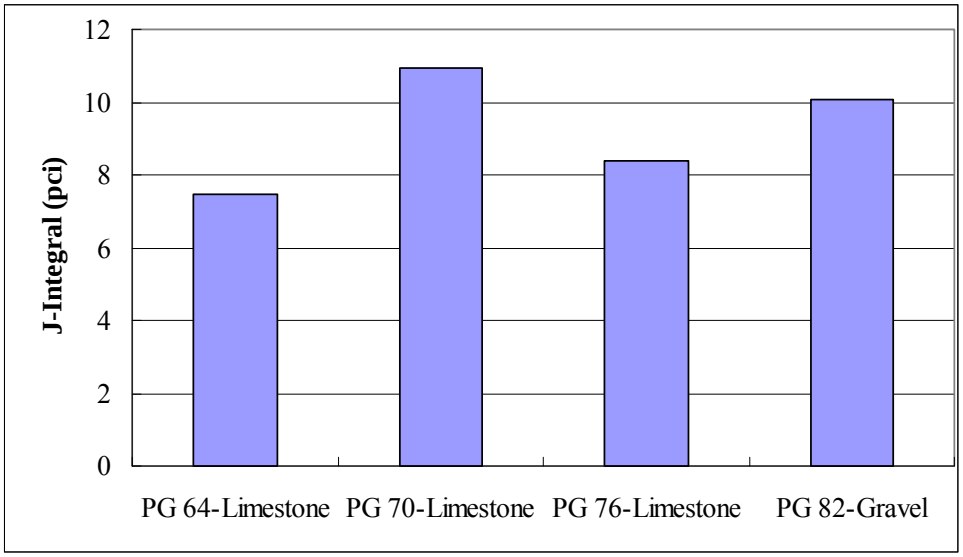

(b) 307 BM-2 Mixtures

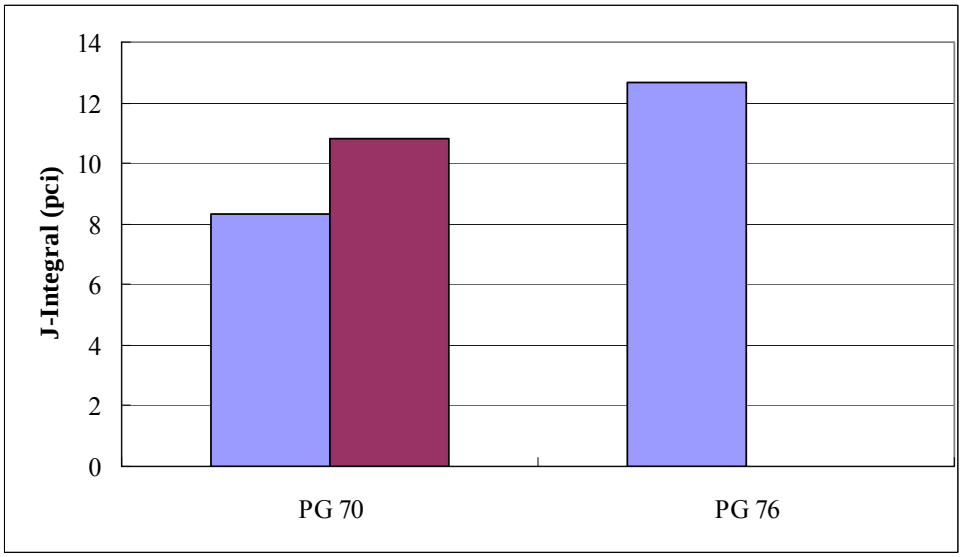

(c) 307 A Mixtures

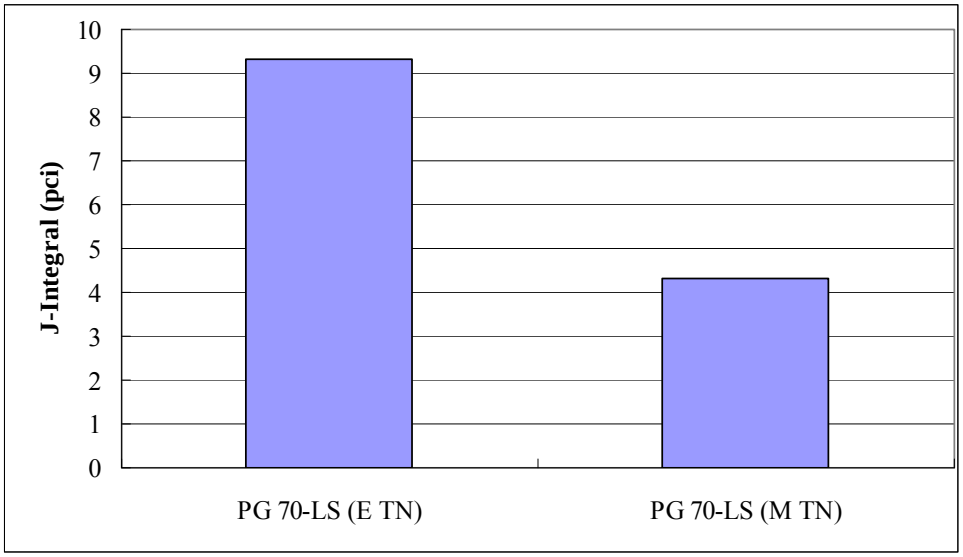

(d) 307 A-S Mixtures

Figure 4-22 J-Integral Results from SCB Notched Test

4.8 Determination of Structural Layer Coefficients

The structural layer coefficient a_i is a measure of the relative ability of a unit thickness of a given material to function as a structural component of the pavement and thus used to convert the actual thicknesses of asphalt layers into the structural number required in the structural design of pavement. The layer coefficient values was initially determined from the AASHO road test for different layer materials and provided in the 1986 and 1993 AASHTO design guides. Without road test, layer coefficients are usually determined from the empirical correlation between layer coefficients and the layer material properties. Resilient modulus has long been used as a fundamental material property to estimate layer coefficients from.

Table 4-3 shows the structural layer coefficients determined from the indirect tensile resilient modulus results for 411-D and 307 BM-2 mixtures using the chart for estimating layer coefficient of dense-graded asphalt concrete mixtures (Huang 2004). It should be noted that usually the resilient modulus at 70°F (21°C) is used to determine the layer coefficient of asphalt materials. However, resilient modulus was tested at 77°F (25°C) in this study. Due to its viscoelastic property, the resilient modulus is slightly lower at the testing temperature of 77°F (25°C) than at 70°F (21°C) and thus the determined layer coefficients were slightly smaller than they should be.

Table 4-3 Layer Coefficients Determined from IDT Resilient Modulus for 411 D and 307 BM-2 Mixtures

Mixture	M_R (psi)	Layer Coefficient
411D Limestone PG 64-22	3.7E+05	0.40
411D Limestone PG 70-22	5.5E+05	0.48
411D Limestone PG 76-22	4.7E+05	0.45
411D Gravel PG 64-22	5.3E+05	0.48
411D Gravel PG 70-22	6.3E+05	0.50
411D Gravel PG 76-22	5.4E+05	0.48
411D Granite PG 64-22	3.6E+05	0.40
BM-2 Limestone PG 64-22	6.2E+05	0.50
BM-2 Limestone PG 70-22	6.4E+05	0.50
BM-2 Limestone 76-22	5.2E+05	0.46
BM-2 Gravel PG 82-22	3.2E+05	0.38

The layer coefficient values for different layer materials can also be determined from the following empirical equations given by Ullidtz (1987):

Asphalt concrete:

$$a_1 = 0.40 * \log[E/(3000\text{MPa})] + 0.44, \qquad 0.20 < a_1 < 0.44 \qquad (4\text{-}1)$$

Bituminous-treated base:

$$a_2 = 0.30 * \log[E/(3000\text{MPa})] + 0.33, \qquad 0.10 < a_2 < 0.30 \qquad (4\text{-}2)$$

Using equations (4-1) and (4-3), the layer coefficients for all the mixtures used in this study was determined and presented in Table 4-4.

Table 4-4 Layer Coefficients Determined from Equations Given by Ullidtz (1987)

Mixture	M_R (psi)	Layer Coefficient
411D Limestone PG 64-22	3.67E+05	0.41
411D Limestone PG 70-22	5.48E+05	0.48
411D Limestone PG 76-22	4.73E+05	0.45
411D Gravel PG 64-22	5.26E+05	0.47
411D Gravel PG 70-22	6.34E+05	0.51
411D Gravel PG 76-22	5.36E+05	0.48
411D Granite PG 64-22	3.57E+05	0.41
BM-2 Limestone PG 64-22	6.21E+05	0.50
BM-2 Limestone PG 70-22	6.35E+05	0.51
BM-2 Limestone 76-22	5.18E+05	0.47
BM-2 Gravel PG 82-22	3.19E+05	0.39
A Limestone PG 70-22 (Knoxville)	5.43E+05	0.36
A Limestone PG 70-22 (Davidson)	4.41E+05	0.33
A Limestone PG 76-22	8.34E+05	0.41
AS Limestone PG 70-22 (Knoxville)	9.90E+05	0.44
AS Limestone PG 70-22 (Nashville)	6.83E+05	0.39

However, lower fatigue life values were observed for 307 BM-2 asphalt materials compared to 411-D mixtures. The beam fatigue test results for 307 A and A-S materials showed higher variation than other materials. The lower fatigue life values and the higher

variation in fatigue life indicate that these materials may not have a relatively good resistance to fatigue cracking. These layer coefficient values need to be adjusted for practical design usage. The layer coefficients for all the mixtures are recommended in Table 4-5.

Table 4-5 Recommended Structural Layer Coefficients

Mixture	Layer Coefficient
411D Limestone PG 64-22	0.40
411D Limestone PG 70-22	0.44
411D Limestone PG 76-22	0.44
411D Gravel PG 64-22*	0.40 – 0.42
411D Gravel PG 70-22*	0.44
411D Gravel PG 76-22*	0.44
411D Granite PG 64-22	0.44
BM-2 Limestone PG 64-22	0.42
BM-2 Limestone PG 70-22	0.42
BM-2 Limestone 76-22	0.42
BM-2 Gravel PG 82-22*	0.42
A Limestone PG 70-22 (Knoxville)	0.40
A Limestone PG 70-22 (Davidson)	0.40
A Limestone PG 76-22	0.40
AS Limestone PG 70-22 (Knoxville)	0.30
AS Limestone PG 70-22 (Nashville)	0.30

*Gravel: The gravel used in this study is mainly from Eastern Tennessee. When Western Tennessee gravel is used in asphalt mixture, caution should be taken for the determination of layer coefficients

CHAPTER 5 CONCLUSIONS AND RECOMMENDATIONS

5.1 Conclusions

A laboratory study has been conducted to evaluate the structural layer coefficients for the asphalt mixtures used in the state of Tennessee. The asphalt mixtures included 411-D surface mixtures, 307 BM-2 base mixtures, and 307 A and 307 A-S base mixtures. The performance of asphalt mixtures were evaluated by following laboratory tests: dynamic modulus and flow number tests, Asphalt Pavement Analyzer (APA) test, Superpave indirect tensile (IDT) tests (including resilient modulus, creep, and strength tests), beam fatigue test, and semi-circular bending (SCB) strength and notched fracture tests. Based on the laboratory experiments and analyses, the following can be summarized and concluded:

- With the increase in the upper grade limit of asphalt binder, asphalt mixtures exhibited relatively better performance, which included increase in the dynamic modulus ($|E^*|$), flow number, IDT resilient modulus (M_R), IDT tensile strength, IDT failure strain, fracture energy, dissipated creep strain energy threshold (DCSEf), energy ratio, fatigue life and reduction in APA rut depth, creep compliance, m-value, plateau value.
- The improved performance of asphalt mixtures with the increase in the upper

grade limit of asphalt binder indicates that use of modified asphalt binder could lead to the increase in the structural layer coefficients for structural design of asphalt pavements.

5.2 Recommendations

- Based on the laboratory test results, the structural layer coefficients for all the asphalt mixtures used in this study were recommended and presented in Table 5-1 (same as Table 4-5).

Table 5-1 Recommended Structural Layer Coefficients

Mixture	Layer Coefficient
411D Limestone PG 64-22	0.40
411D Limestone PG 70-22	0.44
411D Limestone PG 76-22	0.44
411D Gravel PG 64-22*	0.40 – 0.42
411D Gravel PG 70-22*	0.44
411D Gravel PG 76-22*	0.44
411D Granite PG 64-22	0.44
BM-2 Limestone PG 64-22	0.42
BM-2 Limestone PG 70-22	0.42
BM-2 Limestone 76-22	0.42
BM-2 Gravel PG 82-22*	0.42
A Limestone PG 70-22 (Knoxville)	0.40
A Limestone PG 70-22 (Davidson)	0.40
A Limestone PG 76-22	0.40
AS Limestone PG 70-22 (Knoxville)	0.30
AS Limestone PG 70-22 (Nashville)	0.30

*Gravel: The gravel used in this study is mainly from Eastern Tennessee. When Western Tennessee gravel is used in asphalt mixture, caution should be taken for the determination of layer coefficients

- The commonly used gravel HMA mixtures collected for the present study only reflected the materials from Eastern Tennessee sources; whereas, the majority of gravel aggregates used in TDOT HMA are from Western Tennessee. Further study is needed to evaluate the potential increase in the structural layer coefficients for the asphalt mixtures containing Western Tennessee gravel.

REFERENCES

AASHTO. AASHTO Guide for Design of Pavement Structures, Washington, D.C., 1993.

"AASHTO T 321-03 Determining the Fatigue Life of Compacted Hot-Mix Asphalt (HMA) Subjected to Repeated Flexural Bending," *Standard Specifications for Transportation Materials and Methods of Sampling and Testing, Part 2B*, American Association of State Highway and Transportation Officials, Washington D.C., 2005.

Bahia, H.U., Bosscher, P.J., Christensen, J., Hu, Y. Layer Coefficients for New and Reprocessed Asphalt Mixes, Res. Rpt No. WI/SPR-04-00, Wisconsin Department of Transportation, Madison, WI, 2000.

Buttlar, W.G., and Roque, R., "Experimental Development and Evaluation of the New SHRP Measurement and Analysis System for Indirect Tensile Testing at Low Temperature," Transportation Research Record, National Academy Press, Washington D.C., No. 1454, 1994, pp. 163-171.

Carpenter, S.H., Ghuzlan, K., Shen, S., "Fatigue Endurance Limit for Highway and Airport Pavements," Transportation Research Record, No.1832, 2003, pp. 131– 138.

George, K.P., "Structural Layer Coefficient for Flexible Pavement," Journal of Transportation Engineering, Vol.110, No.3, 1984, pp.251–267.

Ghuzlan, K., Carpenter, S.H., "Energy-Drived/Damage-Based Failure Criteria for Fatigue Testing," Transportation Research Record, No. 1723, 2000, pp. 141–149.

Hossain, M., Habib, A., LaTorella, T.M., "Structural Layer Coefficients of Crumb Rubber-Modified Asphalt Concrete Mixtures," Transportation Research Record, No. 1583, 1997, pp. 62–70.

Huang, B., Zhang, Z., Kingery, W., Zuo, G., "Fatigue Crack Characteristics of HMA Mixtures Containing RAP," Cracking in Pavements, RILEM PRO 37, May 2004.

Janoo, V. C., Layer Coefficients for NH DOT Pavement Materials. Special Report 94-30. Cold Regions Research & Engineering Laboratory, U.S. Army Corps of Engineers, 1994.

Mohammad, L.N., Wu, Z., Myers, L., Cooper, S., and Abadie, C., "A Practical Look at the Simple Performance Tests: Louisiana's Experience," Journal of the Association of Asphalt Paving Technologists, Volume 74, 2005, pp. 557-600.

Molenaar, A.A.A., Scarpas, A., Liu, X., and Erkens, S.M.J.G., "Semi-Circular Bending Test; Simple but Useful?," Journal of Asphalt Paving Technologists, Vol. 71, 2002, pp. 794 – 815.

Mull, M.A., Stuart, K., Yehia, A., "Fracture Resistance Characterization of Chemically Modified Crumb Rubber Asphalt Pavement," Journal of Materials Science, Vol.37, 2002, pp. 557-566.

Noureldin, S., Zhu, K., Harris, D., Li, S., Non-Destructive Estimation of Pavement Thickness, Structural Number and Subgrade Resilience along INDOT Highways. Res. Rpt No. FHWA/IN/JTRP-2004/35, Indiana Department of Transportation, West Lafayette, IN, 2005.

Pellinen, T. K., and Witczak, M. W., "Stress Dependent Master Curve Construction for Dynamic (Complex) Modulus", Journal of the Association of Asphalt Paving Technologists, Volume 71, 2002, pp. 281-309.

Pologruto, M., "Procedure for Use of Falling Weigh Deflectometer to Determine AASHTO Layer Coefficients," Transportation Research Record, No.1764, 2001, pp. 11–19.

Roque, R., Birgisson, B., Drakos, C., Dietrich, B., "Development and Field Evaluation of Energy-Based Criteria for Top-Down Cracking Performance of Hot Mix Asphalt, Journal of the Association of Asphalt Paving Technologists, Vol. 73, 2004, pp. 229-260.

Roque, R., and Buttlar, W.G., "The Development of a Measurement and Analysis System to Accurately Determine Asphalt Concrete Properties Using the Indirect Tensile Mode," Journal of the Association of Asphalt Paving Technologists, Vol. 61, pp. 304-332, 1992

Shen, S., Carpenter, S.H., "Application of Dissipated Energy Concept in Fatigue Endurance Limit Testing," Transportation Research Record, No. 1929, 2005, pP. 165–173.

Ullidtz, P. Pavement Analysis. Elsevier, N.Y., 1987, pp. 221-223.

Van de Ven, M., Smit, A., Karns, R., "Possibilities of a Semi-Circular Bending Test," Road and Hydraulic Engineering Division Ministry of Transport and Public Works, Netherlands, 1997.

Witczak, M. W., Kaloush, K. E., and H. Von Quintus, "Pursuit of the Simple Performance Test for Asphalt Mixture Rutting," Journal of the Association of Asphalt Paving Technologists, Volume 71, 2002, pp. 671-691.

Zhou, F., and Scullion, T., "Preliminary Field Validation of Simple Performance Tests for Permanent Deformation: Case Study," Transportation Research Record, n 1832, 2003, pp. 209-216.